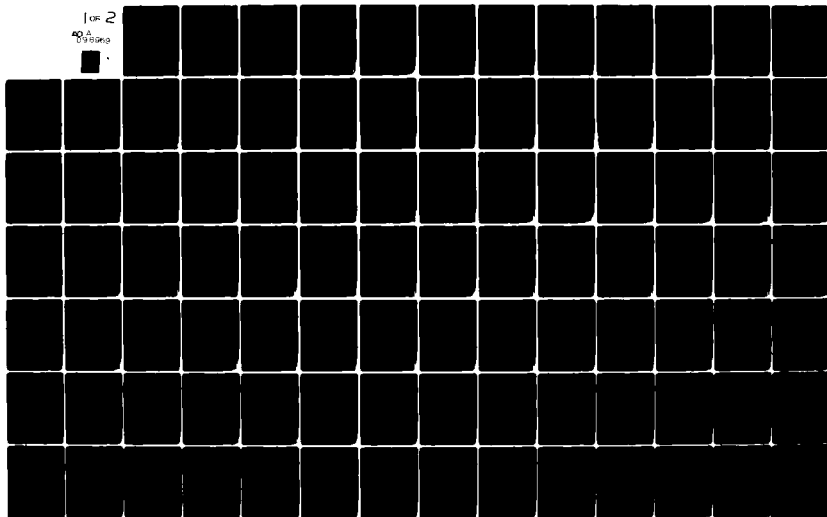


AD-A096 969 LOCKHEED MISSILES AND SPACE CO INC SUNNYVALE CA ADVA--ETC. F/6 9/1  
HIGH CONTRAST CRT FACEPLATE.(U)  
JAN 81 T 6 MAPLE, I D LIU, 6 COX DAAK20-79-C-0282  
UNCLASSIFIED LMSC/D767020 DELET-TR-79-0282-F NL

1 OF 2  
NO A  
DURING





(1.2)

LEVEL

## Research and Development Technical Report

DELET-TR-79-0282-F

HIGH CONTRAST CRT FACEPLATE

T. G. Maple

I. D. Liu

G. Cox

Advanced Systems Division  
Lockheed Missiles & Space Co., Inc.  
1111 Lockheed Way  
Sunnyvale, California 94086

ERADCOM  
MAR 30 1981

January, 1981

A

Final Report for Period 19 Sept. 1979 - 19 Oct. 1980

### Distribution Statement:

Approved for public release; distribution unlimited

Prepared for:

ELECTRONICS TECHNOLOGY AND DEVICES LABORATORY

# ERADCOM

US ARMY ELECTRONICS RESEARCH AND DEVELOPMENT COMMAND  
FORT MONMOUTH, NEW JERSEY 07703

DTIC FILE COPY

81 3 27 147

HISA-FM 195-78

## NOTICES

### Disclaimers

The citation of trade names and names of manufacturers in this report is not to be construed as official Government indorsement or approval of commercial products or services referenced herein.

### Disposition

Destroy this report when it is no longer needed. Do not return it to the originator.

HISA-FM-633-78

| REPORT DOCUMENTATION PAGE  |  | READ INSTRUCTIONS<br>BEFORE COMPLETING FORM   |
|--|--|---|
| 1. REPORT NUMBER<br>18 DELET-TR-79-0282-F  | 2. GOVT ACCESSION NO.<br>AD-A096   | 3. RECIPIENT'S CATALOG NUMBER<br>969  |
| 4. TITLE (and Subtitle)<br>(6) HIGH CONTRAST CRT FACEPLATE   | 5. TYPE OF REPORT & PERIOD COVERED<br>(9) Final Technical Report<br>19 Sept 1979 - 19 Oct 1980   | 6. PERFORMING ORG. REPORT NUMBER<br>14 LMSC/D767020   |
| 7. AUTHOR(s)<br>10 T. G./Maple<br>I. D./Liu<br>Gerry Fox   | 8. CONTRACT OR GRANT NUMBER(s)<br>15 DAAK20-79-C-0282  | 9. PROGRAM ELEMENT, PROJECT, TASK AREA & WORK UNIT NUMBERS<br>(16) 1L162705AH9403-01<br>17 03 |
| 10. PERFORMING ORGANIZATION NAME AND ADDRESS<br>Advanced Systems Division<br>LOCKHEED MISSILES & SPACE CO., INC.<br>1111 Lockheed Way, Sunnyvale, Ca. 94086  | 11. CONTROLLING OFFICE NAME AND ADDRESS<br>U.S. Army Electronics Research and<br>Development Command Attn: DELET-BD<br>Fort Monmouth, N.J. 07703 | 12. REPORT DATE<br>January, 1981<br>13. NUMBER OF PAGES<br>106<br>15 11                       |
| 14. MONITORING AGENCY NAME & ADDRESS (if different from Controlling Office)  | 15. SECURITY CLASS (of this report)<br>UNCLASSIFIED<br>15a. DECLASSIFICATION/DOWNGRADING SCHEDULE  |   |
| 16. DISTRIBUTION STATEMENT (of this Report)<br>Approved for public release;<br>Distribution unlimited  |  |   |
| 17. DISTRIBUTION STATEMENT (of the abstract entered in Block 20, if different from Report)   |  |   |
| 18. SUPPLEMENTARY NOTES  |  |   |
| 19. KEY WORDS (Continue on reverse side if necessary and identify by block number)<br>3-inch CRT High Contrast Displays<br>Two-Color CRT<br>Thin Film Phosphor<br>Color Penetration Tube   |  |   |
| 20. ABSTRACT (Continue on reverse side if necessary and identify by block number)<br>The objective of this program is the development of a high contrast, two color CRT faceplate employing evaporated thin film phosphors and nonreflective backing, utilizing 1710 glass and also sapphire substrates. Twenty-six faceplates were fabricated using 1710 glass and nineteen using sapphire as substrate. Sapphire was found to possess several advantages over 1710 glass. The 2000°C plus melting point allows sulfurization treatment of the phosphor film at the optimum 1050°C temperature without faceplate distortion. Adhesion of the film is excellent. Thermal conductivity of sapphire, two orders of magnitude greater than 1710 glass, provides excellent dissipation of heat produced by an electron beam. X |  |   |

# PREFACE

This report was prepared by the Advanced Systems Division, Lockheed Missiles & Space Company Inc., Sunnyvale, California under Contract Number DAAK20-79-C-0282 High Contrast CRT Faceplate for the Period 19 September 1979 through 19 October 1980.

This research and development effort was sponsored by the U.S. Army Electronics Research and Development Command, Ft. Monmouth, New Jersey. The work was administered under the direction of Phil Krzyzkowski, Project Engineer; Dr. Elliot Schlam, Team Leader; and Mr. Irving Reingold, Director, Beam, Plasma and Display Division.

Performance of the work under the contract was supervised by Dr. R. A. Buchanan, Manager, NDT Technology Laboratory, Advanced Systems Division, Lockheed Missiles & Space Company, Inc. Dr. T. G. Maple, Staff Scientist, was Project Leader. Dr. Maple fabricated the faceplates and prepared the reports. Cathodoluminescence and optical reflectance measurements were performed by Dr. I.D. Liu, Staff Scientist. The demountable cathodoluminescence measuring system was designed and constructed by Mr. Gerry Cox, Senior Research Engineer, assisted by Mr. William Bradley, Research Engineer.

This is the final report and concludes the work on the contract.

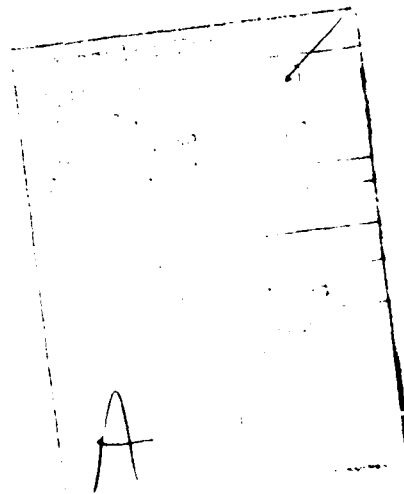


TABLE OF CONTENTS

| <u>Section</u> | <u>Description</u>                                | <u>Page</u> |
|----------------|---|-------------|
| 1.0            | CONFERENCE  | 1           |
| 1.1            | 10 July 1980 at LMSC                              | 1           |
| 2.0            | INTRODUCTION                                      | 4           |
| 2.1            | Background  | 4           |
| 2.2            | Statement of the Problem                          | 4           |
| 3.0            | TECHNICAL APPROACH                                | 6           |
| 4.0            | PROGRESS DURING REPORT PERIOD                     | 7           |
| 4.1            | Fabrication of Faceplates                         | 7           |
| 4.2            | Cathodoluminescence Brightness Measurements       | 13          |
| 4.2.1          | Lot 4   | 13          |
| 4.2.2          | Lot 5   | 13          |
| 4.2.3          | Additional CL Measurements                        | 29          |
| 4.2.3.1        | Brightness vs. "ON" Time                          | 43          |
| 4.2.3.2        | Comparison of 1720 Glass with Sapphire Substrates | 48          |
| 4.3            | Optical Reflectance Measurements                  | 53          |
| 4.3.1          | Lot 1   | 53          |
| 4.3.2          | Lot 4   | 53          |
| 4.3.3          | Lot 5   | 80          |
| 4.4            | Reflectivity Calculations for Sapphire Faceplates | 94          |
| 4.5            | Delivery of Faceplates                            | 102         |
| 5.0            | SUMMARY OF RESULTS                                | 103         |
| 6.0            | CONCLUSIONS                                       | 104         |
| 7.0            | REFERENCES  | 106         |

## LIST OF ILLUSTRATIONS

| <u>Figure #</u> | <u>Description</u>   | <u>Page</u> |
|-----------------|--|-------------|
| 1               | Cathodoluminescence Summary Lot 3                                    | 15          |
| 2               | Cathodoluminescence, Faceplate No. 75                                | 16          |
| 3               | Cathodoluminescence, Faceplate No. 76                                | 17          |
| 4               | Cathodoluminescence, Faceplate No. 77                                | 18          |
| 5               | Cathodoluminescence, Faceplate No. 78                                | 19          |
| 6               | Cathodoluminescence, Faceplate No. 79                                | 20          |
| 7               | Cathodoluminescence, Faceplate No. 80                                | 21          |
| 8               | Cathodoluminescence, Faceplate No. 81                                | 22          |
| 9               | Cathodoluminescence, Faceplate No. 82                                | 23          |
| 10              | Cathodoluminescence, Faceplate No. 83                                | 24          |
| 11              | Cathodoluminescence, Faceplate No. 84                                | 25          |
| 12              | Cathodoluminescence, Faceplate No. 85                                | 26          |
| 13              | Cathodoluminescence, Faceplate No. 86                                | 27          |
| 14              | Cathodoluminescence, Faceplate No. 87                                | 28          |
| 15              | Cathodoluminescence Summary Lot 5                                    | 31          |
| 16              | Cathodoluminescence, Faceplate No. 88                                | 32          |
| 17              | Cathodoluminescence, Faceplate No. 89                                | 33          |
| 18              | Cathodoluminescence, Faceplate No. 90                                | 34          |
| 19              | Cathodoluminescence, Faceplate No. 92                                | 35          |
| 20              | Cathodoluminescence, Faceplate No. 93                                | 36          |
| 21              | Cathodoluminescence, Faceplate No. 95                                | 37          |
| 22              | Cathodoluminescence, Faceplate No. 96                                | 38          |
| 23              | Cathodoluminescence, Faceplate No. 97                                | 39          |
| 24              | Cathodoluminescence, Faceplate No. 98                                | 40          |
| 25              | Cathodoluminescence, Faceplate No. 107                               | 41          |
| 26              | Cathodoluminescence, Faceplate No. 108                               | 42          |
| 27              | Brightness vs. "ON" Time   | 46          |
| 28              | Relative Intensity as a Function of Rise Time                        | 47          |
| 29              | Thermal Quenching of $\text{La}_2\text{O}_2\text{S:Eu}$ Luminescence | 52          |
| 30              | Optical Reflectance, Faceplate No. 40                                | 55          |
| 31              | Optical Reflectance, Faceplate No. 41                                | 56          |
| 32              | Optical Reflectance, Faceplate No. 42                                | 57          |

| <u>Figure #</u> | <u>Description</u>   | <u>Page</u> |
|-----------------|--|-------------|
| 33              | Optical Reflectance, Faceplate No. 44                        | 58          |
| 34              | Optical Reflectance, Faceplate No. 45                        | 59          |
| 35              | Optical Reflectance, Faceplate No. 46                        | 60          |
| 36              | Optical Reflectance, Faceplate No. 48                        | 61          |
| 37              | Reflectance, Mirror, vs. Faceplate 75 and Sapphire Substrate | 63, 64      |
| 38              | Reflectance, Uncoated 1720 Glass                             | 65          |
| 39              | Reflectance, Uncoated Sapphire                               | 66          |
| 40              | Optical Reflectance, Faceplate No. 75                        | 67          |
| 41              | Optical Reflectance, Faceplate No. 76                        | 68          |
| 42              | Optical Reflectance, Faceplate No. 77                        | 69          |
| 43              | Optical Reflectance, Faceplate No. 78                        | 70          |
| 44              | Optical Reflectance, Faceplate No. 79                        | 71          |
| 45              | Optical Reflectance, Faceplate No. 80                        | 72          |
| 46              | Optical Reflectance, Faceplate No. 81                        | 73          |
| 47              | Optical Reflectance, Faceplate No. 82                        | 74          |
| 48              | Optical Reflectance, Faceplate No. 83                        | 75          |
| 49              | Optical Reflectance, Faceplate No. 84                        | 76          |
| 50              | Optical Reflectance, Faceplate No. 85                        | 77          |
| 51              | Optical Reflectance, Faceplate No. 86                        | 78          |
| 52              | Optical Reflectance, Faceplate No. 87                        | 79          |
| 53              | Optical Reflectance, Faceplate No. 88                        | 83          |
| 54              | Optical Reflectance, Faceplate No. 89                        | 84          |
| 55              | Optical Reflectance, Faceplate No. 90                        | 85          |
| 56              | Optical Reflectance, Faceplate No. 92                        | 86          |
| 57              | Optical Reflectance, Faceplate No. 93                        | 87          |
| 58              | Optical Reflectance, Faceplate No. 95                        | 88          |
| 59              | Optical Reflectance, Faceplate No. 96                        | 89          |
| 60              | Optical Reflectance, Faceplate No. 97                        | 90          |
| 61              | Optical Reflectance, Faceplate No. 98                        | 91          |
| 62              | Optical Reflectance, Faceplate No. 107                       | 92          |
| 63              | Optical Reflectance, Faceplate No. 108                       | 93          |
| 64              | Sapphire Plate   | 100         |
| 65              | 1720 Plate   | 101         |

LIST OF TABLES

| <u>Table No.</u> | <u>Description</u>   | <u>Page</u> |
|------------------|--|-------------|
| 1                | Faceplate Fabrication Summary, Lot 4   | 11          |
| 2                | Faceplate Fabrication Summary, Lot 5   | 12          |
| 3                | Cathodoluminescence Brightness, Lot 4  | 14          |
| 4                | Cathodoluminescence Brightness, Lot 5  | 30          |
| 5                | Brightness vs. "ON" Time   | 44          |
| 6                | 1720 Glass vs. Sapphire  | 48          |
| 7                | Optical Reflectance, Lot 1   | 54          |
| 8                | Optical Reflectance, Lot 4   | 62          |
| 9                | Optical Reflectance, Lot 5   | 81, 82      |
| 10               | Sapphire Plate, Oblique Incidence  | 96          |
| 11               | Sapphire Plate over $\text{La}_2\text{O}_2\text{S}$ Film                     | 97          |
| 12               | Sapphire Plate + $\text{La}_2\text{O}_2\text{S}$ Film + Ideal NR Film        | 98          |
| 13               | Sapphire Plate + $\text{La}_2\text{O}_2\text{S}$ Film (Max. Zero Deg. Refl.) | 99          |

1.0 CONFERENCE

1.1 10 July 1980 at LMSC

Report of conference held at LMSC, Mountain View, California, on 10 July 1980 with ERADCOM to review progress on Contract DAAK20-79-C-0282, High Contrast CRT Faceplates.

Personnel Present

ET&D Lab - ERADCOM

P. F. Krzyzkowski

LMSC, Inc.

T. G. Maple

I. D. Liu

G. Cox

The purpose of the meeting was to review and discuss progress under the current contract.

1.1.1 Contract Documentation

The draft copy of the Second Interim Report is still under review by ERADCOM.

1.1.2 Faceplate Processing

LMSC reported that the distortion of 1710 and 1720 glass encountered during the  $H_2 + SO_2$  treatment was solved by incorporating controlled pre-heat and cooling periods into the treatment schedules. The problem can be traced to the faceplates having sufficient thickness that the surface of the glass heats up or cools more rapidly than the interior of the glass; the surface expands or contracts more rapidly than the interior, so that stress is placed on the surface and because the treatment temperature is close to the softening point of the glass, wrinkling or warpage of the surface results. By reducing

the rate of heating or cooling, the temperature difference between surface and interior is reduced, thereby reducing the stress.

Calculations were presented by LMSC showing that 1720 glass has a thermal stress resistance of  $28.5^{\circ}\text{C}$  and that of sapphire is  $5.2^{\circ}\text{C}$ . The sapphire is thus significantly more susceptible to thermal shock than the 1720 glass. Allowance must be made for this in developing the  $\text{H}_2 + \text{SO}_2$  treatment schedule for the sapphire faceplates.

#### 1.1.3 Optical Reflectance Measurements

The LMSC reflectance measuring system gives results similar to those made at ERADCOM. The LMSC system has a longer light path; the "tails" thus occur at a lower level than at ERADCOM.

P. Krzyzkowski discussed some results he had obtained using a Metvac HEA filter to eliminate the front surface reflection, and left a filter for LMSC use.

#### 1.1.4 Cathodoluminescence Measurements

The LMSC cathodoluminescence measuring system has been modified to permit use of a magnetic deflection gun producing 500 microamperes screen current. Focus "blooming" is still a problem. The system was demonstrated with comparison of a 1710 glass faceplate and a sapphire faceplate. At the higher current densities (300 - 500 microamperes) brightness of the TV raster on the 1710 faceplate fell to one-half the initial value within 30 seconds. By contrast, that of the sapphire faceplate decreased by only one to two percent. The thermal conductivity of 1710 is probably about  $0.0017 \text{ cal. cm/cm}^2 \text{ sec}^{\circ}\text{C}$ ; that of sapphire is 0.11, nearly two orders of magnitude greater. The phosphor on the 1710 can thus be expected to attain a higher temperature and the observed difference in brightness is likely due to thermal quenching in the case of 1710 glass.

Visually, the raster at 5 microamperes and 10 kV appeared quite red but at increased screen current, 100 - 500 microamperes, appears orange.

P. F. Krzyzkowski suggested that color coordinates be measured for the raster on faceplates to determine if there is a real change with current density.

P. F. Krzyzkowski described two types of brightness measurements, at 5000 and 20,000 in/sec writing speeds, which would be typical of the intended application for the CRTs. LMSC agreed to explore the capability of its system for making both measurements.

#### 1.1.5 Faceplate Sealing

P. F. Krzyzkowski reported that Thomas Electronics had successfully sealed an experimental sapphire faceplate provided ERADCOM by LMSC, to a CRT. The seal was made at 450°C in argon gas. The black layer was not degraded. He also presented results of measurements made at Thomas Electronics on the completed CRT. He left two of the Thomas electron guns for LMSC examination.

## 2.0

## INTRODUCTION

### 2.1 Background

This program is a continuation of previous work at LMSC as a subcontractor to the Watkins-Johnson Company under Contract No. DAAB-07-77-C-2639 (see Research and Development Technical Reports ECOM-77-2639-1, Jan. 1978; ECOM-77-2639-2, May, 1978; DELET-TR-77-2639-3, Aug. 1979; DELET-TR-77-2639-4, Aug. 1979; DELET-TR-2639-5, Aug. 1979; and DELET-TR-77-2639-F, Feb, 1980).

The progress under the present contract during the period 19 September 1979 - 18 May 1980 has been described in the First Interim Report, DELET-TR-79-0282-1, April, 1980, and the Second Interim Report, DELET-TR-79-0282-2, December 1980.

This Final Report describes the progress during the period.

The faceplates to be fabricated under this program are an essential component of the proposed high contrast multicolor CRT.

### 2.2 Statement of the Problem

The basic problem addressed by this program is the ability to display information generated by various electronic systems with suitable high resolution in two colors with its legibility maintained under ambient illumination ranging from  $10^4$  to  $10^{-3}$  fc.

Existing color tubes cannot satisfy the above requirement. Such tubes which employ aperture masks are severely limited in brightness and resolution by the aperture mask. Their brightness is limited because the aperture mask transmission is only 15 to 20 percent, therefore wasting 80 to 85 percent of the current. The wide spacing between holes degrades the resolution below that required in most military systems. Furthermore, the color purity of such tubes is influenced by their position with respect to the earth's

magnetic field, and it is therefore impractical to incorporate them in airborne systems.

The use of color penetration phosphors overcomes some of the problems of mask type tubes. The color purity is no longer affected by the tube orientation and the resolution is higher than that which can be achieved with a mask type tube. Conventional color penetration tubes which employ powdered phosphors cannot be used for daylight (high brightness) viewing because of their high reflectivity and low brightness, particularly in red, which produces a washed-out low contrast display. The reflectivity of the phosphor is high because of its particulate nature. The brightness of the red, in addition to its lower luminescent efficiency, is low because most of the light generated by the red phosphor is scattered by the green phosphor before it reaches the faceplate of the CRT.

3.0

TECHNICAL APPROACH

The technical guidelines for the program and the technical approach developed to achieve the objectives of the program have been described in the First Interim Report. DELET-TR-79-0282-1, April, 1980. Results to date have not indicated any need for modification of the technical approach.

#### 4.0 PROGRESS DURING REPORT PERIOD

##### 4.1 Fabrication of Faceplates

Corning Type 1710 aluminosilicate glass was used as substrate for the faceplate Lots 1, 2, and 3 fabricated during the earlier part of the program. For Lots 4 and 5, fabricated during the latter part of the program, sapphire was used as substrate.

Sapphire possesses several advantages over 1710 glass. First, the melting point of sapphire is  $2015^{\circ}\text{C}$  as compared to a softening point of  $915^{\circ}\text{C}$  for 1710 glass. It has been previously established that maximum cathodoluminescent brightness of rare earth oxysulfide phosphors is attained by sulfurization at  $1050^{\circ}\text{C}$ . The sulfurization treatment can be readily carried out at this temperature for oxysulfide phosphor films on sapphire, whereas experience has shown that when 1710 substrates are used, the sulfurization temperature must be reduced to  $850^{\circ}\text{C}$  to avoid softening of the substrate during the 1 hour treatment. As a result of the lower treatment temperature, a reduced cathodoluminescent brightness results (Ref. 1).

Although the coefficient of thermal expansion of sapphire ( $7.7 \times 10^{-6}/^{\circ}\text{C}$ ,  $60^{\circ}$  to C-axis) exceeds that of lanthanum oxysulfide ( $\sim 6 \times 10^{-6}/^{\circ}\text{C}$ ,  $0 - 200^{\circ}\text{C}$ ) by nearly as much as that of the oxysulfide exceeds that of 1710 glass ( $42 \times 10^{-6}/^{\circ}\text{C}$ ,  $0 - 300^{\circ}\text{C}$ ); film adhesion and structure of the phosphor film is not affected by the  $1050^{\circ}\text{C}$  treatment on sapphire. On the other hand, the  $850^{\circ}\text{C}$  treatment is sufficiently close to the softening point of 1710 glass, that the stress due to the coefficient mismatch between the film and the glass produces gross distortion and warping of the 1710 faceplates unless a prolonged and careful preheating and cool schedule is adhered to. A somewhat similar preheat and cool schedule has, however, been found advisable for sapphire in order to avoid a visible defect believed to be an incipient crack due to the poorer thermal shock resistance of sapphire.

A third advantage of sapphire is its thermal conductivity which is between ten and one-hundred times greater than that of 1710 glass. This is important because much of the electron beam energy of a cathode-ray tube (CRT) is dissipated as heat. Although the oxysulfide phosphors, due to their melting

points of about  $2200^{\circ}\text{C}$ , have considerable thermal stability, thermal quenching of luminescence can occur at elevated temperatures; for  $\text{La}_2\text{O}_2\text{S:Eu}$  quenching begins at  $100^{\circ}\text{C}$ . Temperature rise of the phosphor film is very small for sapphire faceplates even at high current densities, while experimental evidence has been obtained indicating significant thermal quenching for 1710 faceplates.

The sapphire substrates used for fabrication of Lot 4 were purchased from Crystal Systems, Inc., Salem, Massachusetts, as their standard 3.0 in. dia. single crystal windows, 0.125 in. thickness. Orientation was 60 degrees to the C-axis. Standard dimensional tolerances were dia.  $\pm 0.005$  in. thickness  $\pm 0.001$  in. Standard optical polish of 80-50, flatness 10 waves per inch of diameter. To minimize stress during sulfurization treatment at  $1050^{\circ}\text{C}$  and also during subsequent sealing of the completed faceplate to CRT funnels, an edge to bevel at 45 degrees approximately 0.010 in. wide was requested. Micrometer measurements on the sapphire discs for faceplates 75 through 86 showed all diameters between 2.999 and 3.002 in., indicating supplier was able to hold dimensions well within his standard specifications. Two substrates, however, had small edge chips, which would ordinarily have warranted rejection with request for replacement. In view of the extended delay in delivery beyond the promised delivery date, it was apparent replacement would not be likely within the contract performance period, so the two substrates were retained and processed with the others, but kept in-house for test purposes.

One of the Lot 4 faceplates was accidentally scratched during mounting for the cathodoluminescence measurements and another exhibited an incipient crack after the sulfurization treatment. As the number of Crystal Systems substrates was thus insufficient to fulfill the Lot 5 requirements, the latter was supplemented with sapphire substrates purchased from Union Carbide Corp., San Diego, California. Faceplates No's. 91 and 94 were found to have bad films due to an error in processing. The films were stripped in acid, and reprocessed as No's. 107 and 108. The break in numerical sequence was the result of fabricating some faceplates on 1710 glass (No's 99-106) for in-house test purposes prior to fabricating No's. 107 and 108.

Fabrication of the Lots 4 and 5 sapphire faceplates was essentially identical to that of the previous 1710 faceplate lots, except for the sulfurization treatment temperature.

The sapphire substrates were cleaned in a two-step process, the first step consisting of ultrasonic agitation in hot detergent solution; the second step consisted of immersion in hot chromic acid solution for 15-30 minutes. Each step was followed by rinsing in 5 changes of deionized water. After the final rinse, the faceplates were immersed in isopropyl alcohol, then drained and dried in an oven at 120°C. The chromic acid cleaning step was omitted for the 1710 glass substrates as these had been found susceptible to etching, which would have provided appreciable diffuse reflectance.

The phosphor films were deposited by RF sputtering of 5 in. diameter  $\text{La}_2\text{O}_2\text{S:Tb}$  and  $\text{La}_2\text{O}_2\text{S:Eu}$  targets in an argon atmosphere of 5 microns to which hydrogen sulfide was added at a partial pressure of  $1.5 \times 10^{-5}$  torr. RF power was 300 watts. Deposition time for the initial  $\text{La}_2\text{O}_2\text{S:Tb}$  layer was 120 min., giving a film thickness of 8800Å. Deposition time for the  $\text{La}_2\text{O}_2\text{S:Eu}$  film was 55 min.; thickness of this phosphor film was 4000Å. It was observed occasionally on opening the deposition chamber to remove the faceplates that a trace of powder was present on the surface. The presence of this powder was undesirable because any particles on the surface of the substrates would intercept the depositing vapor, causing pinholes in the phosphor film. Pinholes in the Tb-activated film would cause an absence of green emission in the pinhole area when the CRT screen potential was such as would ordinarily produce green emission. Pinholes in the Eu-activated film would result in excitation of the underlying Tb-activated layer, producing green emission at screen potential intended to produce red emission.

There appears to be three possible sources for powder contaminant during RF sputtering - particles detaching from the sintered target, particles of sulfur due to dissociation of the  $\text{H}_2\text{S}$  gas, and particles resulting from spalling of film deposited on chamber and fixtures during prior runs. The RF sputtering system available for this program was a downward sputtering design, that is, the target was situated on the top plate of the chamber, with the substrates below.

It was recognized that the particle contamination problem could be avoided by use of an upward sputtering design with the substrates placed above the target. Inquiries were made of several vacuum and sputtering equipment manufacturers as to availability of upward sputtering systems or modification of the existing system; none were able to quote a delivery or modification within the time span of the present contract.

Periodic removal of accumulated film from the chamber and fixtures by sanding and scraping was therefore resorted to, and the incidence of powder contamination appeared to be reduced, but not eliminated altogether.

Following deposition of the second phosphor film, the sapphire faceplates were treated in an  $H_2 + SO_2$  atmosphere at  $1050^{\circ}C$  for one hour.

After sulfurization, the faceplates were successively treated with 3 changes of hot TCE followed by a hot isopropyl alcohol rinse to remove any traces of elemental sulfur, prior to deposition of the nonreflective (NR) vanadium film. This was considered necessary to avoid a possible subsequent poisoning of the cathode of assembled CRT's. Cathodoluminescent brightness and optical reflectance measurements were made on the completed faceplates.

Fabrication of the Lot 4 faceplates is summarized in Table 1, and for Lot 5 in Table 2.

Table 1

## Faceplate Fabrication Summary, Lot 4

| F.P. # | Substrate   | La <sub>2</sub> O <sub>3</sub> :S:Tb<br>Run # Min. | La <sub>2</sub> O <sub>3</sub> :S:Eu<br>Run # Min. | H <sub>2</sub> + SO <sub>2</sub><br>°C Min. | NR(%)<br>Run # | Remarks       |
|--------|-------------|--|--|---|----------------|---------------|
| 75     | CS Sapphire | 26-80  | 26-80  | 1050  | 60 52-80       | Scratched     |
| 76     | CS Sapphire | 27-80  | 27-80  | 1050  | 60 53-80       | "Crack"       |
| 77     | CS Sapphire | 28-80  | 28-80  | 1050  | 60 54-80       | Sm. Chip (E)  |
| 78     | CS Sapphire | 29-80  | 29-80  | 1050  | 60 55-80       | (E)           |
| 79     | CS Sapphire | 30-80  | 30-80  | 1050  | 64 56-80       | (E)           |
| 80     | CS Sapphire | 31-80  | 31-80  | 1050  | 60 57-80       | Scratched (E) |
| 81     | CS Sapphire | 32-80  | 32-80  | 1050  | 61 58-80       | (E)           |
| 82     | CS Sapphire | 33-80  | 33-80  | 1050  | 65 59-80       | Scratched (E) |
| 83     | CS Sapphire | 34-80  | 34-80  | 1050  | 67 6080        | "Crack" (E)   |
| 84     | CS Sapphire | 36-80  | 36-80  | 1050  | 60 61-80       | (E)           |
| 85     | CS Sapphire | 36-80  | 36-80  | 1050  | 60 62-80       | Scratch (E)   |
| 86     | CS Sapphire | 37-80  | 37-80  | 1050  | 60 63-80       | (E)           |
| 87     | CS Sapphire | 38-80  | 38-80  | 1050  | 60 64-80       | Chip          |

LMSC-D767020

CS - Supplied by Crystal Systems, Inc.

E - Delivered to ERADCOM

Table 2

## Faceplate Fabrication Summary, Lot 5

| F.P. # | Substrate   | La <sub>2</sub> O <sub>3</sub> :Tb<br>Run # | La <sub>2</sub> O <sub>3</sub> :Eu<br>Run # | H <sub>2</sub> + SO <sub>2</sub><br>o <sub>c</sub> Min. | NR(V)<br>Run # | Remarks       |
|--------|-------------|---|---|---|----------------|---------------|
| 88     | CS Sapphire | 39-80                                       | 49-80                                       | 1050  | 60             | 69-80 (E)     |
| 89     | CS Sapphire | 40-80                                       | 49-80                                       | 1050  | 64             | 70-80         |
| 90     | CS Sapphire | 41-80                                       | 50-80                                       | 1050  | 60             | 71-80 (E)     |
| 91     | CS Sapphire | 42-80                                       | 51-80                                       | 1050  | 60             | 72-80 Shadow  |
| 92     | CS Sapphire | 43-80                                       | 52-80                                       | 1050  | 60             | 73-80 (E)     |
| 93     | CS Sapphire | 44-80                                       | 53-80                                       | 1050  | 60             | 74-80 (E)     |
| 94     | CS Sapphire | 45-80                                       | 54-80                                       | 1050  | 60             | 75-80 Bad NR  |
| 95     | UC Sapphire | 46-80                                       | 55-80                                       | 1050  | 60             | 76-80 (E)     |
| 96     | UC Sapphire | 47-80                                       | 56-80                                       | 1050  | 64             | 77-80 (E)     |
| 97     | UC Sapphire | 48-80                                       | 57-80                                       | 1050  | 64             | 78-80 (E)     |
| 98     | UC Sapphire | 49-80                                       | 58-80                                       | 1050  | 62             | 79-80 "Crack" |
| 107    | CS Sapphire | 58-80                                       | 59-80                                       | 1050  | 60             | 81-80 (E)     |
| 108    | CS Sapphire | 59-80                                       | 60-80                                       | 1050  | 63             | 82-80 (E)     |

CS - Supplied by Crystal Systems, Inc., Salem, Mass.

UC - Supplied by Union Carbide Corp., San Diego, California

E - Delivered to ERADCOM

LMSC-D767020

#### 4.2 Cathodoluminescent Brightness Measurements

During the course of the program, extensive modifications were made to the original demountable cathodoluminescent brightness measuring system. The principal modifications have been described in the Second Interim Report, DELET TR-79-0282-2. For characterization of the faceplates, measurements at a writing speed of 5000 in./sec. and high current densities were desirable as these would closely approximate the intended use of the assembled CRT. An electron gun capable of providing screen currents exceeding 500 microampere with a spot size less than 0.016 in. was required. The existing 5UP1 gun was found incapable of meeting this requirement. The 5UP1 gun utilizes both electrostatic focus and deflection. It was found to have poor spot definition and limited to about 120 microamperes screen current.

As the result of poor spot definition, it was observed that for a nominal 0.5 x 0.5 cm raster most of the energy was concentrated in an 0.3 x 0.3 cm area. The electronics was modified to allow use of magnetically deflected guns. Samples of both bipotential and Einzel type guns were obtained from Southwest Vacuum Devices, Inc., Tucson, Arizona.

4.2.1 Lot 4. Measurements on Lot 4 sapphire faceplates were made with a magnetic deflection bipotential gun which produced a well-defined raster with ample deflection. Table 3 presents the results obtained with an 0.5 x 0.5 cm raster and screen current of 5.0 microamperes. This measurement was intended to permit comparison with the results obtained for Lots 1-3. The more uniform energy distribution of the raster for the Lot 4 measurements resulted in an apparent decrease in measured luminescent intensity; however, which must be taken into account. The results are summarized graphically in Fig. 1. Figures 2 through 14 are plots of brightness vs. electron energy for each faceplate of this lot.

4.2.2 Lot 5. The spot size provided by the bipotential gun was observed to be sensitive to both screen potential and screen current. By contrast, the focus of an Einzel-type gun is in principal independent of screen potential, although current dependence is still a factor.

Table 3

Cathodoluminescent Brightness (ft-L) Lot #4

| Electron<br>Energy<br>Kev | Faceplate Number |      |      |      |      |      |      |      |      |      |      |      |      |
|---------------------------|------------------|------|------|------|------|------|------|------|------|------|------|------|------|
|                           | 75               | 76   | 77   | 78   | 79   | 80   | 81   | 82   | 83   | 84   | 85   | 86   | 87   |
| 8                         | 6.1              | 1.6  | 7.6  | 4.2  | 3.4  | 2.3  | 1.7  | 3.1  | 4.5  | 6.0  | 3.5  | 3.4  | 1.6  |
| 9                         | 10.6             | 3.9  | 13.7 | 9.2  | 7.4  | 6.4  | 4.7  | 6.9  | 7.3  | 11.5 | 8.3  | 7.7  | 4.5  |
| 10                        | 17.1             | 8.3  | 19.5 | 14.8 | 12.7 | 9.3  | 8.8  | 12.8 | 15.2 | 18.1 | 17.7 | 13.3 | 12.0 |
| 11                        | 25.4             | 13.1 | 30.6 | 24.2 | 19.3 | 20.3 | 13.7 | 18.6 | 25.0 | 24.4 | 26.6 | 22.4 | 20.5 |
| 12                        | 35.3             | 20.8 | 40.7 | 31.5 | 25.3 | 35.2 | 22.7 | 25.5 | 46.0 | 37.8 | 42.2 | 36.3 | 34.7 |
| 13                        | 45.4             | 27.9 | 54.8 | 43.6 | 38.7 | 50.3 | 42.1 | 39.6 | 56.7 | 56.4 | 57.4 | 41.5 | 51.8 |
| 14                        | 61.3             | 40.9 | 80.8 | 60.5 | 50.7 | 63.2 | 52.1 | 57.1 | 68.0 | 78.6 | 78.2 | 54.3 | 64.1 |
| 15                        | 70.0             | 50.0 | 89.1 | 73.9 | 64.6 | 77.0 | 67.2 | 76.3 | 80.6 | 91.1 | 89.7 | 63.4 | 86.8 |
| 16                        | 82.0             | 68.5 | 116  | 81.6 | 82.9 | 85.2 | 88.3 | 95.6 | 93.5 | 109  | 105  | 80.2 | 105  |
| 17                        | 98.8             | 78.1 | 120  | 108  | 95.5 | 105  | 123  | 106  | 111  | 131  | 121  | 102  | 125  |
| 18                        | 113              | 90.7 | 162  | -    | 108  | 138  | 129  | 125  | 133  | 139  | 135  | 109  | 142  |
| 19.6                      | 138              | 102  | 173  | 156  | 135  | 151  | 141  | 159  | 167  | 151  | 157  | 142  | 165  |
|                           |                  |      | (E)  | (E)  | (E)  | (E)  | (E)  | (E)  | (E)  | (E)  | (E)  | (E)  |      |

Raster Size:  $0.5 \times 0.5 \text{ cm}^2$   
 Screen Current:  $5.0 \mu\text{A}$   
 Pressure:  $\sim 2 \times 10^{-7} \text{ Torr}$

E - Delivered to ERADCOM

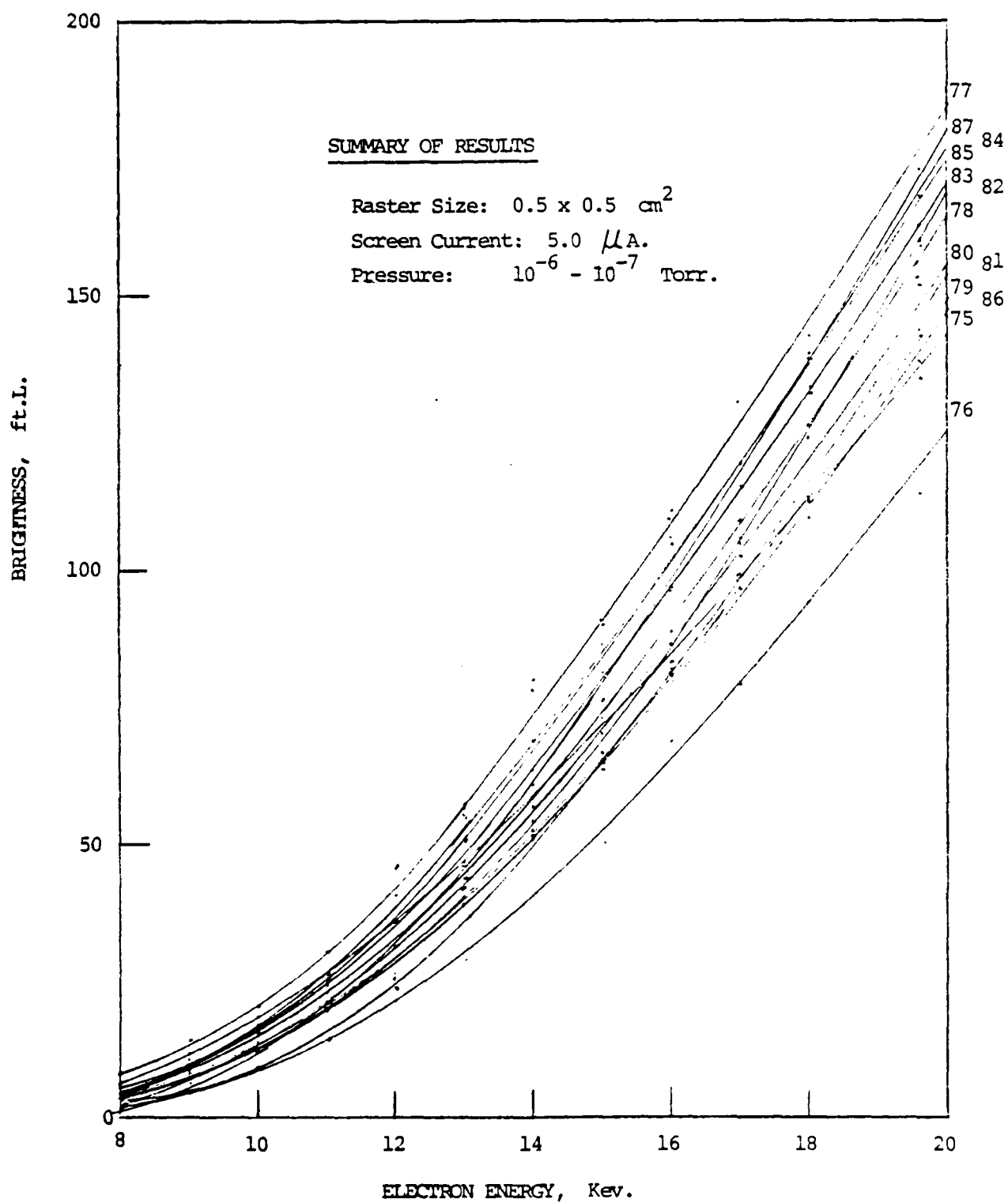


Fig. 1 Cathodoluminescence Summary, Loc 4

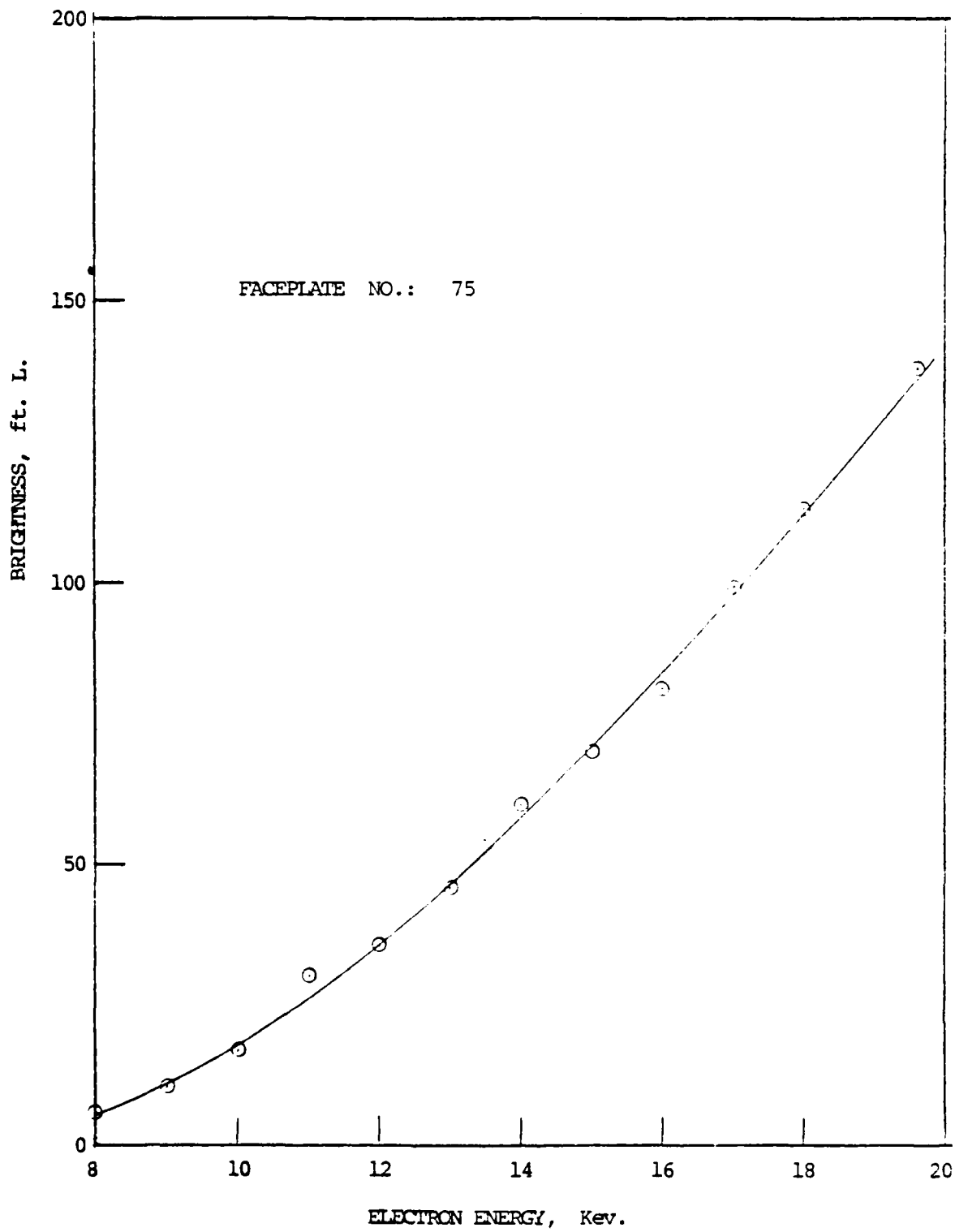


Fig. 2 Cathodoluminescence, Faceplate No. 75

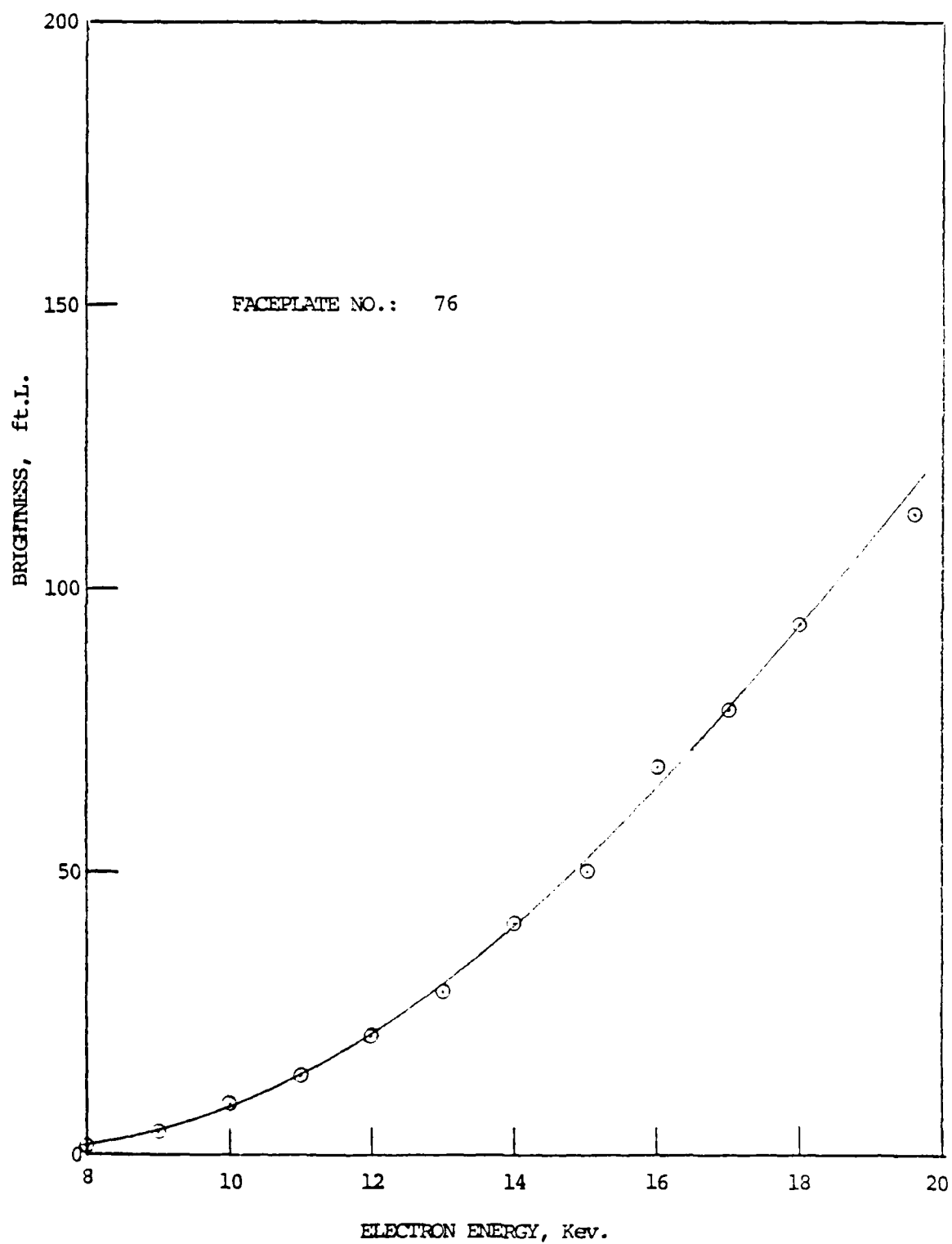


Fig. 3 Cathodoluminescence. Faceplate No. 76

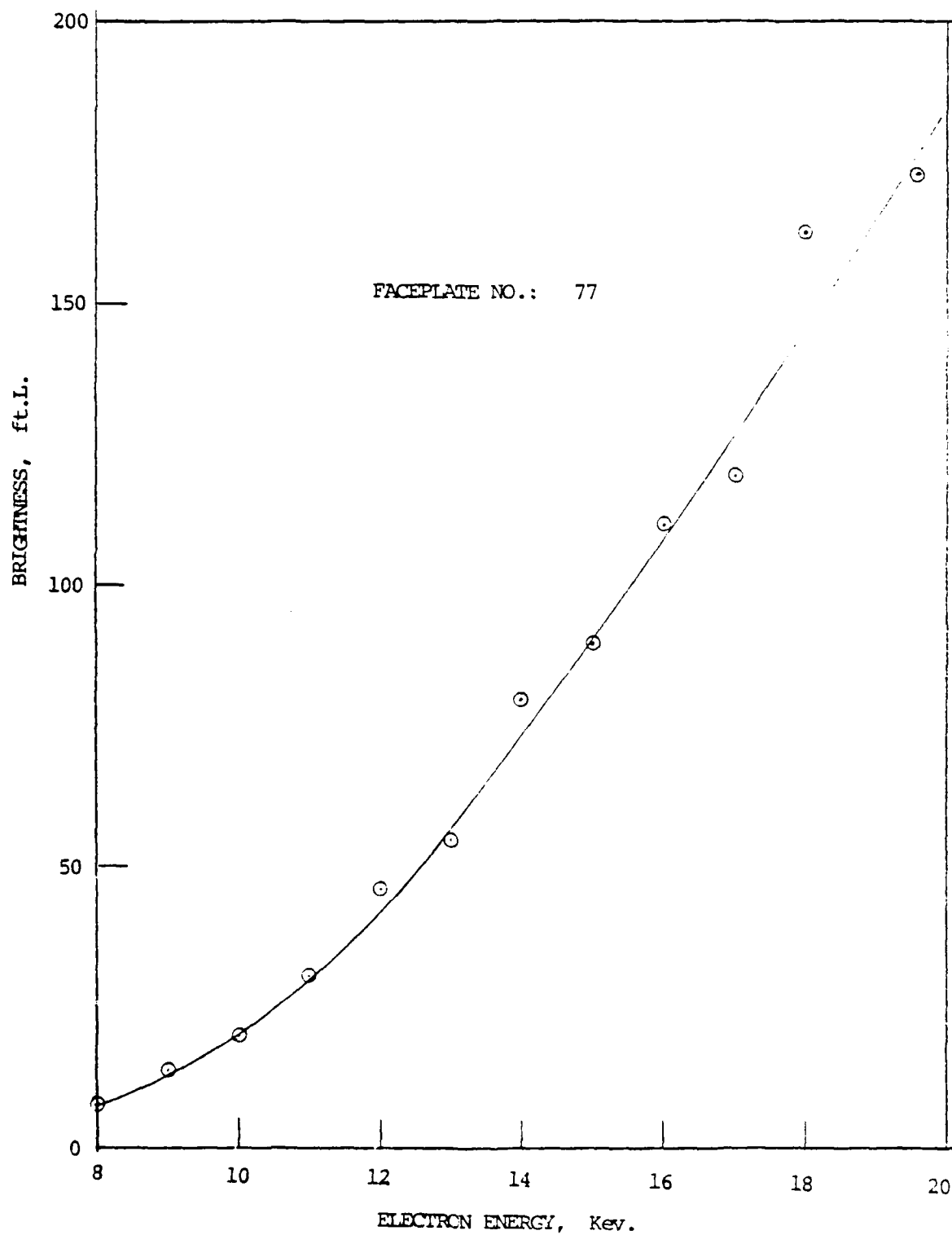


Fig. 4 Cathodoluminescence, Faceplate No. 77

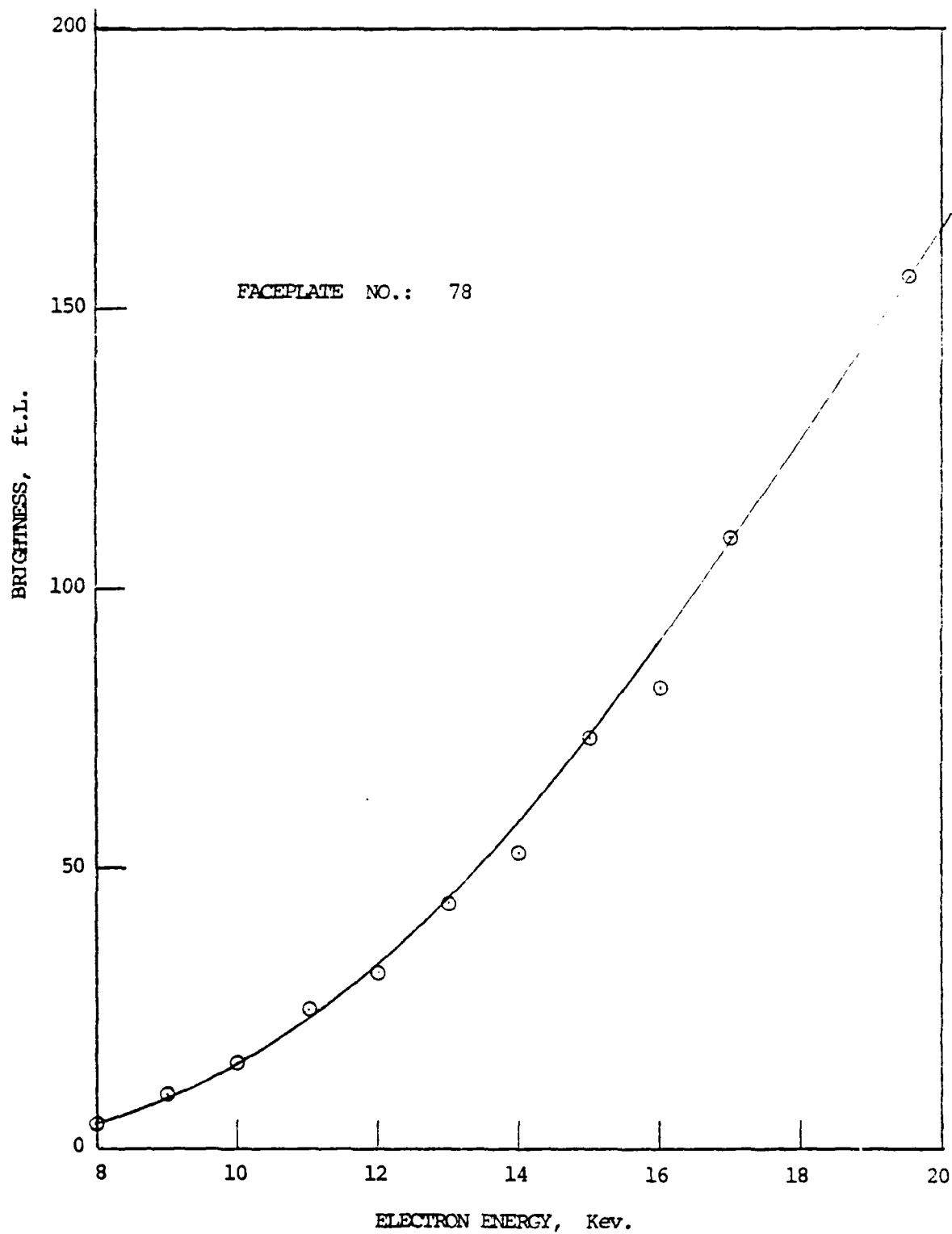


Fig. 5 Cathodoluminescence, Faceplate No. 78

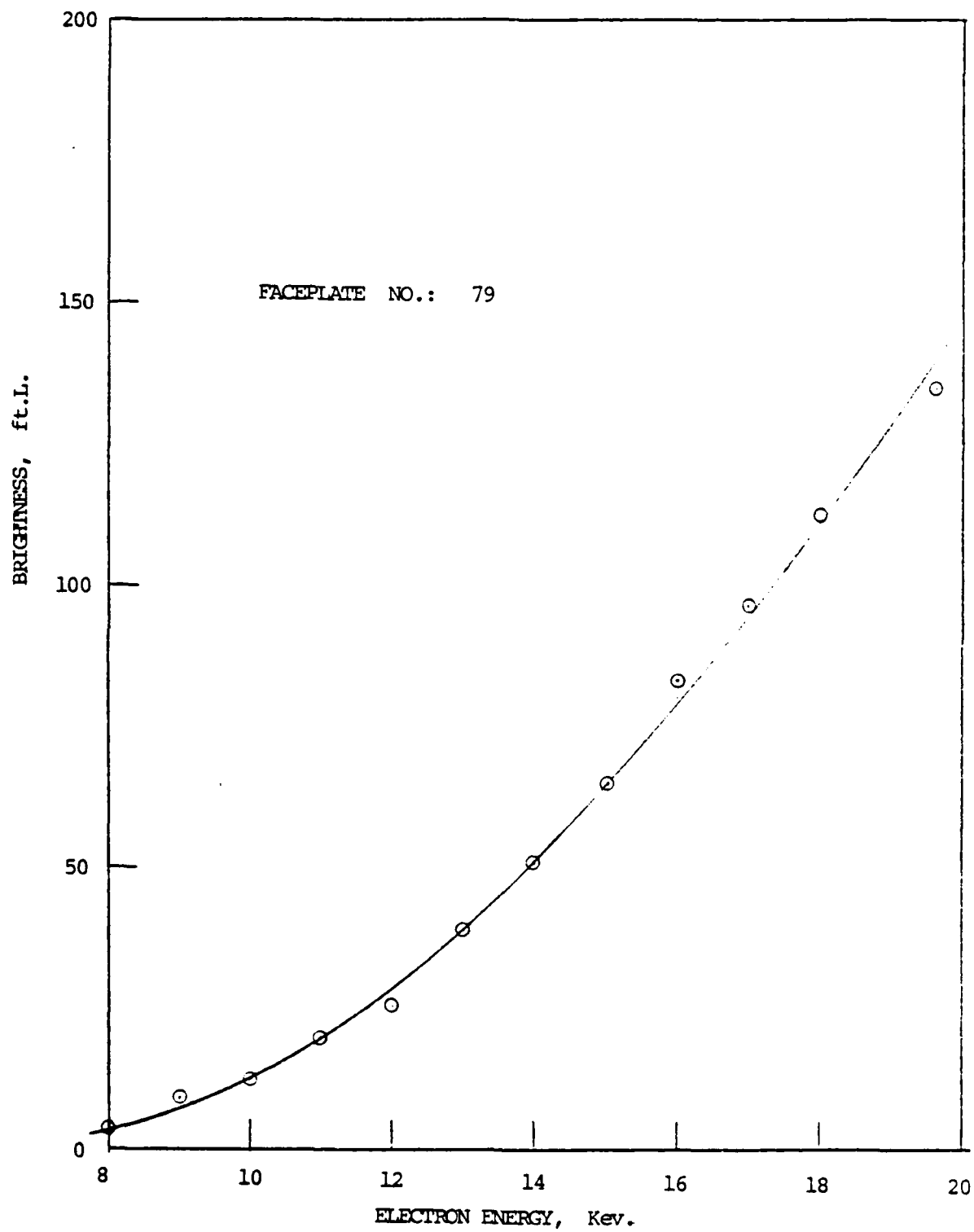


Fig. 6 Cathodoluminescence, Faceplate No. 79

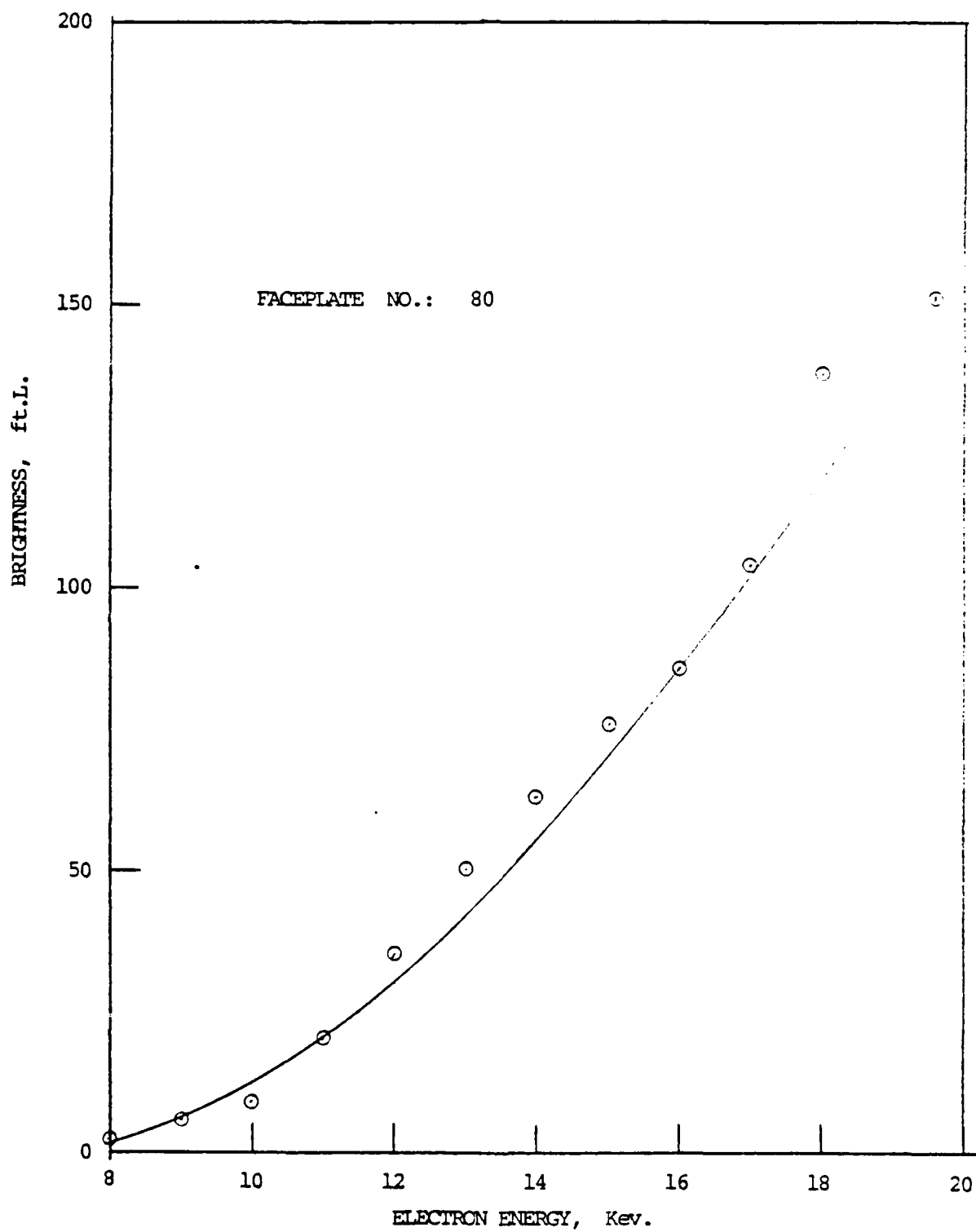


Fig. 7 Cathodoluminescence, Faceplate No. 80

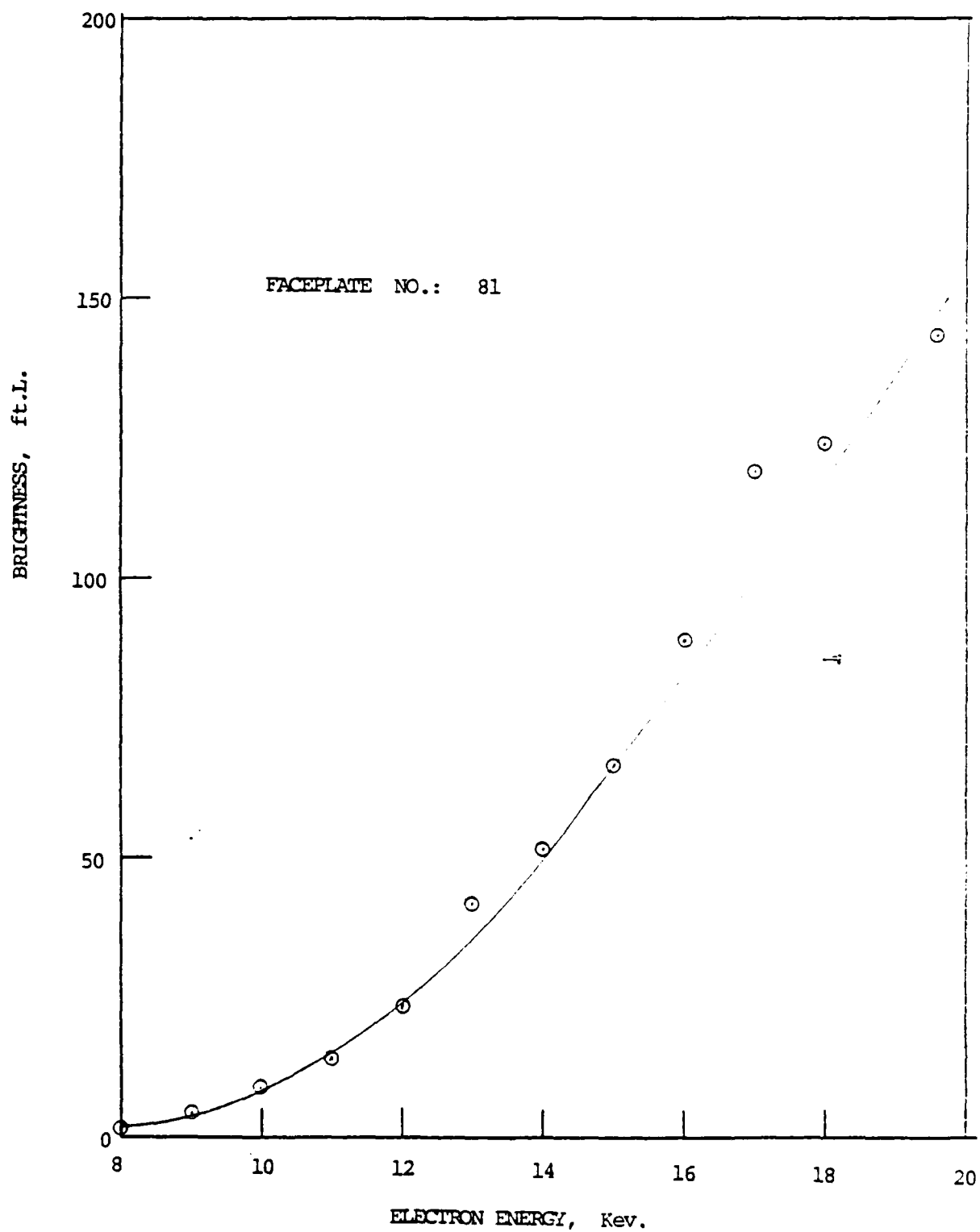


Fig. 8 Cathodoluminescence, Faceplate No. 81

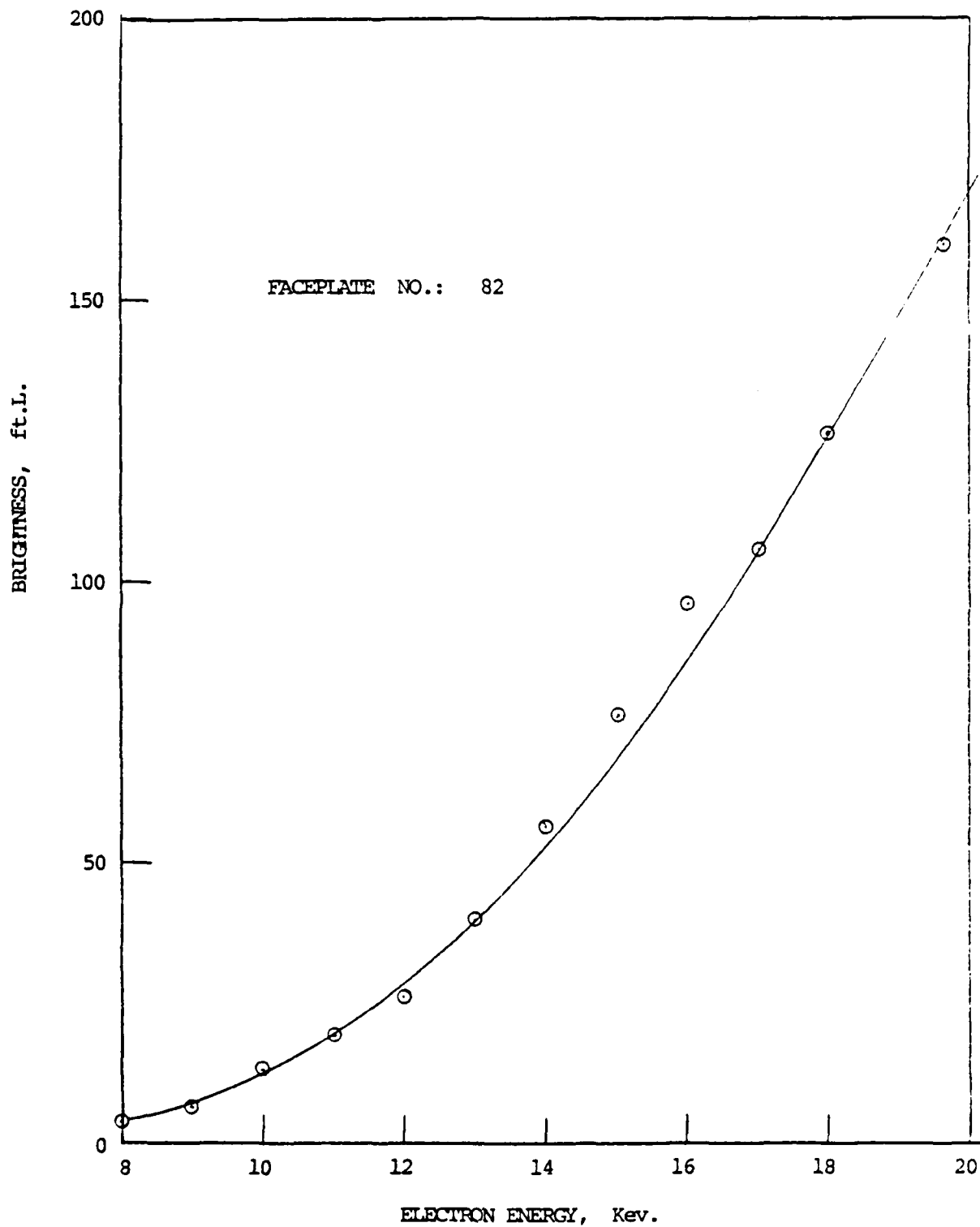


Fig. 9 Cathodoluminescence. Faceplate No. 82

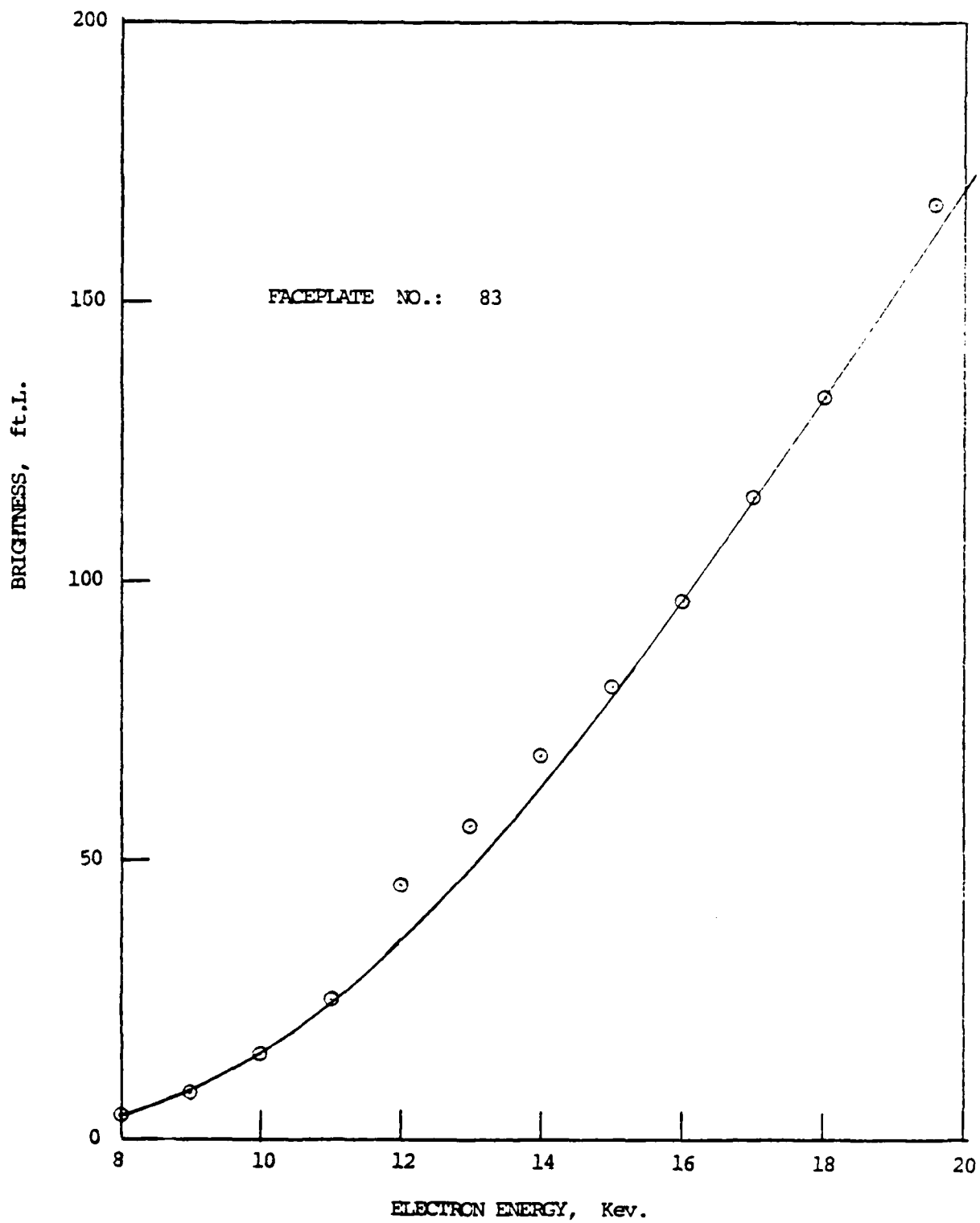


Fig. 10 Cathodoluminescence, Faceplate No. 83

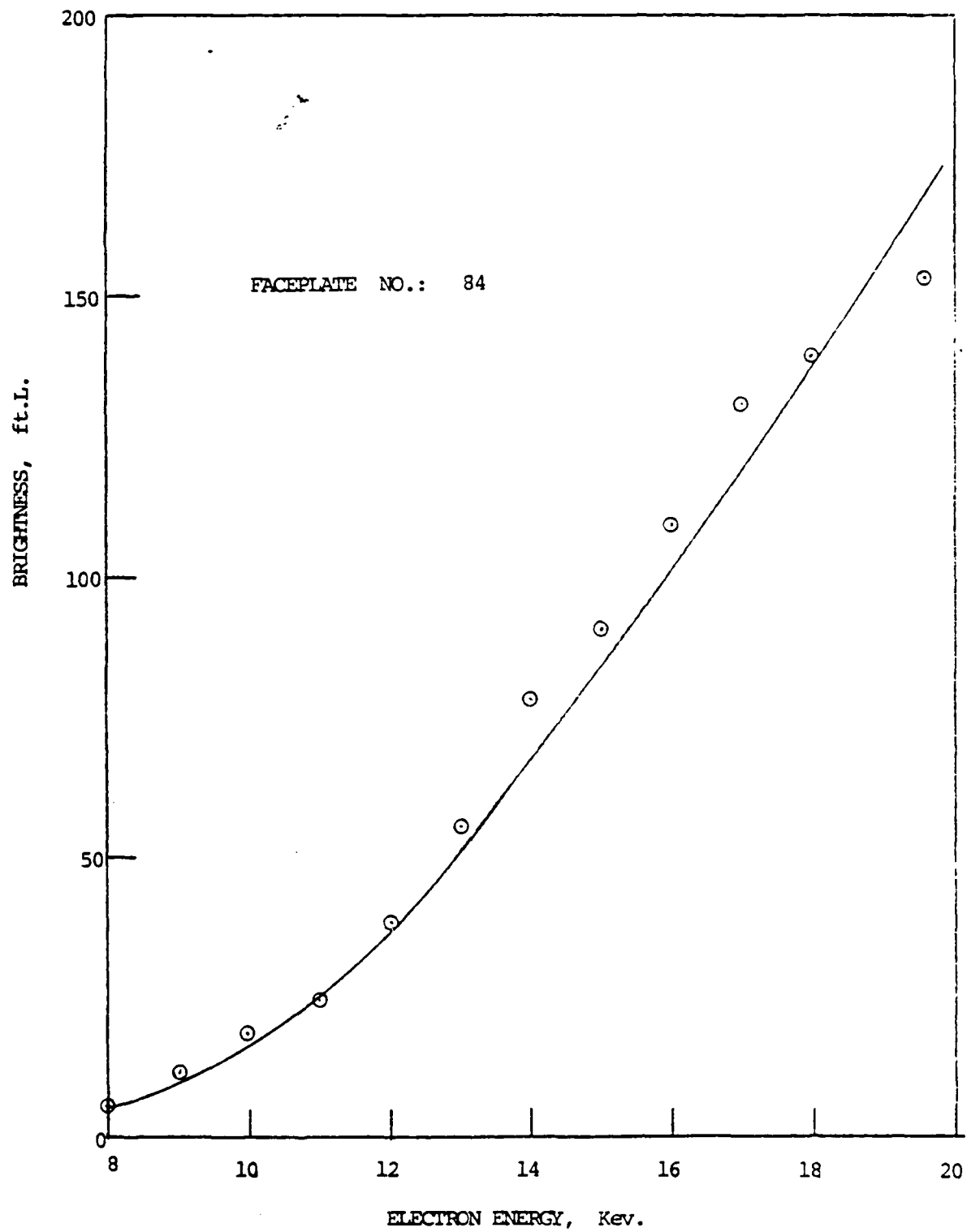


Fig. 11 Cathodoluminescence. Faceplate No. 84

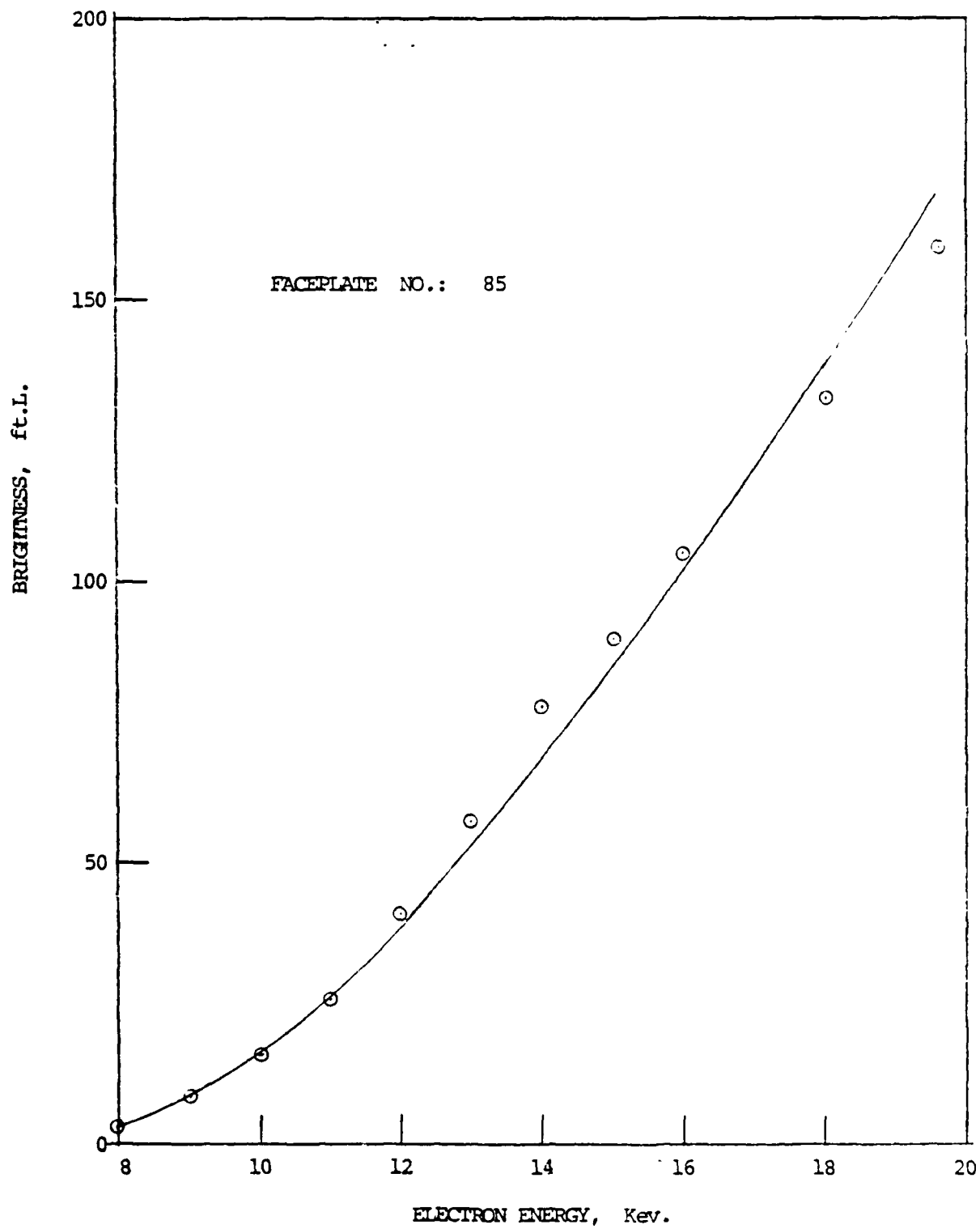


Fig. 12 Cathodoluminescence, Faceplate No. 85

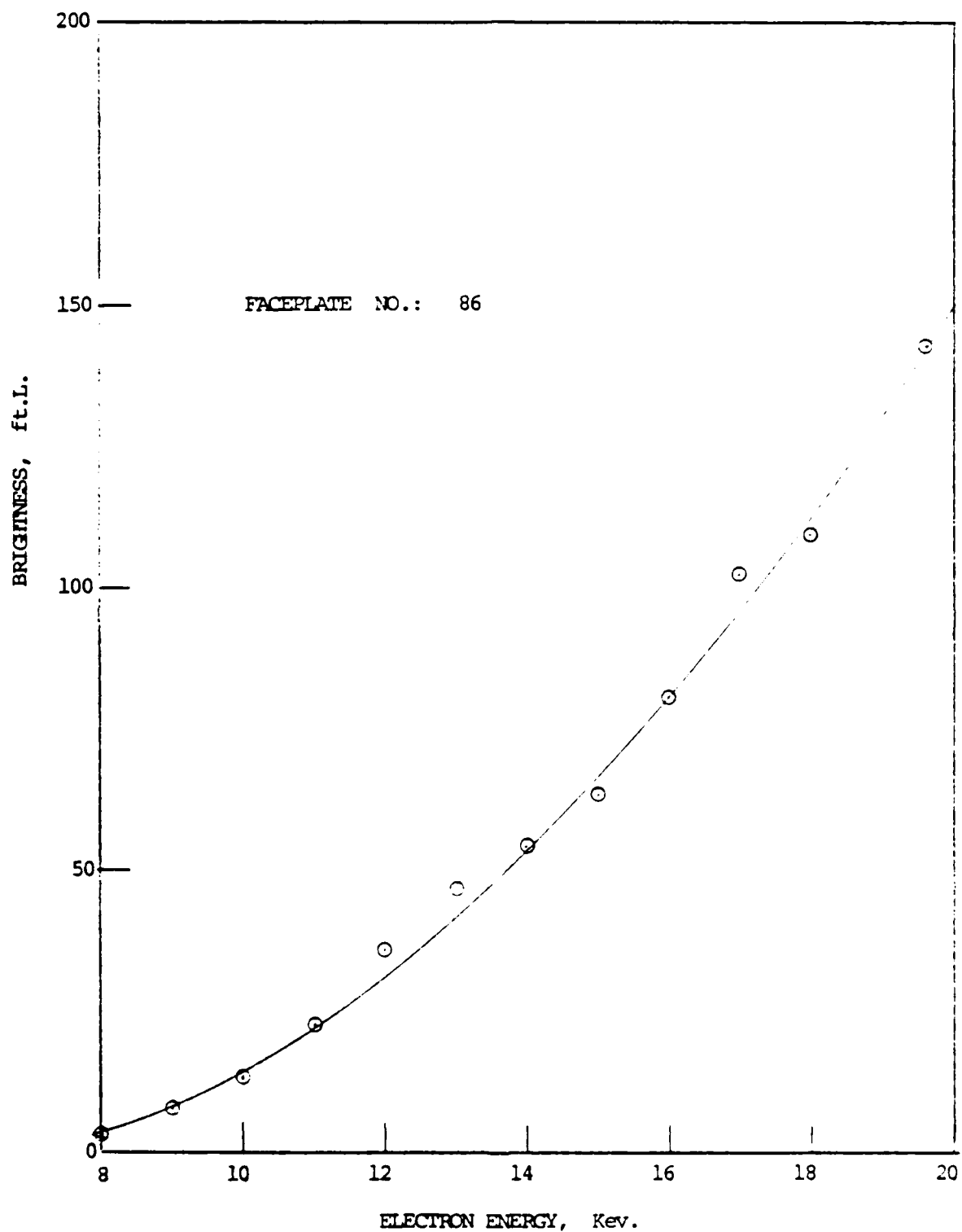


Fig. 13 Cathodoluminescence. Faceplate No. 86

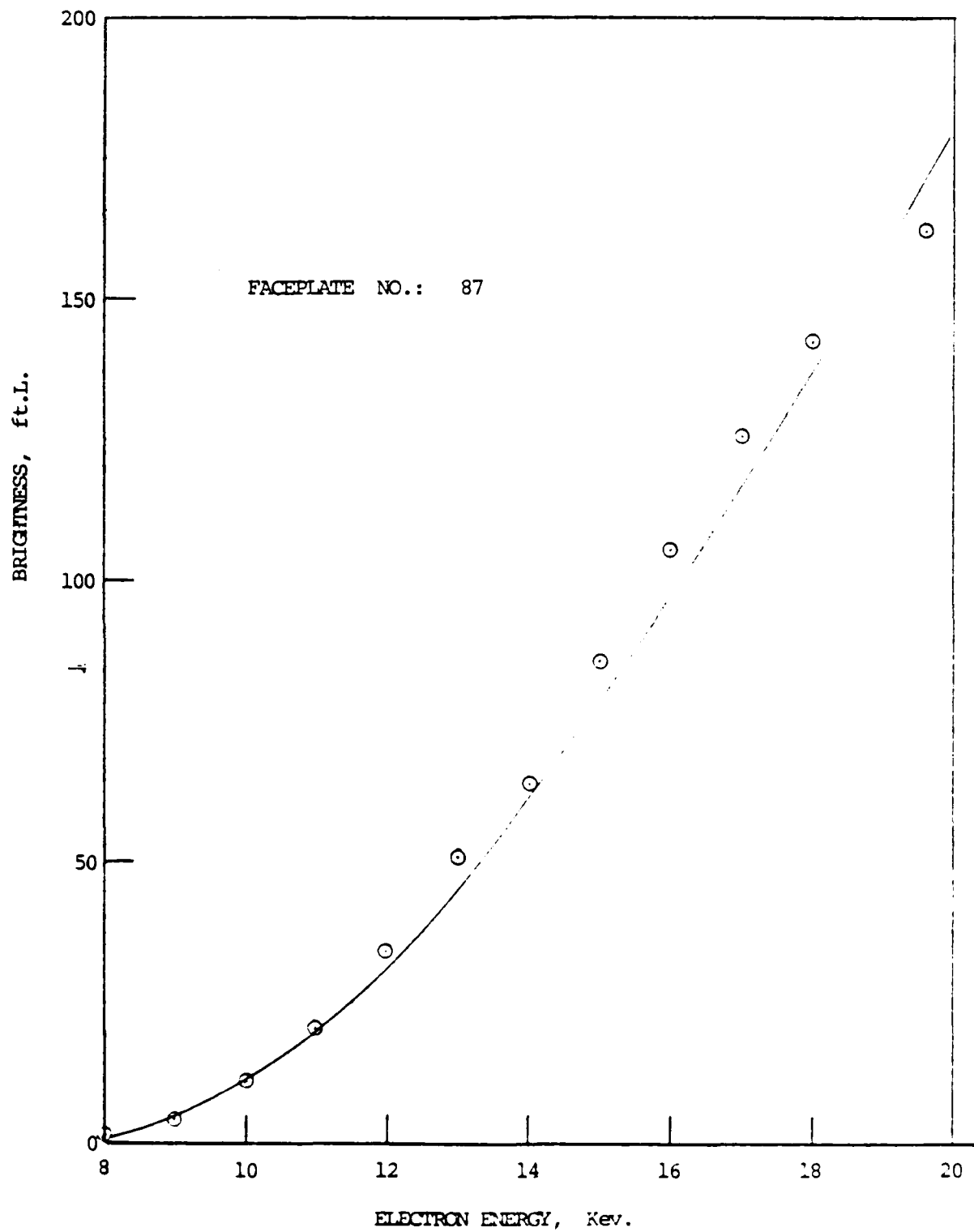


Fig. 14 Cathodoluminescence. Faceplate No. 87

In a cathodoluminescence measurement, the electron beam power density is limited by the minimum spot diameter obtainable and the emission current capability of the electron gun used. The electron gun used was of Einzel-focus type with a 6.3V, 450ma filament and oxide coated cathode. This gun was designed for use in a small CRT having a cathode to screen distance of nominally 4 to 5 inches, and was thus a potential component of the High Contrast CRT for which the faceplates of the present program were intended.

Because the minimum cathode to screen spacing of the demountable testing system was more than twice the above, the spot size obtained was larger than would be expected for a small CRT. The minimum spot diameter at 50 microamperes peak current was found to be about 0.035 in. Currents as great as 2 milliamperes were obtained by increasing the filament power in excess of the manufacturer's recommendation for short periods. All faceplates of the lot were measured at peak densities up to 100 watts/cm<sup>2</sup> and in some instances nearly twice the value. The Lot 5 measurements were made with a single line trace at a writing speed of 5,000 in/sec., refreshed at a 60 Hz rate, and a screen potential of 10 kV. For 10 kV, only the Eu<sup>3+</sup> red emission is to be expected. Study of the red emission was desirable because some previous measurements (Ref. 2) had suggested a possible saturation of the red phosphor film at high current densities.

The cathodoluminescent brightness was measured with a Spectra Pritchard Model 1980A-PL photometer, using the 6" aperture, the standard 7 in. lens plus supplementary SL-20 lens, and an ND-3 filter. Use of the ND-3 filter is necessary to avoid saturation of the photomultiplier tube in the photometer. The results are presented in Table 4 and summarized graphically in Figure 15. Figures 16 through 26 are plots for the individual faceplates of the lot. The brightness values are average brightness; peak brightness would be the average value multiplied by 1.47, the duty factor of the measurement (ratio of refresh time to beam "ON" time). The curves in Figure 15 are all concave upwards, and thus do not indicate saturation.

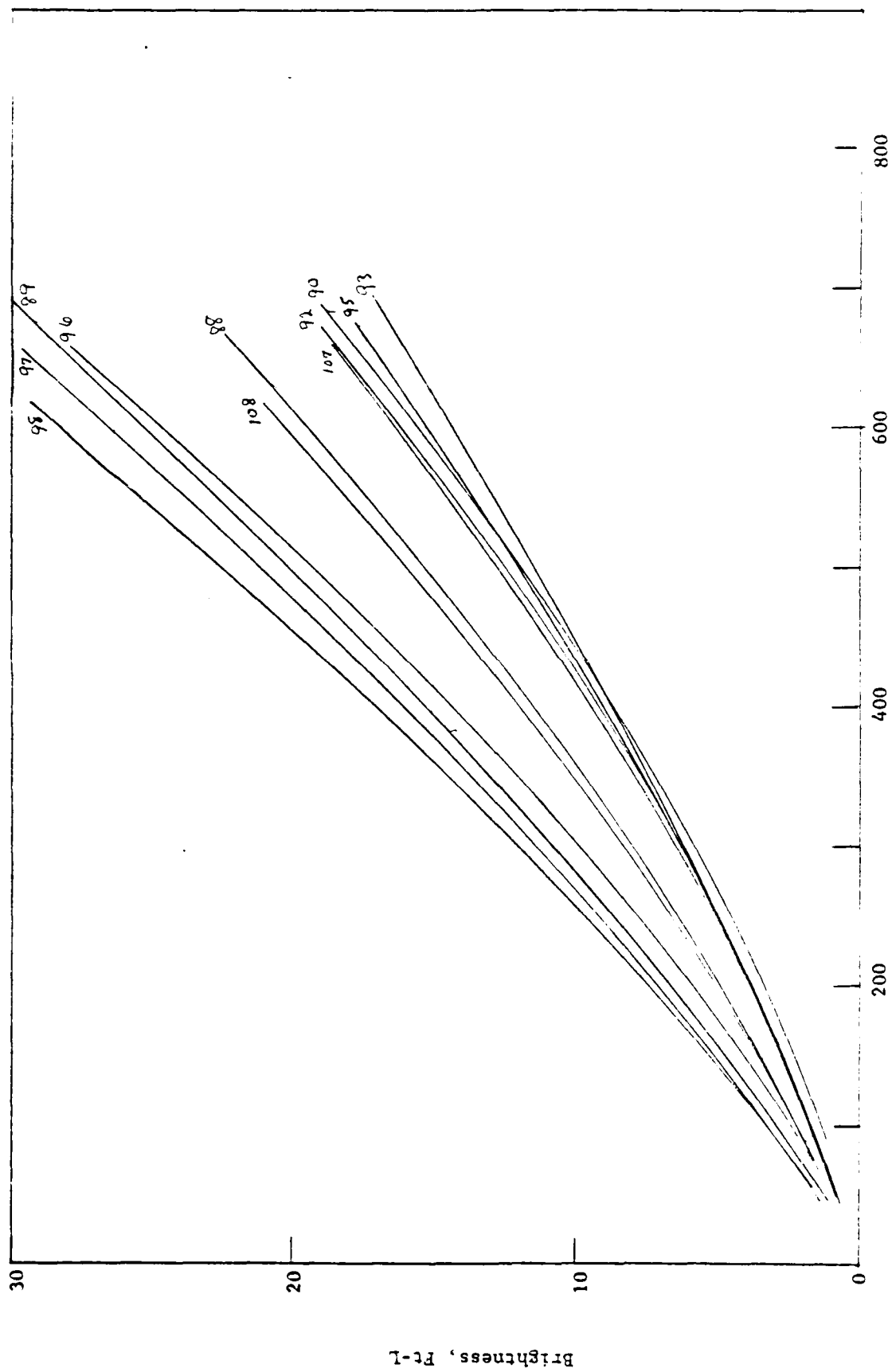
#### 4.2.3 Additional CL Measurements

To provide further information on the phosphor film characteristics, some additional measurements were made, as described in the following section.

Table 4  
Cathodoluminescent Brightness, Lot #5, in Ft. L.

| Average Current $\mu$ A      | 0.30 | 0.60 | 0.90 | 1.10 | 1.60 | 1.90 | 2.20 | 2.40 | 2.90 | 3.29 | 3.59 | 2.89 | 4.90 |
|------------------------------|------|------|------|------|------|------|------|------|------|------|------|------|------|
| Peak Screen Current, $\mu$ A | 50   | 100  | 150  | 200  | 267  | 317  | 367  | 400  | 484  | 550  | 600  | 650  | 818  |
| Faceplate 88 (E)             | 1.2  | 2.0  | 2.9  | 4.5  |      | 8.0  |      | 13.6 | 16.0 |      |      |      |      |
| Faceplate 89                 | 1.0  | 2.5  | 5.9  | 6.7  |      | 12.6 | 16.0 |      | 23.0 | 27.1 |      | 29.6 | 33.6 |
| Faceplate 90 (E)             | 1.0  | 1.5  | 2.2  | 3.5  | 4.9  | 5.8  |      | 9.5  | 11.4 | 13.3 | 16.0 | 17.4 |      |
| Faceplate 92                 | 1.0  | 1.8  | 2.8  | 4.0  | 5.4  | 6.8  | 8.7  | 10.2 | 12.2 | 14.2 | 16.0 | 18.3 |      |
| Faceplate 93 (E)             | 1.0  | 1.6  | 2.4  | 3.6  | 5.7  | 6.6  | 7.9  | 9.8  | 11.6 |      | 14.5 | 15.5 |      |
| Faceplate (E)                | 1.0  | 1.6  | 2.6  | 3.8  | 5.5  | 6.8  | 7.4  | 9.4  | 11.8 | 14.2 |      | 16.5 |      |
| Faceplate 96 (E)             | 1.1  | 2.4  | 3.9  | 5.9  |      | 10.7 | 13.1 | 14.6 | 19.6 |      |      |      |      |
| Faceplate 97 (E)             | 1.3  | 3.2  | 5.2  | 7.1  | 10.0 | 12.2 | 14.7 | 18.1 | 20.8 | 23.7 |      | 29.7 |      |
| Faceplate 98                 | 1.3  | 3.2  | 2.6  | 7.1  |      | 12.7 | 16.2 | 19.8 | 23.4 | 26.7 | 30.0 |      |      |
| Faceplate 107 (E)            | 1.0  | 1.9  | 2.6  | 4.0  | 5.9  | 6.9  | 8.4  | 10.4 | 12.4 | 14.5 |      | 18.5 |      |
| Faceplate 108 (E)            | 1.1  | 2.2  | 3.2  | 5.0  | 7.0  | 8.6  | 10.6 | 12.5 | 15.5 | 18.7 |      | 21.5 |      |

Electron Energy 10 Kv  
Spot Velocity 5,000 in./sec  
Linewidth 0.035 in.  
Trace Length 0.5 in.  
(E) - Delivered to ERADCOM



Peak Screen Current,  $\mu A$

Fig. 15 Cathodoluminescence Summary, Lot #5

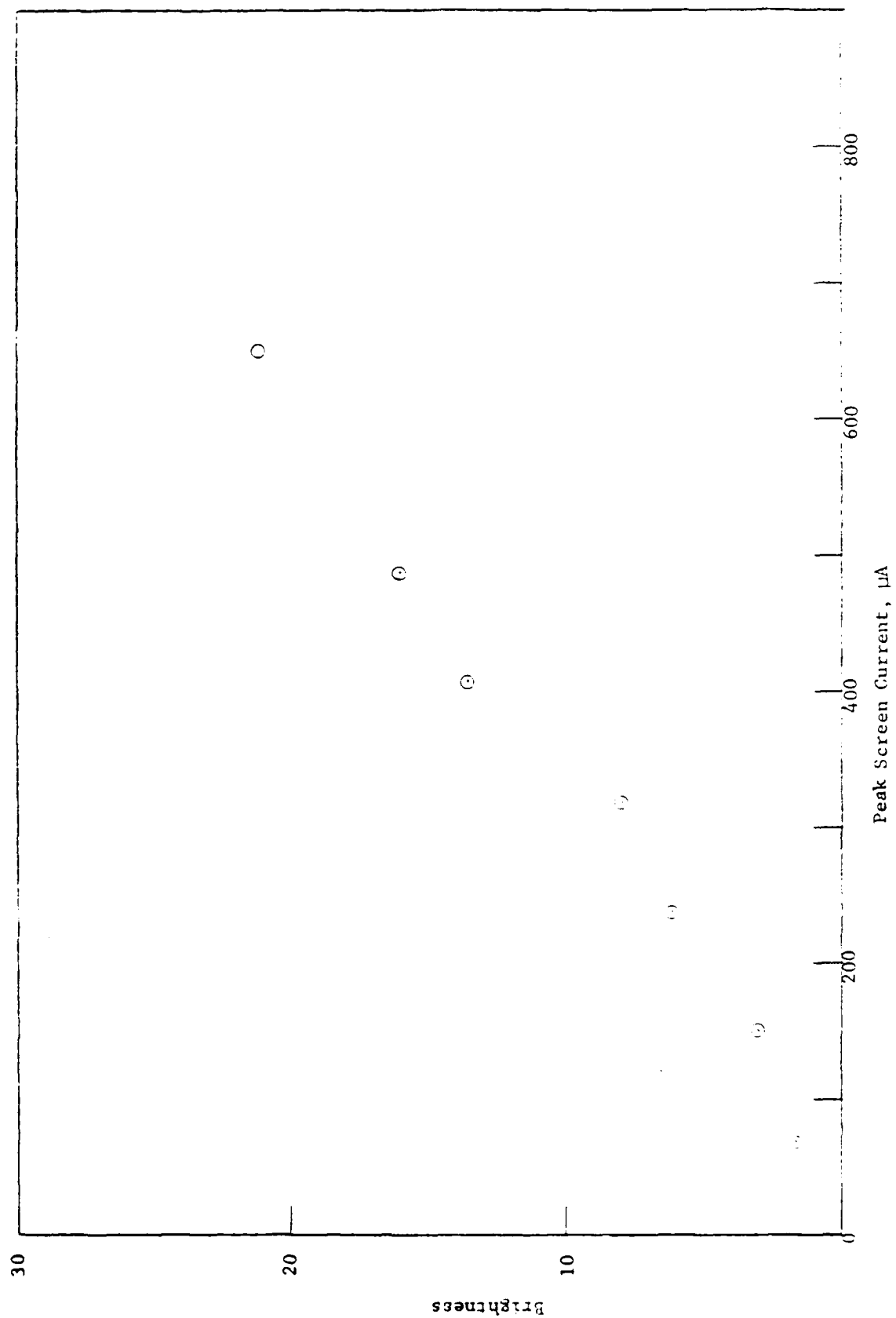


Fig. 16 Cathodoluminescence, Faceplate No. 88

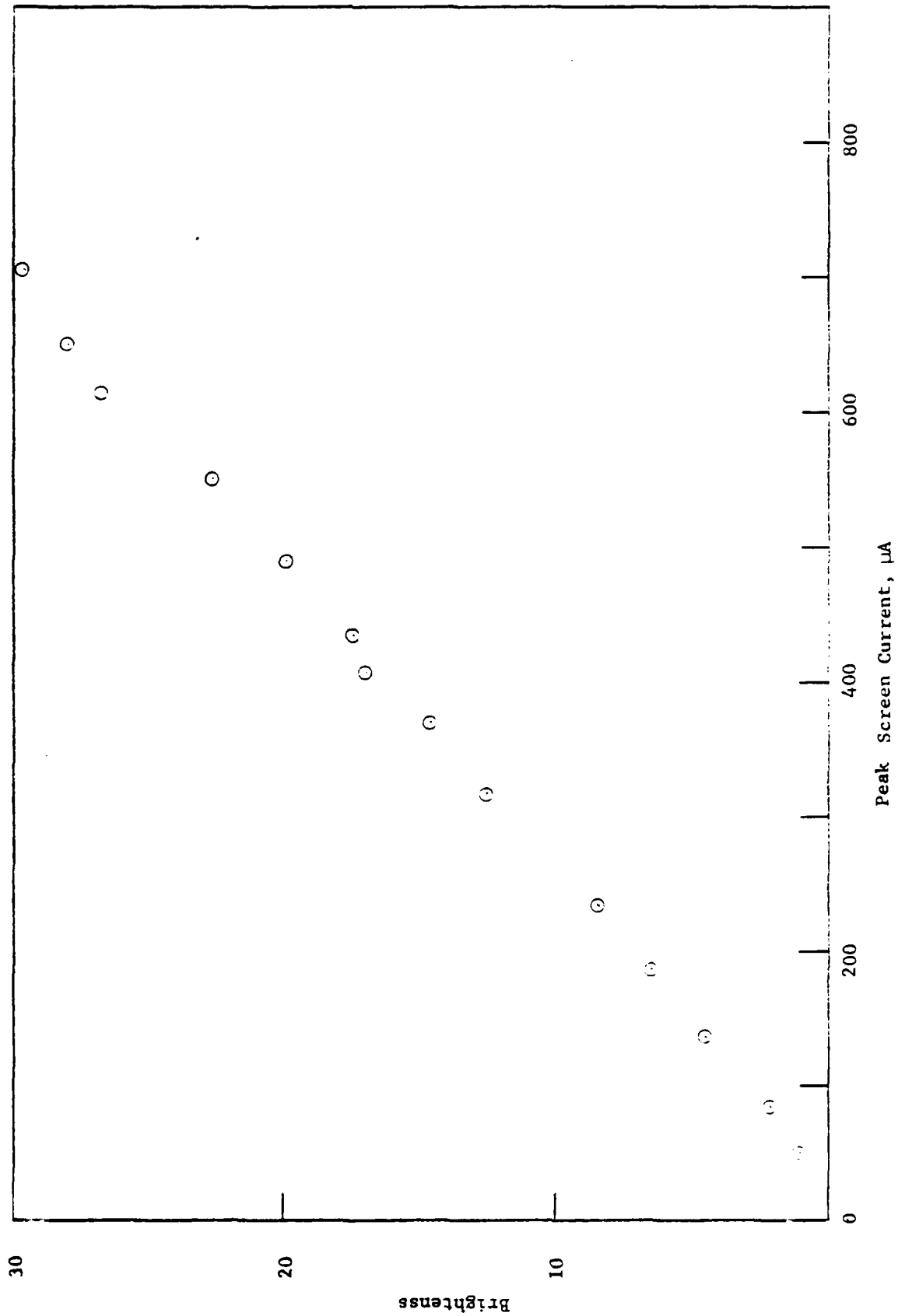


Fig. 17 Cathodoluminescence, Faceplate No. 89

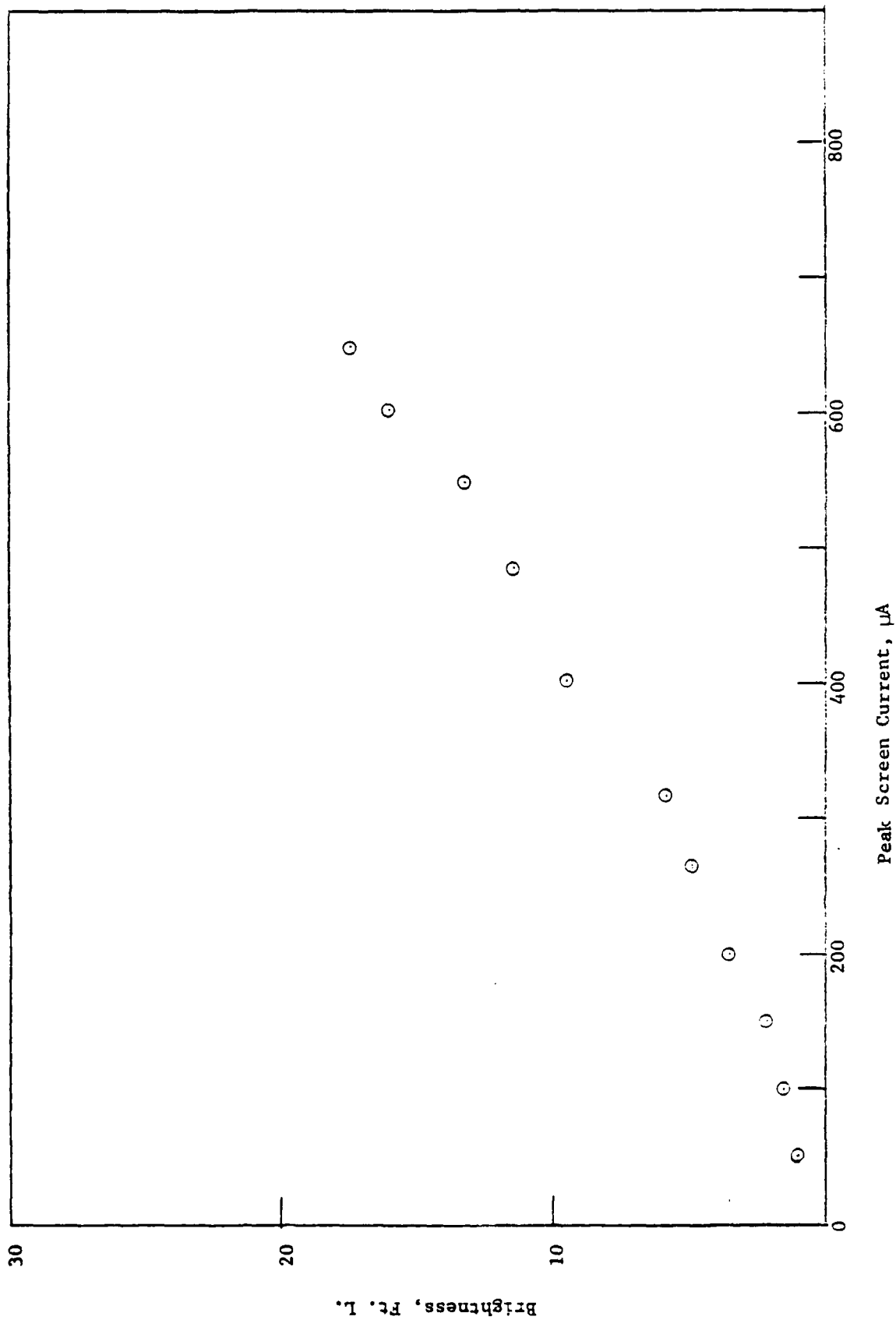


Fig. 18 Cathodoluminescence, Faceplate No. 90

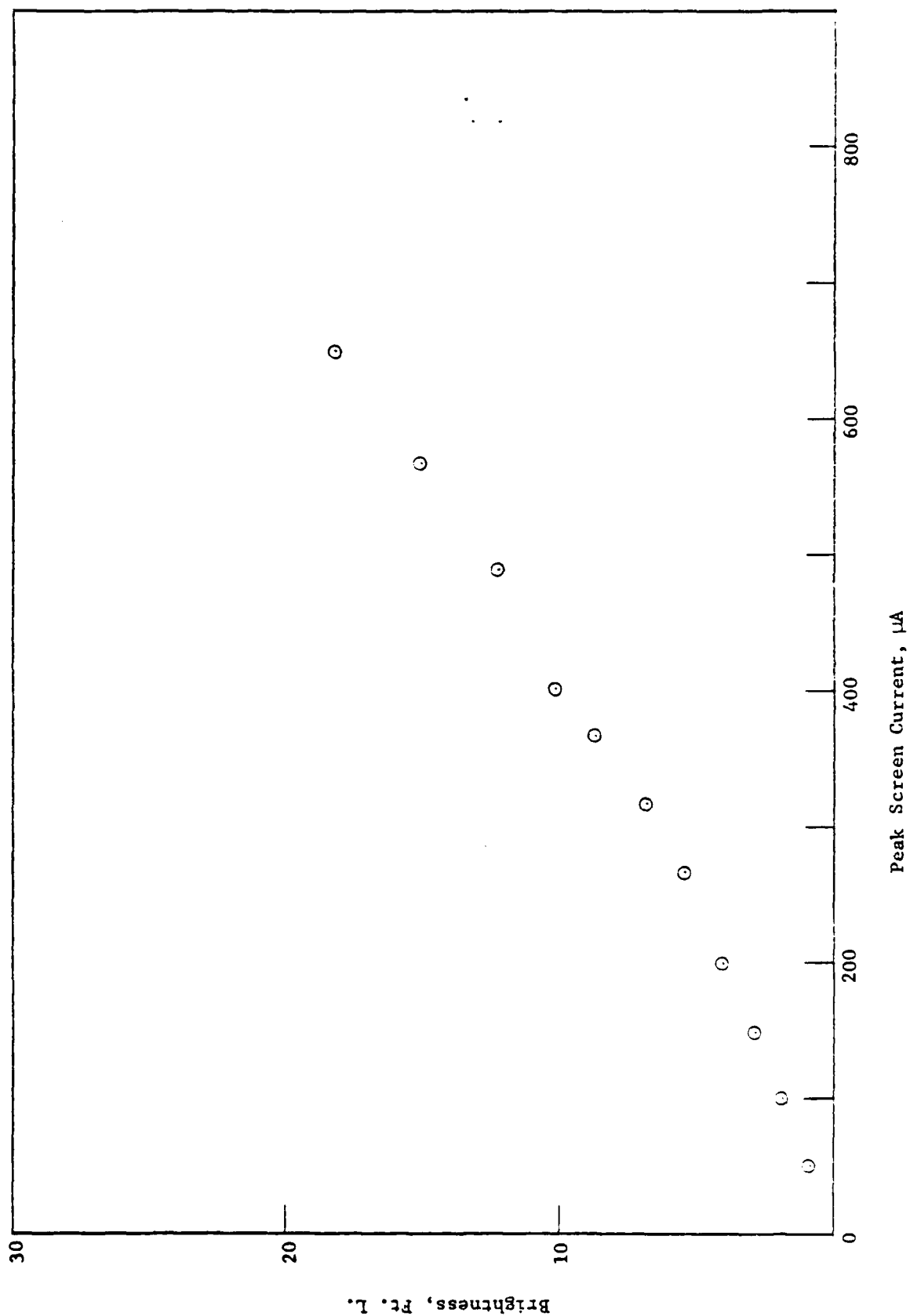


Fig. 19 Cathodoluminescence, Faceplate No. 92

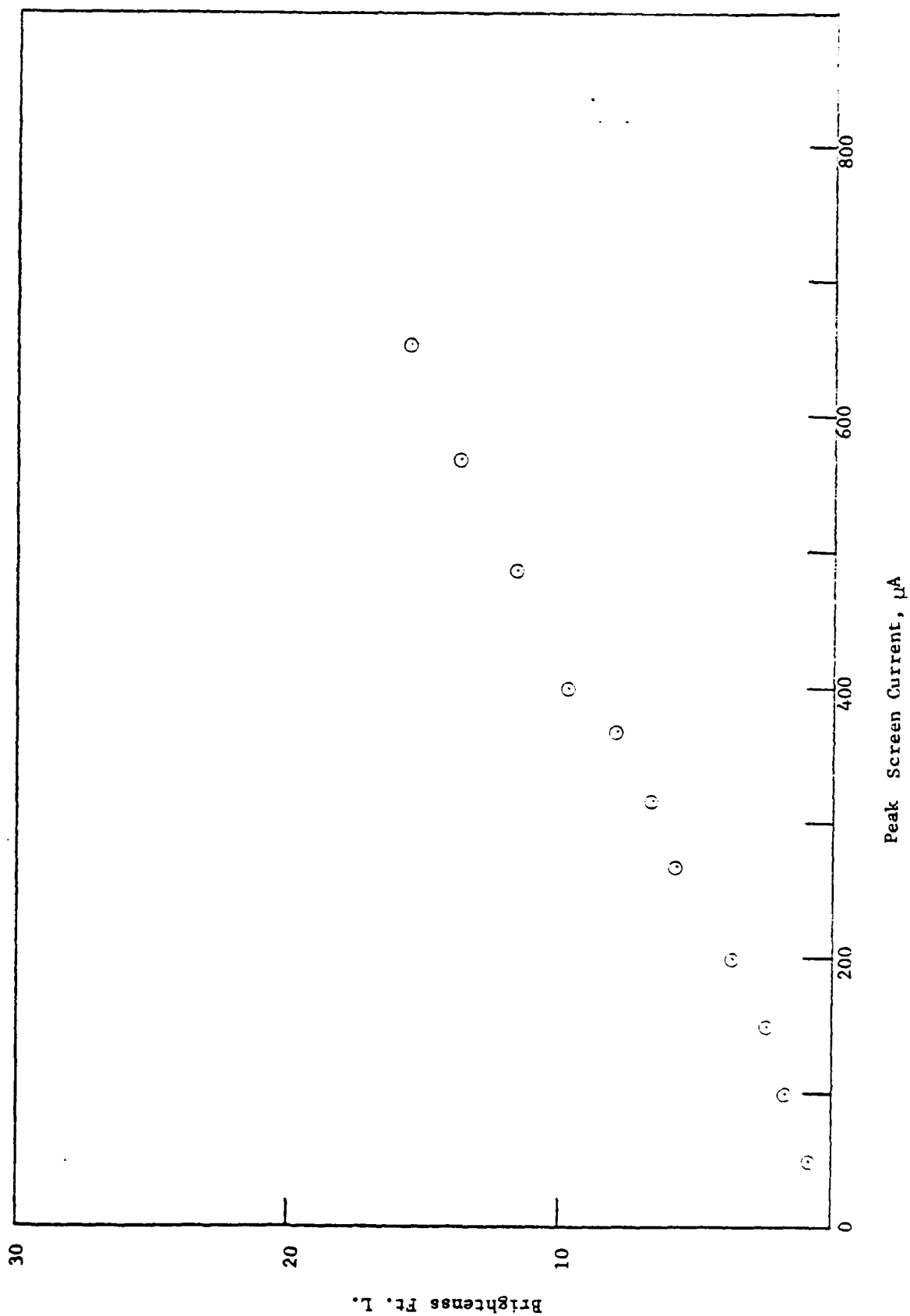


Fig.20 Cathodoluminescence, Faceplate No. 93

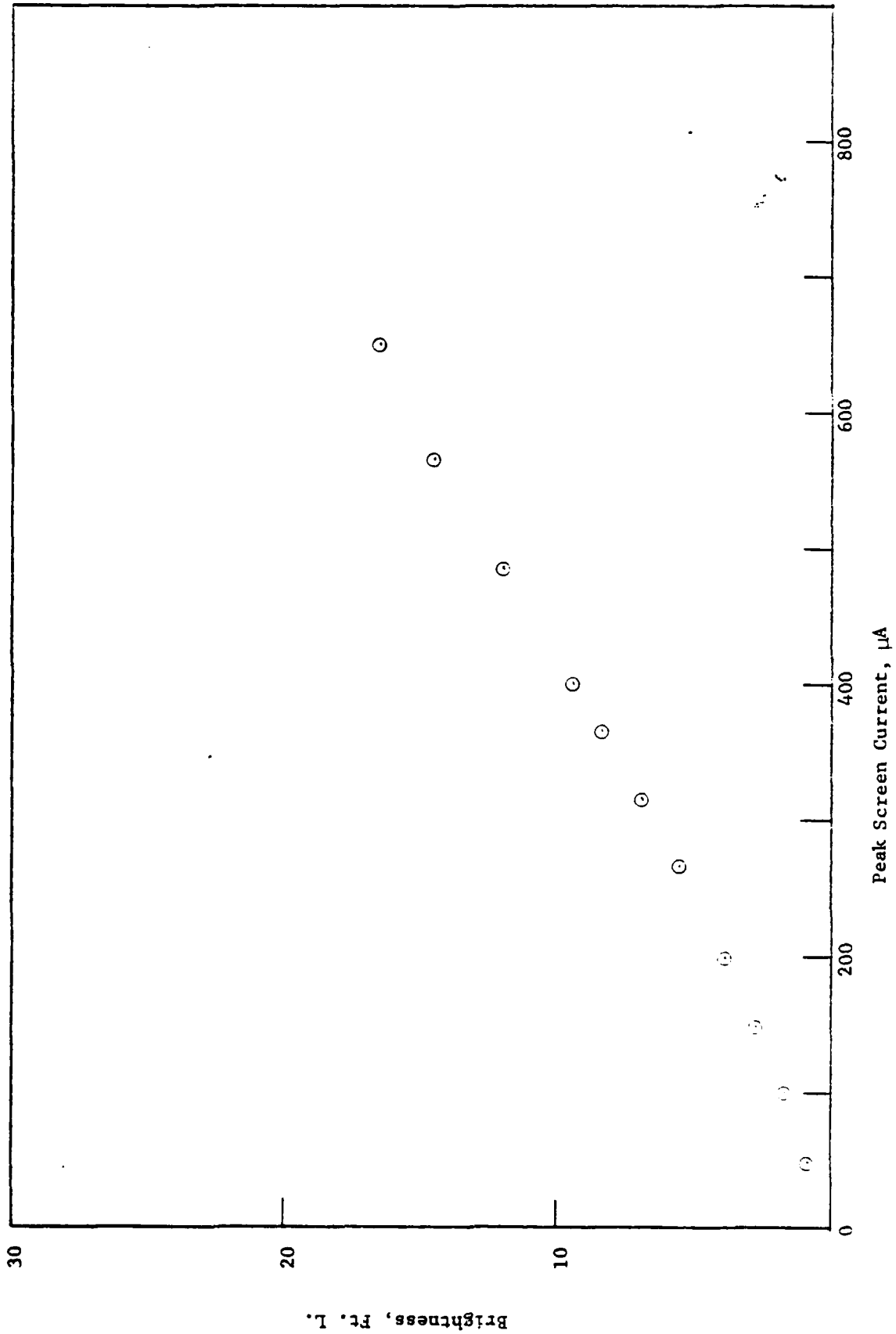


Fig.21 Cathodoluminescence, Faceplate No. 95

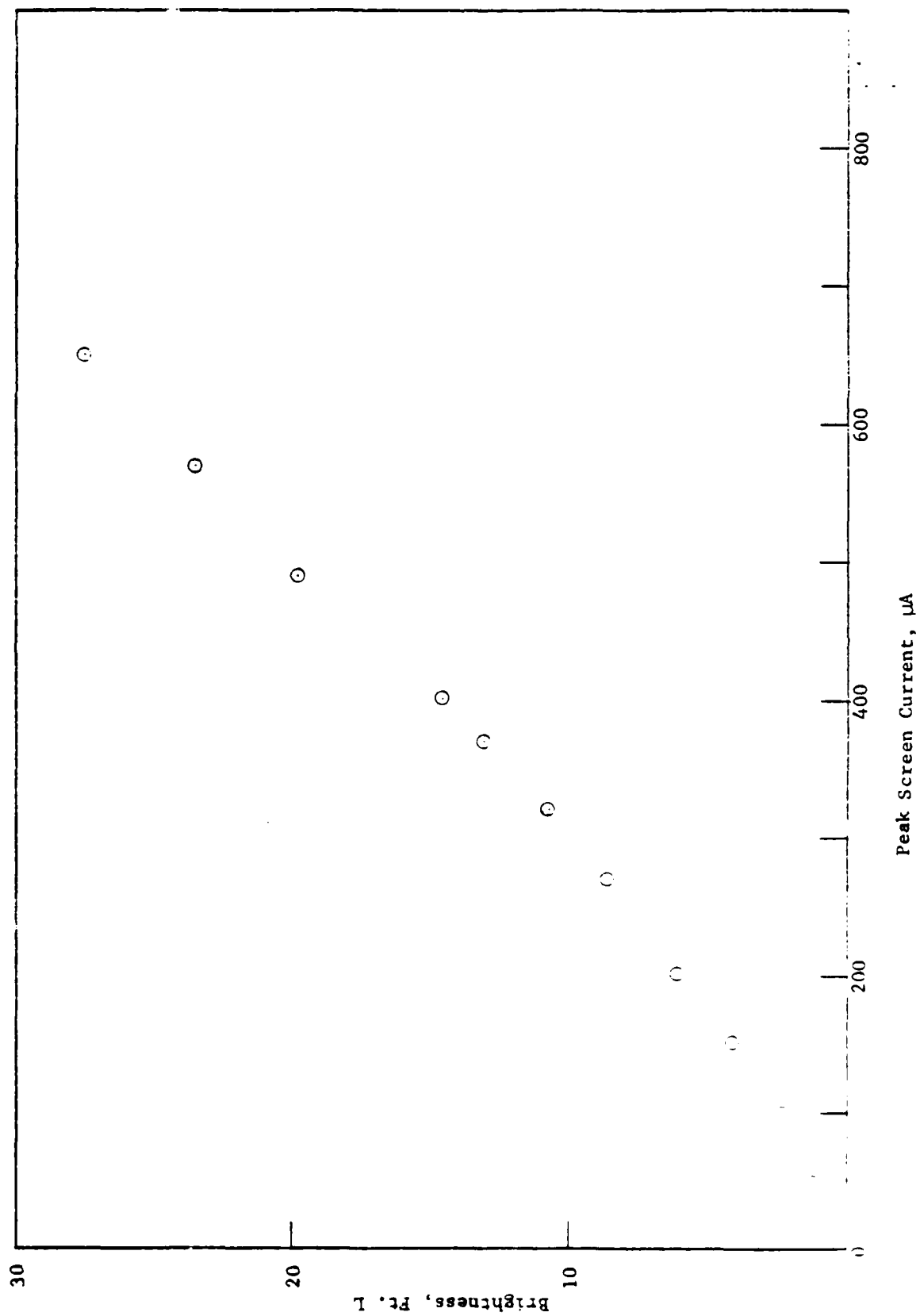


Fig. 22 Cathodoluminescence, Faceplate No. 96

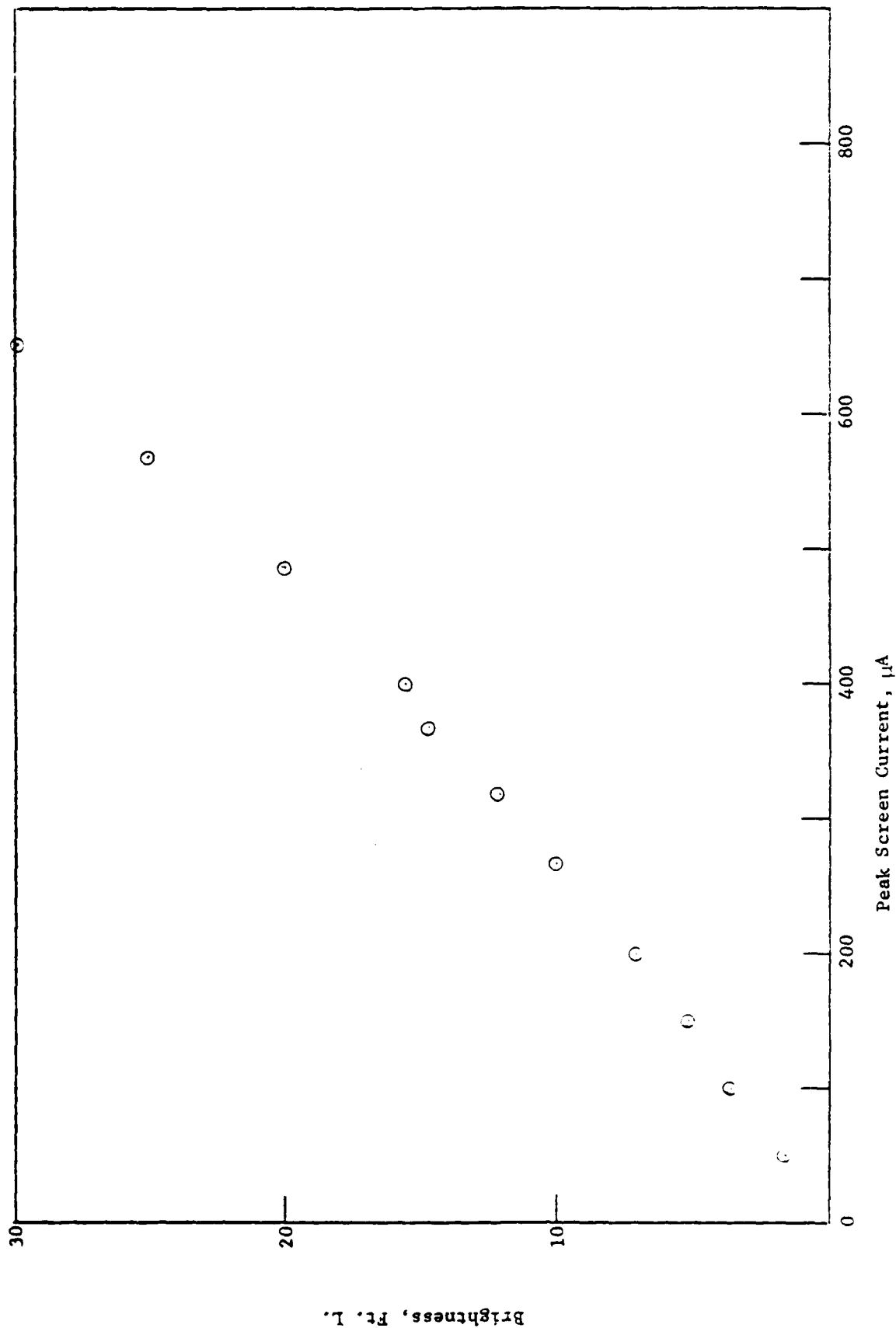


Fig.23 Cathodoluminescence, Faceplate No. 97

Brightness, Ft. L.

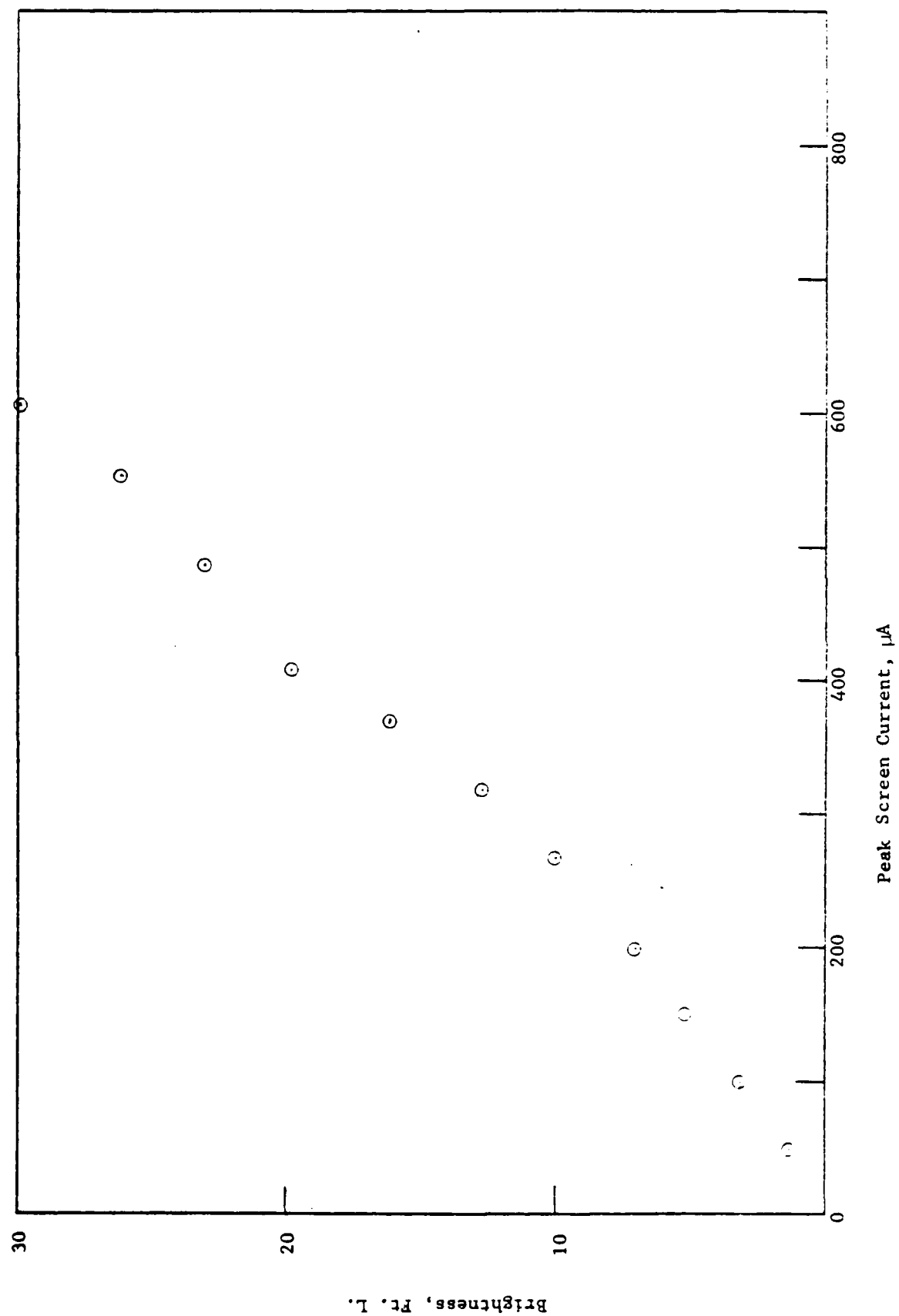


Fig. 24 Cathodoluminescence, Faceplate No. 98

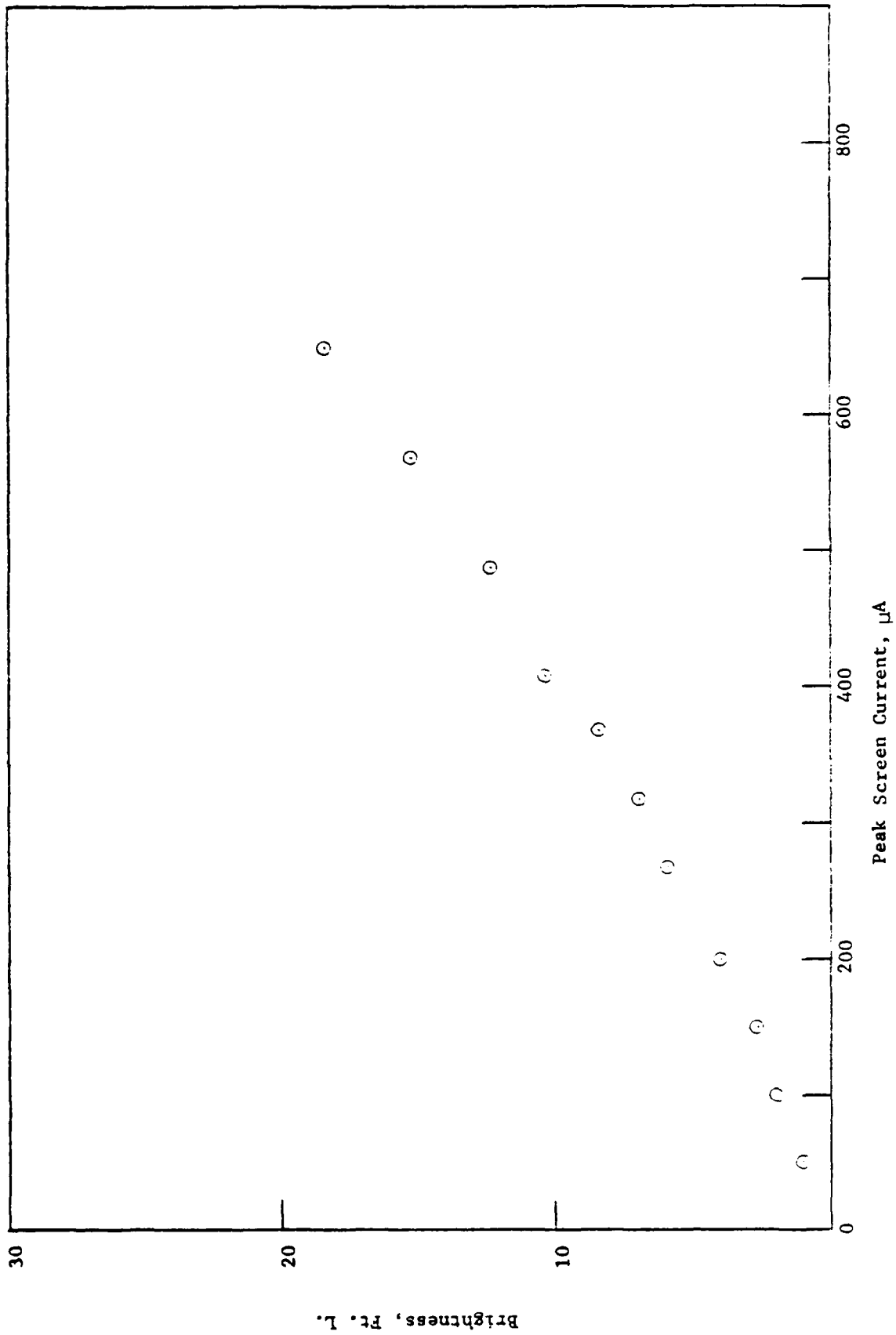


Fig.25 Cathodoluminescence, Faceplate No. 107

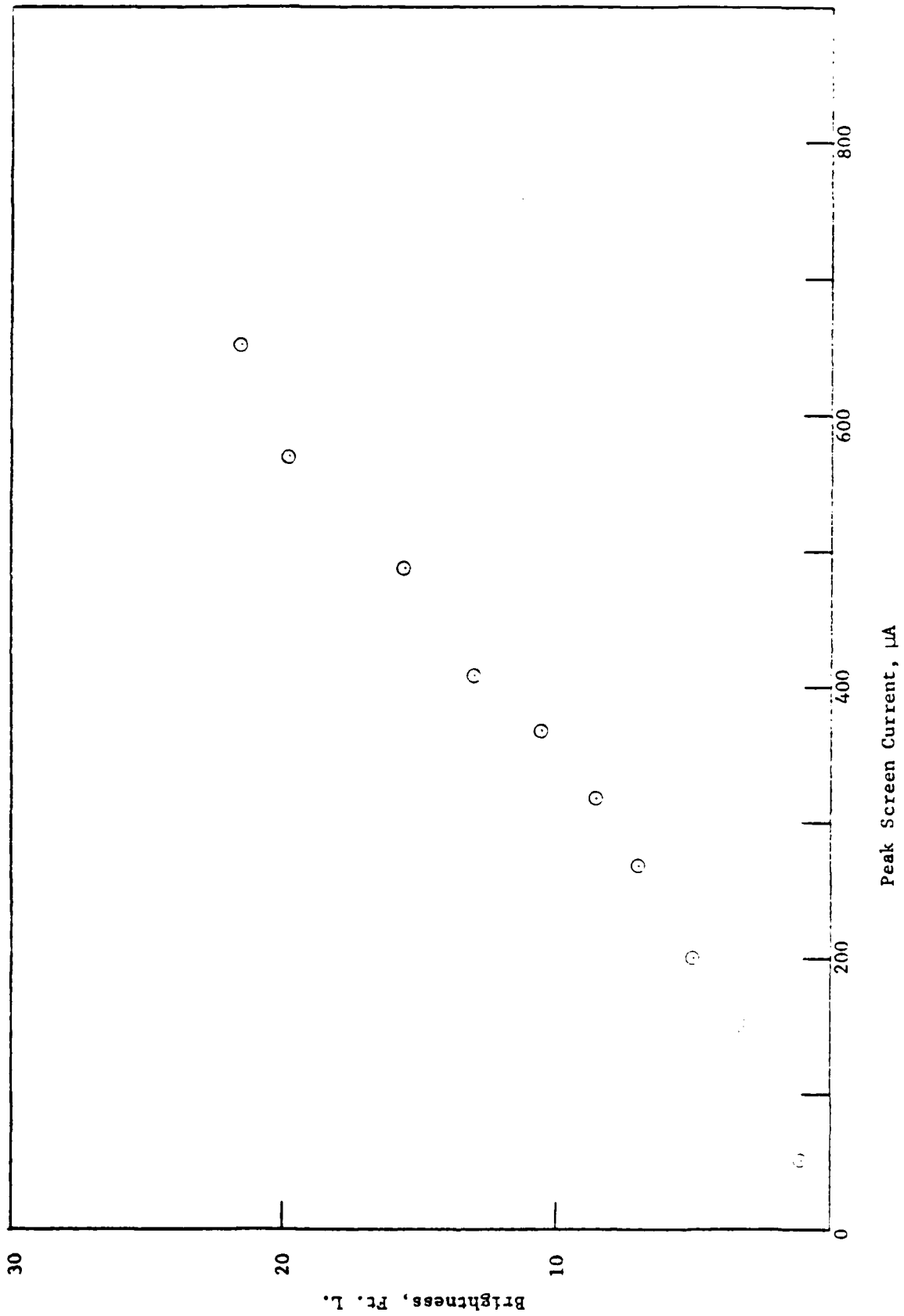


Fig.26 Cathodoluminescence, Faceplate No. 108

#### 4.2.3.1 Brightness vs. "ON" Time

In the absence of any saturation effect, when a given area of phosphor is repeatedly excited by a pulsed electron beam, the average brightness should be a linear function of the beam "ON" time. Thus, if the peak brightness is  $B_{pk}$ , the "ON" time is  $t_{ON}$ , the refresh rate is  $f_r$ , the duty factor is  $F_d$ , the average brightness  $B_{av}$  should be

$$\begin{aligned} B_{av} &= f_r t_{ON} B_{pk} \\ &= \frac{t_{ON}}{t_r} B_{pk} = F_d B_{pk} \end{aligned}$$

where

$$t_r = \frac{1}{f_r} \quad \text{and} \quad F_d = f_r t_{ON}.$$

Measurements were made on sapphire faceplate No. 87 to determine if the faceplate did indeed exhibit the expected relationship. Experimental conditions were screen potential 10 kV, peak screen current 410 microamperes, gated on for various times with a square wave pulse at a 60 Hz refresh rate. The beam was not deflected. The spot diameter was 0.10 in. Brightness was measured with the Spectra Pritchard Model 1980A-pL photometer using a 30' aperture (0.11 in. dia.) and an ND-3 filter. Under these conditions, the current density and power density were  $8.1 \text{ mA/cm}^2$  and  $8.1 \text{ watts/cm}^2$ , respectively.

Results are shown in Table 5 and Figure 27. The plot is seen to be linear from 400 microseconds upward. Below, it deviates from a straight line. The deviation can be ascribed to a rise time effect, in accordance with the following equation:

$$I_t = (1 - e^{-t/\tau}) I_\infty$$

where  $I_t$  is the brightness at time  $t$ ,  $I_\infty$  is the final brightness for an extended "ON" time, and  $\tau$  is the rise time. This relationship is shown graphically in Figure 28. It is seen that the brightness attains

Table 5  
Brightness vs. "ON" Time

| $t_{on}$ , sec. | $F_d$ Duty Factor | $I_{av}$ , mA | Brightness, Ft-L |
|-----------------|-------------------|---------------|------------------|
| 20              | 0.0012            | 0.5           | 3.84             |
| 40              | 0.0024            | 1.0           | 6.83             |
| 60              | 0.0036            | 1.5           | 9.65             |
| 80              | 0.0048            | 1.9           | 11.8             |
| 100             | 0.0060            | 2.4           | 13.9             |
| 120             | 0.0072            | 2.9           | 15.8             |
| 140             | 0.0084            | 3.3           | 17.8             |
| 160             | 0.0096            | 3.9           | 19.7             |
| 180             | 0.0108            | 4.3           | 21.7             |
| 200             | 0.012             | 4.8           | 23.7             |
| 300             | 0.018             | 7.5           | 33.7             |
| 400             | 0.024             | 9.8           | 42.4             |
| 500             | 0.030             | 12.3          | 51.5             |
| 600             | 0.036             | 14.8          | 60.3             |
| 700             | 0.042             | 17.1          | 69.1             |
| 800             | 0.048             | 19.5          | 77.7             |
| 900             | 0.054             | 22.0          | 86.5             |
| 1000            | 0.060             | 24.5          | 95.6             |

Rated - undeflected spot

Refresh rate - 50 Hz

Spot Dia. - 0.1 mm

Voltage - 300 V

98 percent of the final brightness in 4 time constants. Thus we estimate the rise time of the phosphor as about 100 microseconds for the given current density. This is consistent with a known decay time for the  $^5D_0$  (red) emission of  $La_2O_2W:Eu$  (Ref. 3) of about 350 microseconds, rise times of phosphors being usually shorter than decay times.

#### 4.2.4 Sample to Sample Variation, Lot #5

Figure 15 indicates a considerable sample to sample variation between faceplates of Lot #5. The reason for this variation is not understood, and is rather surprising because additional measures had been taken during fabrication of Lot 5 with the view of attaining greater reproducibility than for previous lots. A timer was connected to the RF power supply to terminate deposition of the  $La_2O_2S:Eu$  layer at precisely 55 minutes for each run, and this is reflected in the identical run times shown in Table 2. Each run was performed at 300 watts RF and care taken to adjust the impedance match frequently during the run and thus maintain a constant deposition rate. Unfortunately, difficulties have been experienced with RF leaking into the op amp of the laser thickness monitor despite extensive filtration, so it was not possible to confirm that identical  $La_2O_2S:Eu$  layer thicknesses were obtained.

A slight variation in sulfurization treatment times is shown in Table 2, but the largest variation is only six percent of the treatment time, so it is doubtful that the variation in luminescent brightness of the Lot 5 faceplates can be accounted for by this factor. We can only conclude that there is some unidentified factor associated with the deposition or treatment process responsible for the variation. In the interests of reproducibility and optimization of the faceplates, it would be desirable to identify the factor.

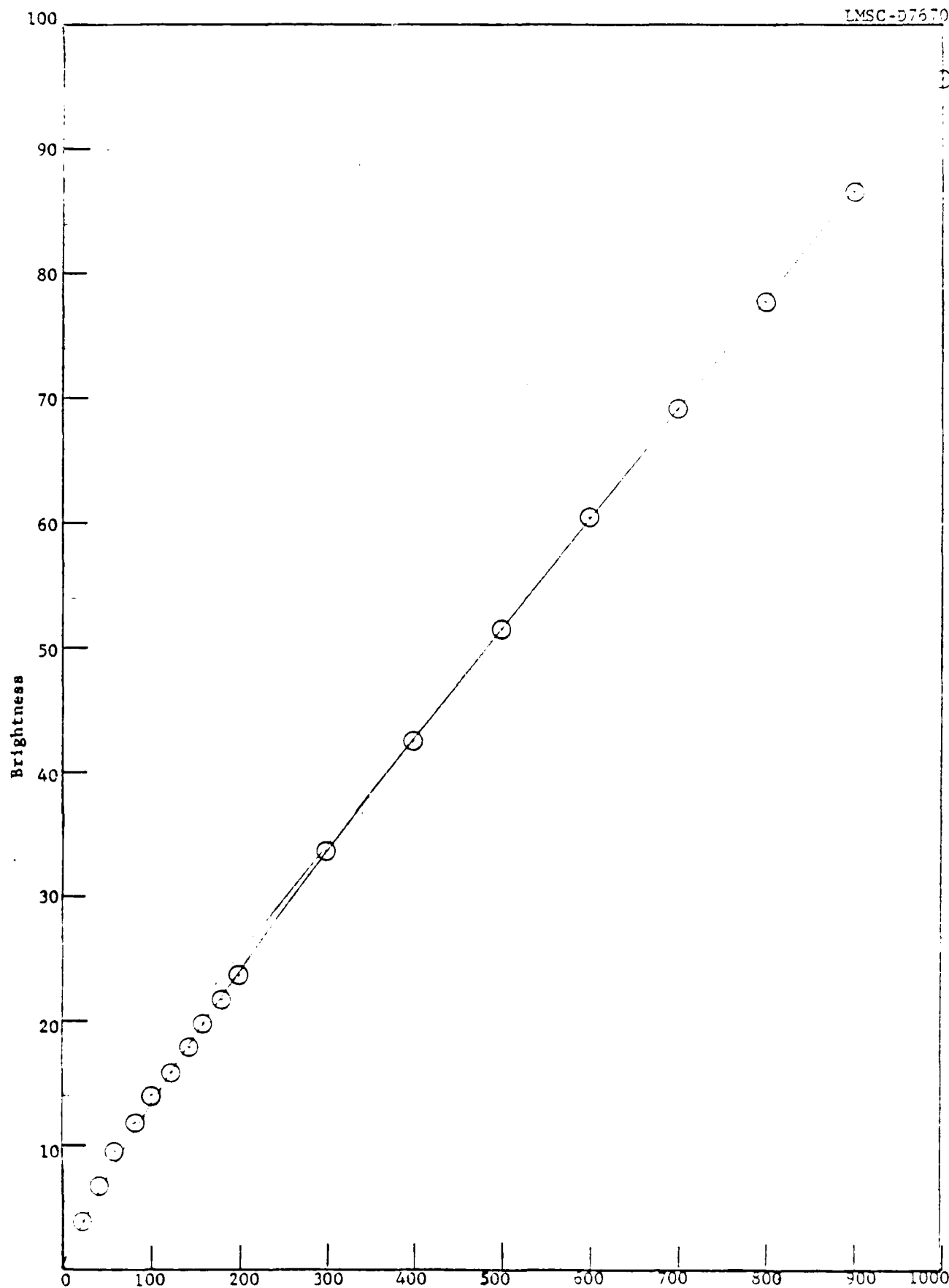


Fig. 27 Brightness vs. "ON" Time

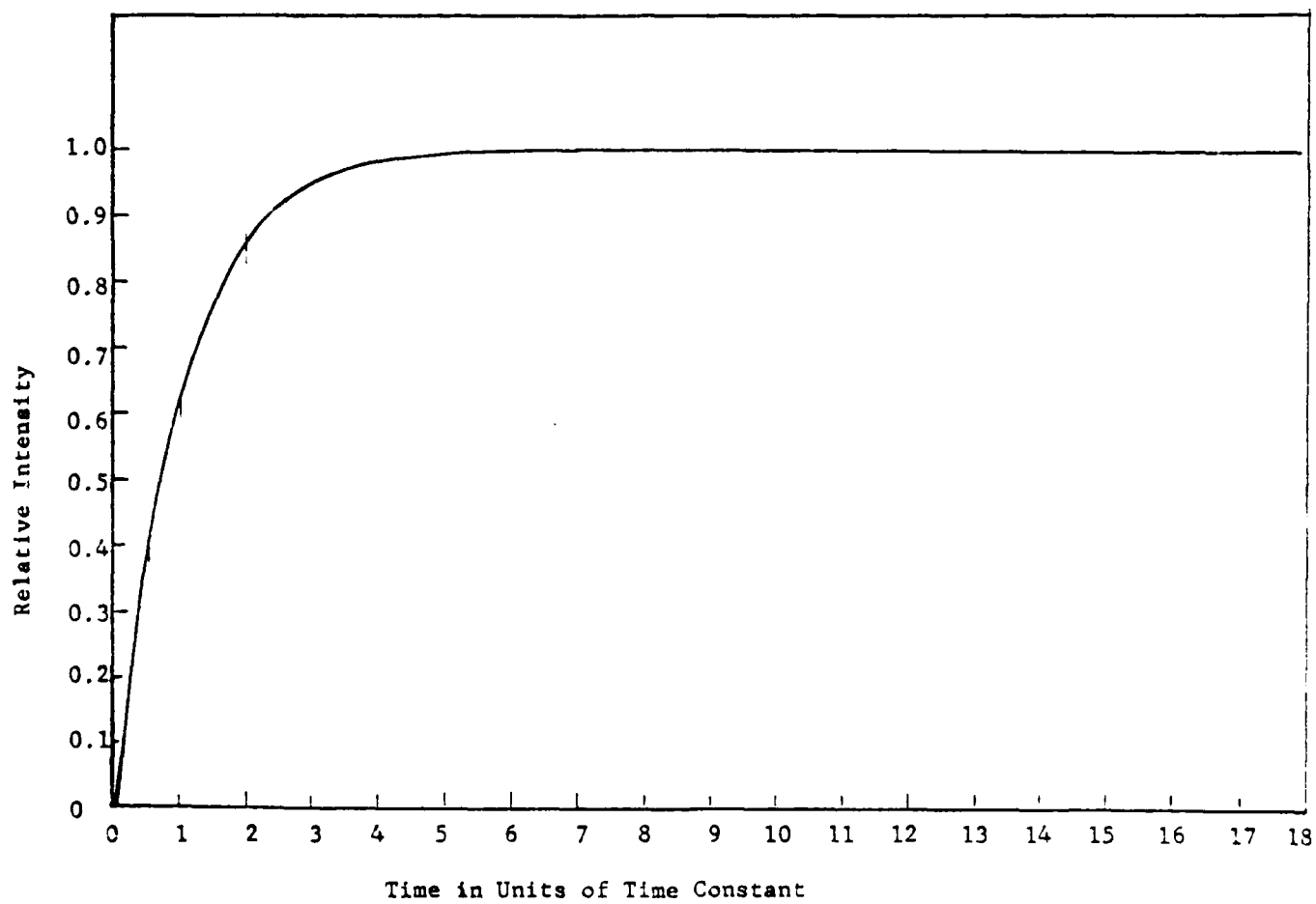


Fig.28 Relative Intensity as a Function of Rise Time

## 4.2.3.2 Comparison of 1720 Glass with Sapphire Substrates

Measurements were made on a faceplate fabricated on 1720 glass and on one fabricated on sapphire using a TV-type raster 0.5 in. x 0.5 in. with a screen potential of 10 Kv and average screen current of 180 microamperes. The brightness was measured just after the display was turned on, and again 30 seconds later. Results in terms relative to initial brightness are shown in Table 6.

Table 6  
1720 Glass vs. Sapphire Substrate

| <u>F.P. No.</u> | <u>Substrate</u> | <u>Initial</u> | <u>Relative Brightness % 30 sec.</u> |
|-----------------|------------------|----------------|--------------------------------------|
| 39              | 1720 Glass       | 100            | 60.3                                 |
| 87              | Sapphire         | 100            | 95.7                                 |

As indicated in the table, the brightness of the sapphire faceplates remained essentially unchanged in time; whereas that of the 1720 faceplate decreased substantially within 30 sec. Very little further reduction in brightness occurred for extended times.

The effect was reproducible. As it is known that much of the energy of an electron beam incident on a phosphor appears as heat and the thermal conductivity of sapphire is superior to that of glass, it appeared that the decrease in brightness of the 1720 faceplate might be due to thermal quenching of the phosphor on the 1720 faceplate.

It is known that the cathodoluminescent emission of oxysulfide phosphors undergoes thermal quenching at elevated temperatures. For  $\text{La}_2\text{O}_2\text{S}:\text{Eu}$  the thermal quenching is in the sequence  $^5\text{D}_2$ ,  $^5\text{D}_1$ ,  $^5\text{D}_0$  as shown in Fig. 29 (Ref. 3) so that a shift in color toward the red would be expected.

The question arises whether significant thermal quenching might be expected to occur when the phosphor film of the faceplate is subjected to a high current density electron beam.

Although the heat capacity of lanthanum oxysulfide has not been measured, that for  $\text{La}_2\text{O}_3$  is known to be 24.2 cal/mol at room temperature. That of  $\text{La}_2\text{O}_2\text{S}$  should not differ greatly from that of  $\text{La}_2\text{O}_3$ . The law of Dulong and Pettit states that  $C_v = 3nR$  Cal/mol where  $n$  is the number of atoms per molecule and  $R$  is the gas constant ( $\approx 2$ ), so an expected value of 30 cal/mol is probably a close estimate of the true heat capacity of  $\text{La}_2\text{O}_2\text{S}$ . This value when divided by the molecular weight (341.88), corresponds to a specific heat of  $8.775 \times 10^{-2} \text{ cal-gm}^{-1} \text{ } ^\circ\text{C}^{-1}$ .

The area of an 0.5 in. x 0.5 in. TV raster is  $0.25 \text{ in.}^2$  or  $1.613 \text{ cm}^2$ . The mass of phosphor film in the raster area is

$$m = Ad\rho$$

where

$A$  is the area,  $d$  the thickness, and  $\rho$  the density of the film. Assuming the film has the bulk density of  $\text{La}_2\text{O}_2\text{S}$ ,  $5.73 \text{ g/cm}^3$ , the mass of a  $4000 \text{ \AA}$  thick film of  $\text{La}_2\text{O}_2\text{S:Eu}$  is

$$m = 1.613 \times 4 \times 10^{-5} \times 5.73 = 3.697 \times 10^{-4} \text{ grams.}$$

For a 10 Kv beam and screen current of 180  $\mu\text{A}$ , the energy  $W$  delivered to the raster during ea. 60 Hz cycle is

$$W = VI/60$$

$$= 1 \times 10^4 \times 180 \times 10^{-6}/60 = 3 \times 10^{-2} \text{ joule}$$

$$= 3 \times 10^{-2} \times 0.23906 = 7.17 \times 10^{-3} \text{ cal.}$$

Assuming no energy is transferred to the substrate during the instant the beam is incident on a given point of the raster, the instantaneous temperature rise of the film is given by

$$\Delta T = W/cm$$

where  $c$  is the specific heat of the film.

The instantaneous temperature rise is then

$$\Delta T = \frac{7.17 \times 10^{-3}}{8.775 \times 10^{-2} \times 3.697 \times 10^{-4}} = 221^{\circ}\text{C}$$

The calculated value of  $\Delta T$  is an upper limit. The actual temperature rise will be lower because the energy is not delivered instantaneously; the beam has a finite diameter and thus a finite time will be required for the beam to traverse a given point. During this finite time, some energy will be transferred to the substrate.

If the thermal conductivity of the substrate is sufficiently large, the energy is dissipated throughout the massive substrate and produces in insignificant temperature rise. If the conductivity is small, there will be a significant localized temperature increase of the substrate under the trace which can be reinforced by subsequent pulses. In the latter event, the phosphor film might experience a temperature rise of  $100^{\circ}\text{C}$  or more, resulting in appreciable thermal quenching. The thermal conductivity of light borate crown glass (composition similar to 1720 glass) is  $1.7 \times 10^{-3}$ , while that of sapphire is  $1.1 \times 10^{-1}$  cal/cm sec. $^{\circ}\text{C}$ , nearly two orders of magnitude greater.

It can be seen in Figure 29 that thermal quenching of emission from the  $^5D_1$  state of  $La_2O_2S:Eu$  begins at room temperature and becomes substantial at  $100^\circ C$ .

We conclude that the difference in behavior of the 1720 and sapphire faceplates is attributable to the poor thermal conductivity of the former as compared with the latter. As a result, the 1720 faceplate experiences a substantial temperature increase, producing significant thermal quenching of the luminescence. In the case of sapphire, however, the heat is dissipated sufficiently rapidly that negligible increase in temperature of the phosphor film takes place and thermal quenching is not a problem.

This test demonstrates a very significant advantage of sapphire as faceplate substrate.

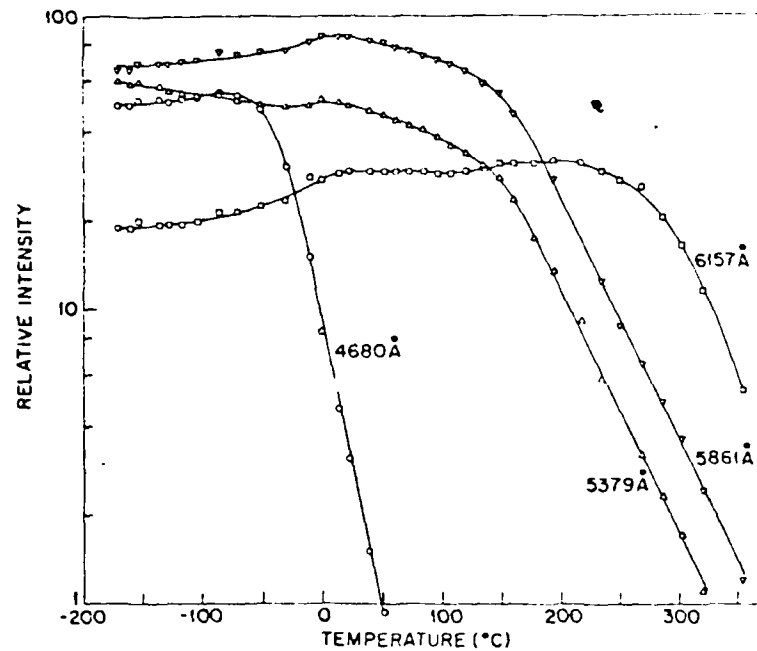


Fig. 29 Thermal Quenching of  $\text{La}_2\text{O}_2\text{S:Eu}$  Luminescence

Intensities of selected emission lines as a function of temperature. The 4680Å line originates from the  $^3\text{D}_2$  state, the 5379 and 5861Å lines from the  $^3\text{D}_1$  state and the 6157Å line from the  $^3\text{D}_0$  state. Ultraviolet excitation was used to obtain these data.

### 4.3 OPTICAL REFLECTANCE MEASUREMENTS

#### 4.3.1 Lot 1

The plots of the bidirectional optical reflectance measurements on Lot 1 (see Second Interim Report, DELET-TR-79-0282-2, May, 1980) showed a broad maximum at the specular reflection angle, contrary to an expected sharp peak. Also, no tails characteristic of diffuse reflectance as previously found in ERADCOM measurements, were observed. It was concluded that the broad peak was due to insufficient collimation of the incident light beam. The measurement assembly was subsequently modified, as described in the Second Interim Report, to provide improved collimation. The expected sharp peaks and tails were observed for Lots 2 and 3.

To allow comparison with the subsequent lots, the reflectance of Lot 1 was re-measured using the modified assembly. The results are summarized in Table 7. Plots for the individual faceplates are shown in Figures 30 - 36. The plots are similar to those for Lots 2 and 3, with a sharp peak at the specular angle and the tails usually between  $10^{-1}$  and  $10^{-2}$  Ft-L. For a few faceplates in those lots the tails appear in the  $10^0$ - $10^{-1}$  Ft-L region, indicating some variability in quality of the optical polish of the glass, or inhomogeneities within the glass.

#### 4.3.2 Lot 4

Results of optical reflectance measurements on Lot 4 are summarized in Table 8. Figures 40 through 52 present plots for the individual faceplates. The shoulders on the curves occur at about an order of magnitude lower than the previous lots. A similar difference was also found between uncoated sapphire substrates and an uncoated 1710 substrate. This suggests that the surface polish of the sapphire substrates may be superior to that of the 1710 aluminosilicate glass substrates. Because the position of the shoulder of the curves has been interpreted as a measure of the diffuse reflectance and it appears essential for the intended application that diffuse reflectance be a minimum, integrating sphere measurements on the uncoated substrates may be desirable. Should a real difference in diffuse reflectance be found and correlation with the bidirectional measurements established, the latter could then serve as an incoming inspection criteria. It would also provide a basis for discussion with substrate suppliers towards improved polishing. (Text continued on page 80).

Table 7  
Reflectance of Lot 1 Faceplates  
in Percentage

| Faceplate No. | Angular Displacement from Specular Angle, Degree |                       |                       |                       |                       |                       |                       |
|---------------|--|-----------------------|-----------------------|-----------------------|-----------------------|-----------------------|-----------------------|
|               | 0  | 1                     | 3                     | 5                     | 10                    | 15                    | 30                    |
| 40            | 7.58   | $3.64 \times 10^{-3}$ | $5.12 \times 10^{-4}$ | $3.56 \times 10^{-4}$ | $2.46 \times 10^{-5}$ | $2.04 \times 10^{-4}$ | $5.66 \times 10^{-5}$ |
| 41            | 7.71   | $1.36 \times 10^{-2}$ | $1.46 \times 10^{-4}$ | $8.11 \times 10^{-5}$ | $6.52 \times 10^{-5}$ | $4.87 \times 10^{-5}$ | $9.80 \times 10^{-6}$ |
| 42            | 7.64   | $1.84 \times 10^{-2}$ | $2.91 \times 10^{-4}$ | $1.00 \times 10^{-4}$ | $6.80 \times 10^{-5}$ | $5.11 \times 10^{-5}$ | $8.86 \times 10^{-6}$ |
| 44            | 6.10   | $2.33 \times 10^{-2}$ | $2.85 \times 10^{-4}$ | $1.13 \times 10^{-4}$ | $6.39 \times 10^{-5}$ | $4.45 \times 10^{-5}$ | $5.49 \times 10^{-6}$ |
| 45            | 8.10   | $3.35 \times 10^{-3}$ | $1.20 \times 10^{-3}$ | $1.03 \times 10^{-4}$ | $7.89 \times 10^{-5}$ | $5.82 \times 10^{-5}$ | $1.25 \times 10^{-5}$ |
| 46            | 8.19   | $1.64 \times 10^{-2}$ | $3.57 \times 10^{-6}$ | $2.37 \times 10^{-4}$ | $1.48 \times 10^{-6}$ | $1.02 \times 10^{-6}$ | $1.50 \times 10^{-5}$ |
| 48            | 8.30   | $7.17 \times 10^{-3}$ | $2.64 \times 10^{-3}$ | $1.79 \times 10^{-6}$ | $1.16 \times 10^{-4}$ | $8.62 \times 10^{-5}$ | $1.89 \times 10^{-5}$ |

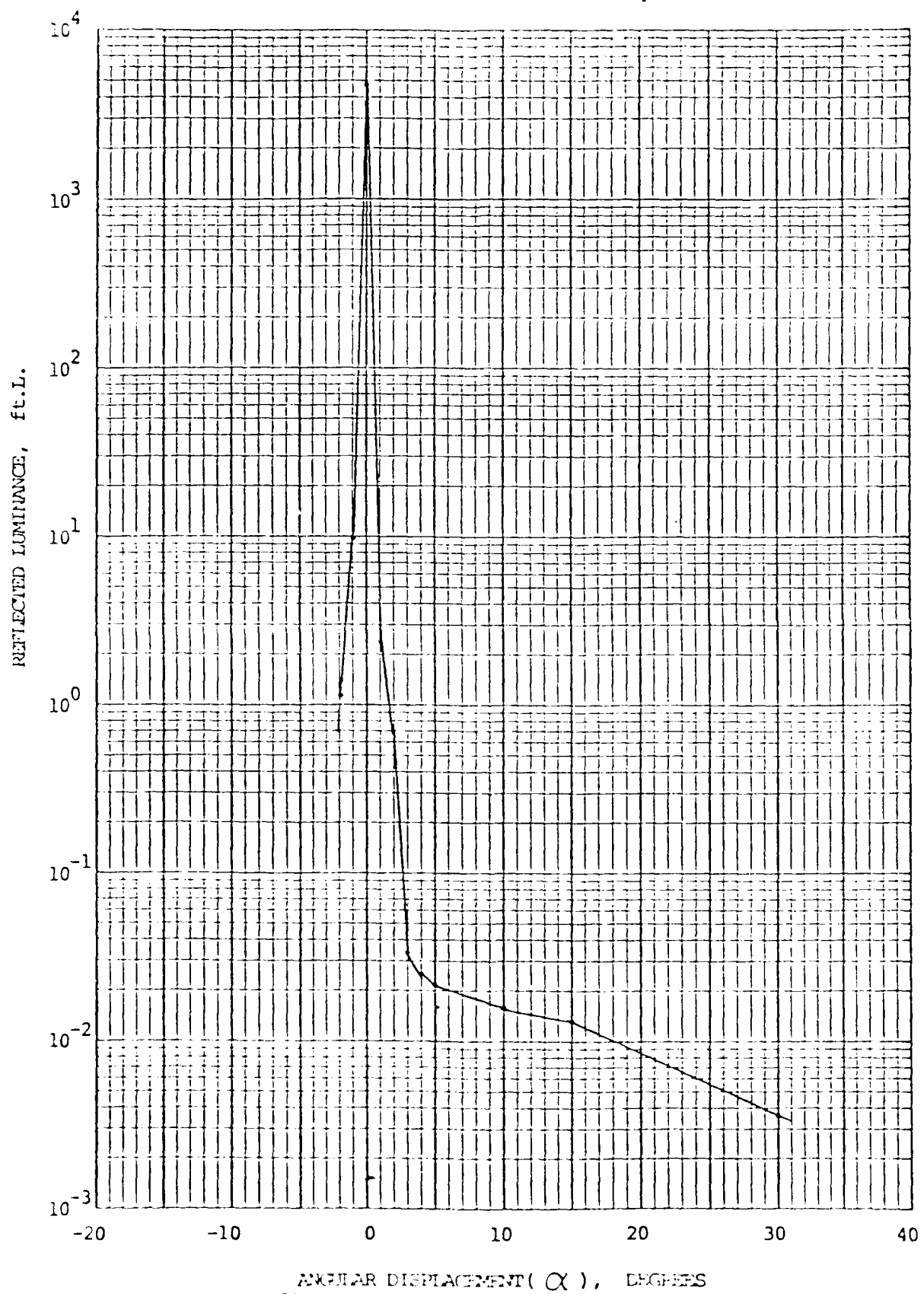


Fig. 30 Reflectance, Faceplate No. 40

KOE SEMI-LOGARITHMIC 48 6483  
7 CYCLES & 40 DIVISIONS PER INCH  
REUPPEL & EBER CO.

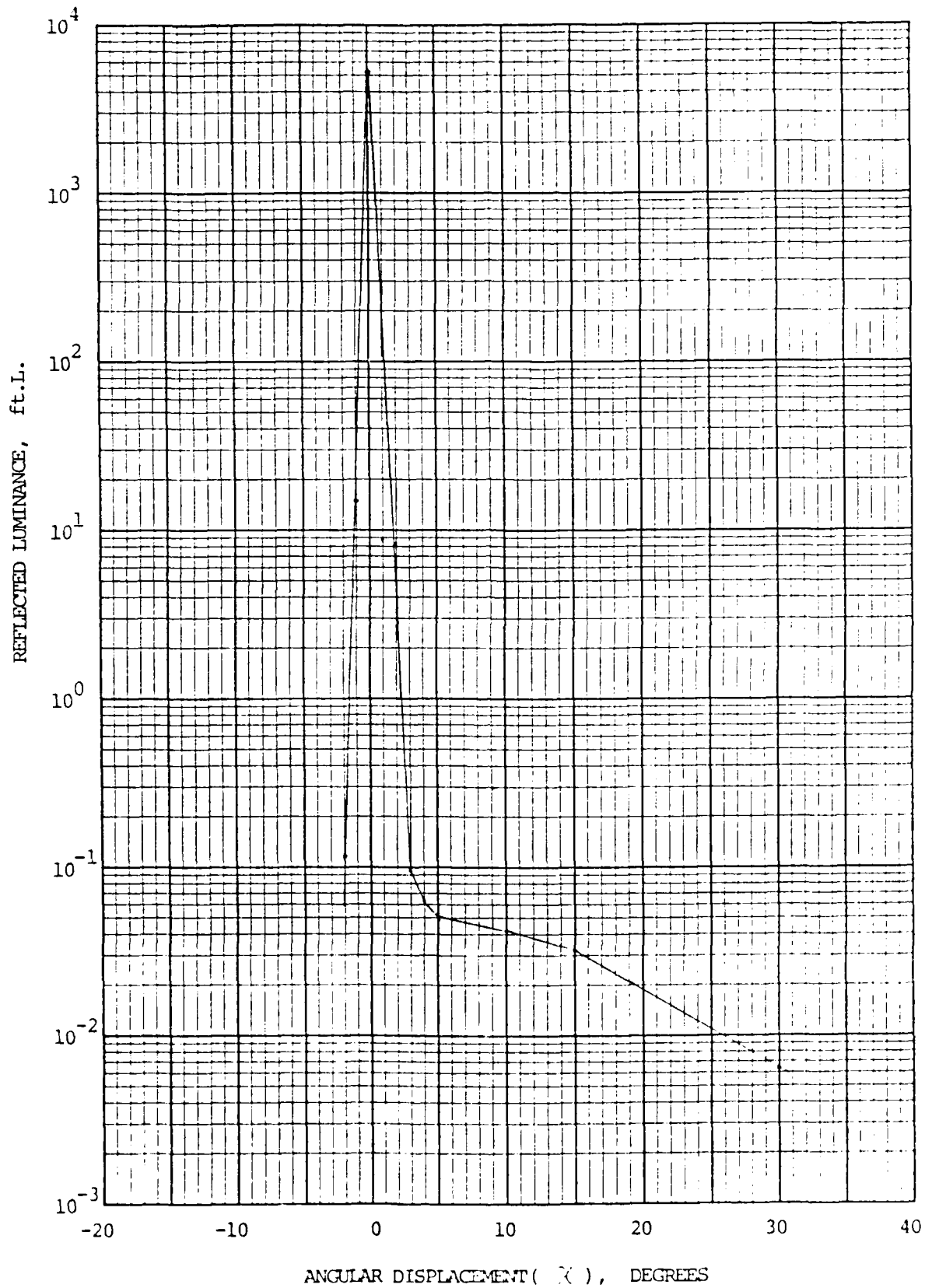


Fig. 31 Reflectance, Faceplate No. 41

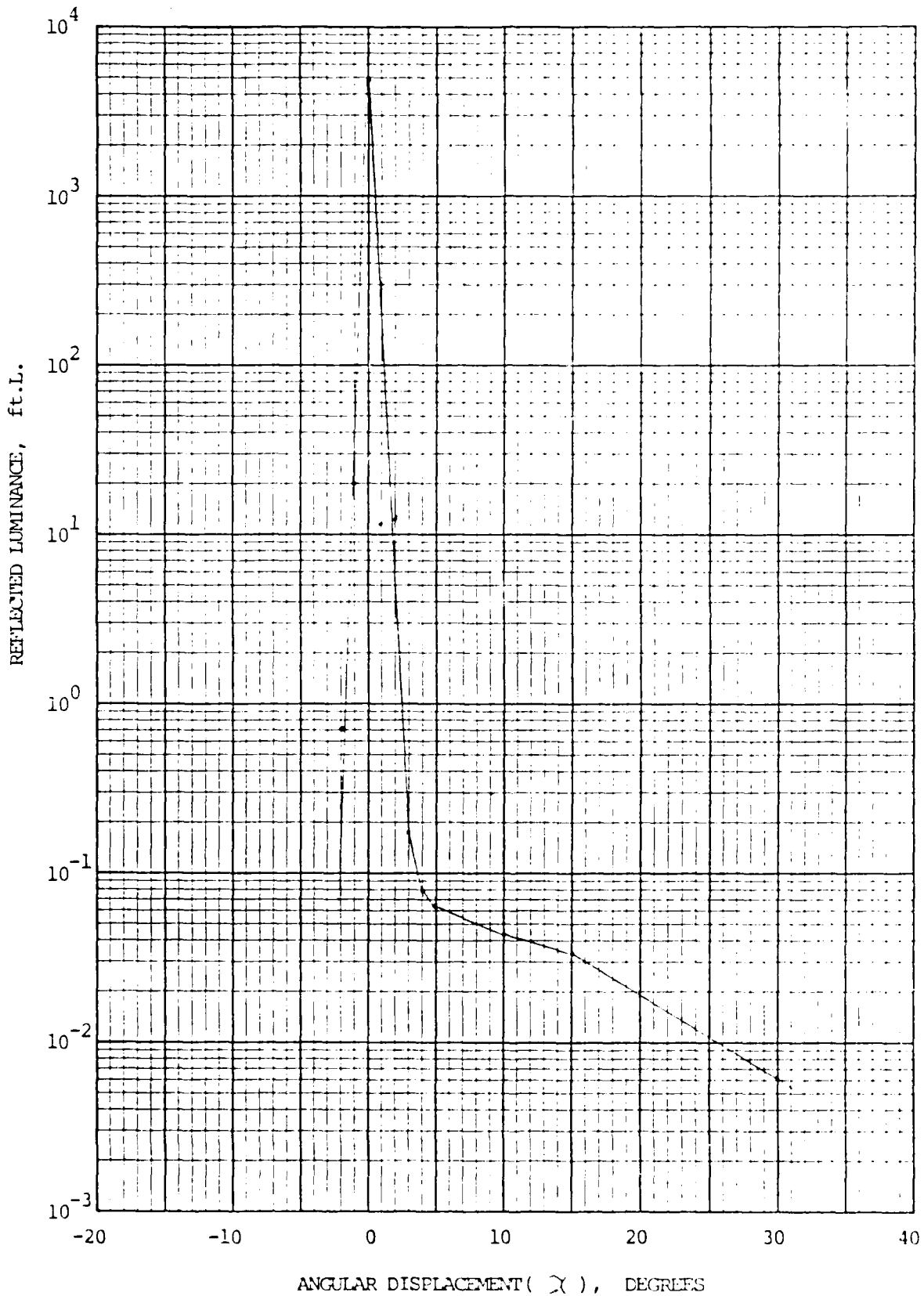


Fig. 32 Reflectance, Faceplate No. 42

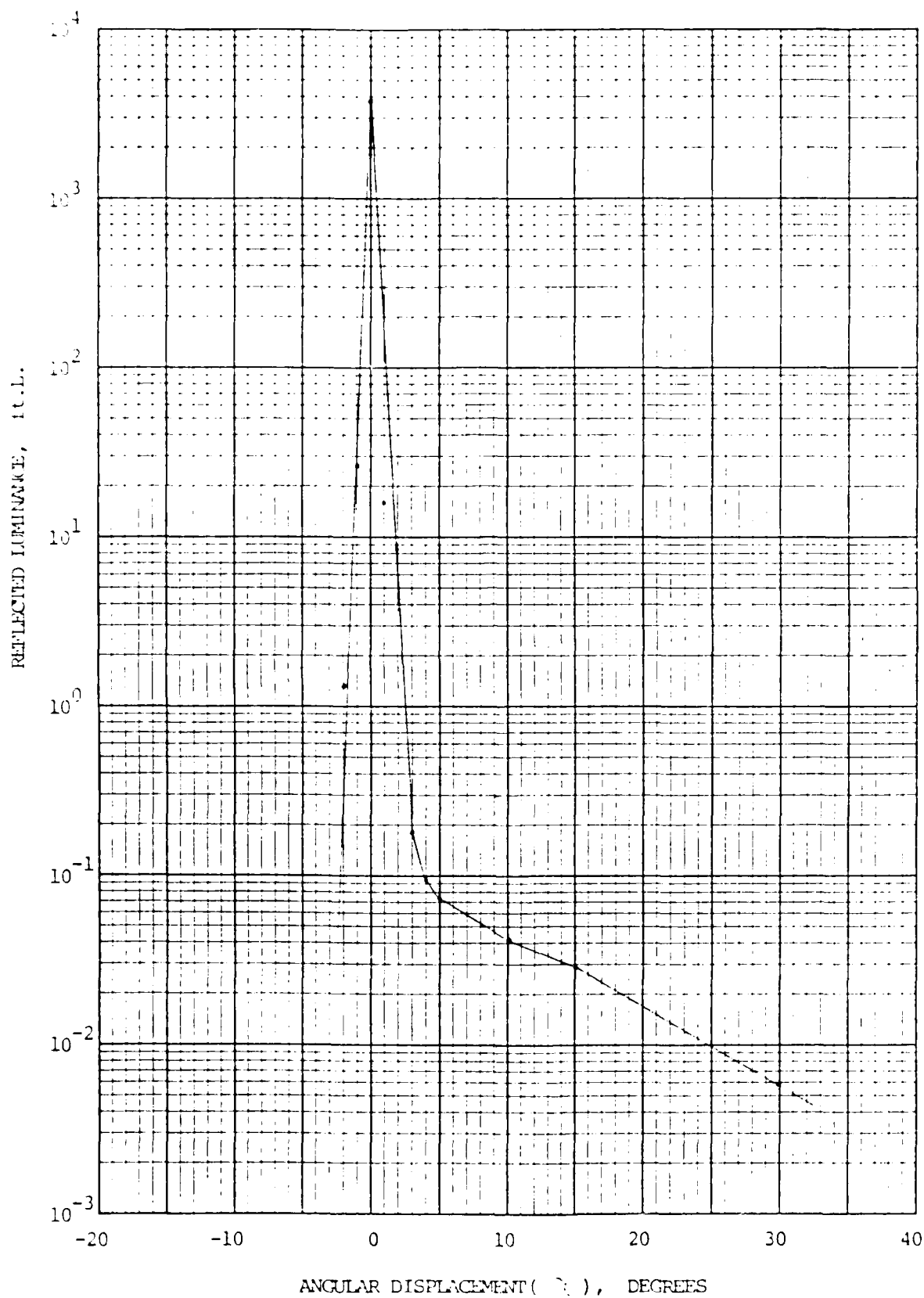


Fig.33 Reflectance, Faceplate #44

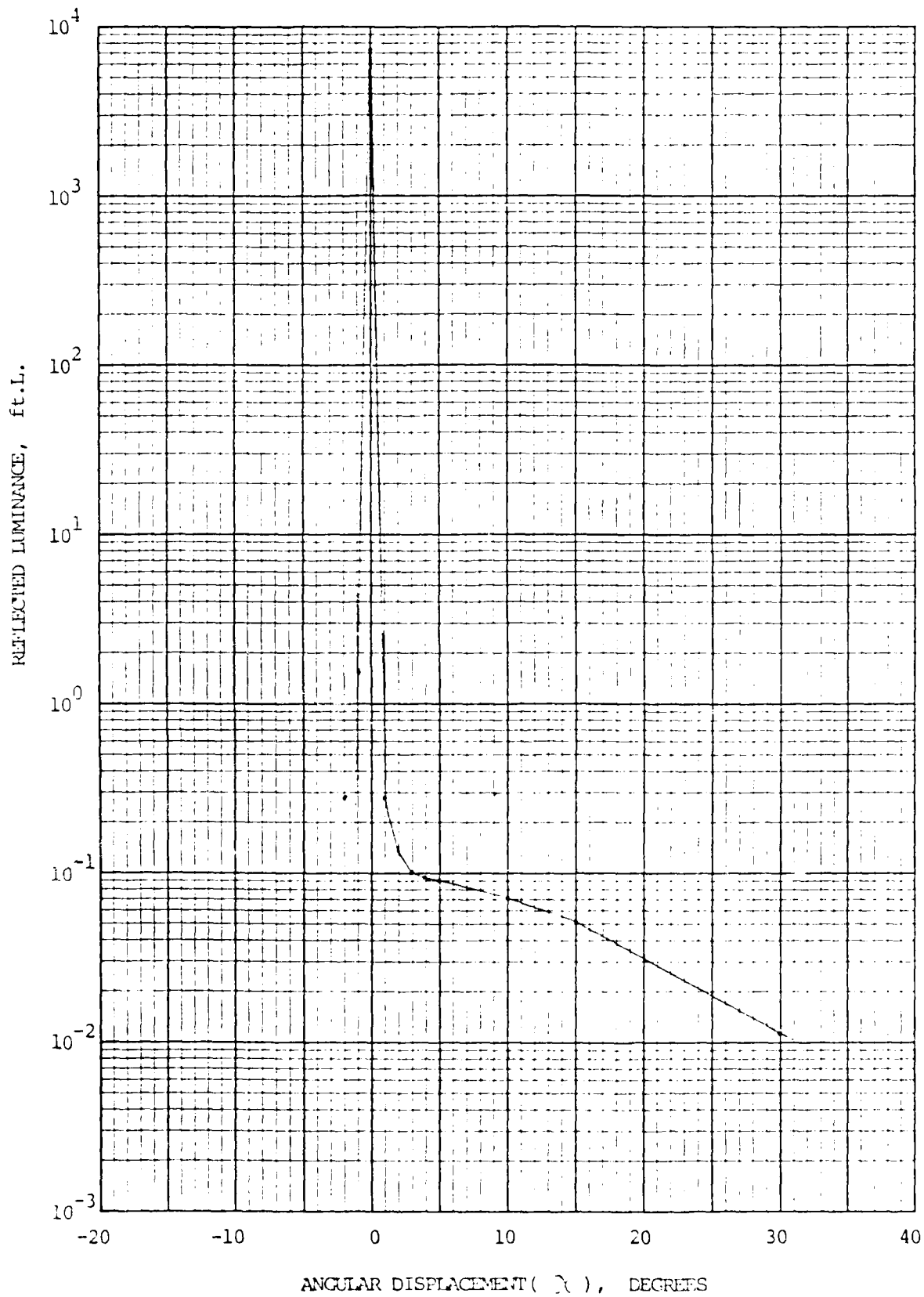


Fig.34 Reflectance, Faceplate No. 45

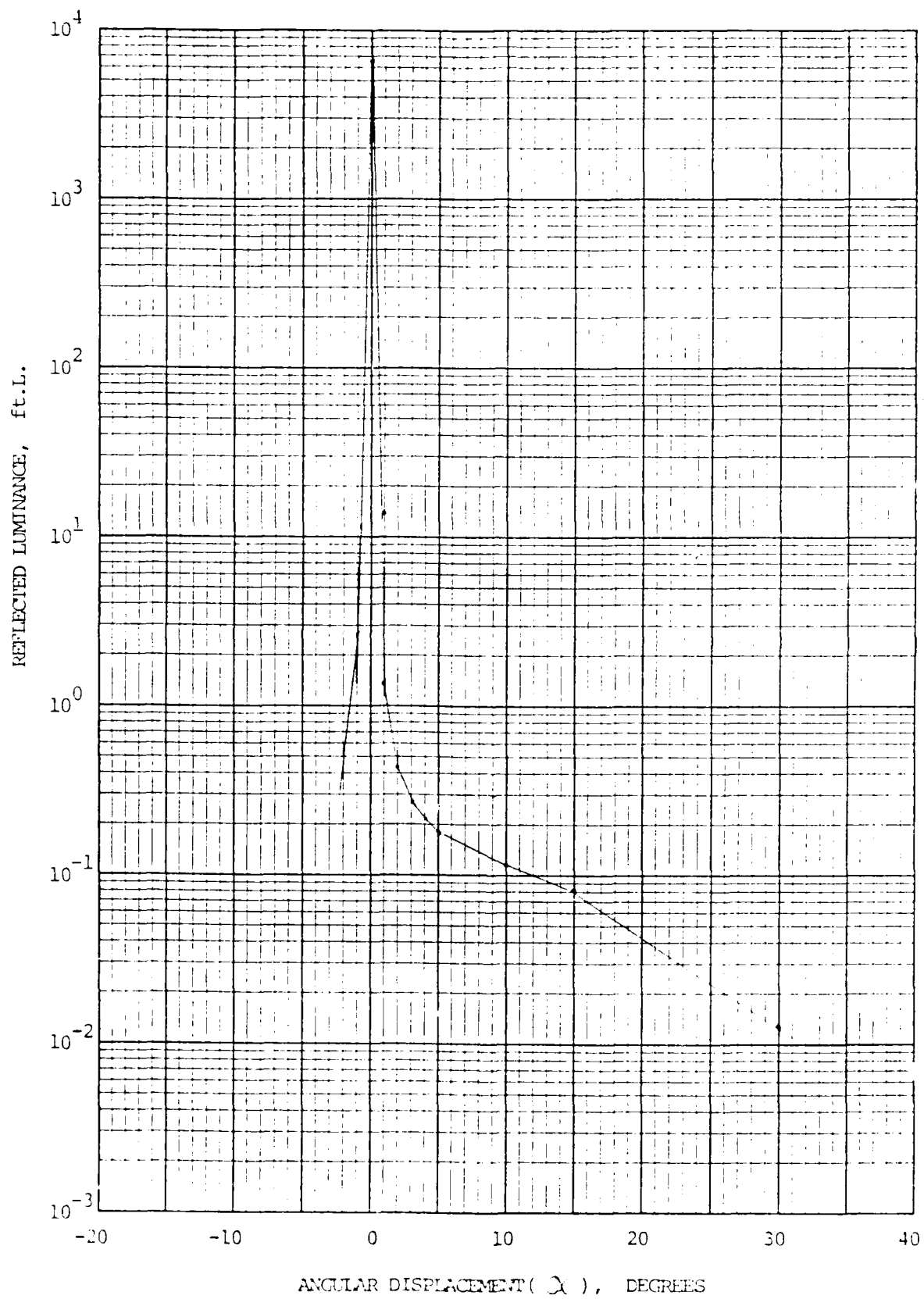


Fig. 35 Reflectance Faceplate No. 46

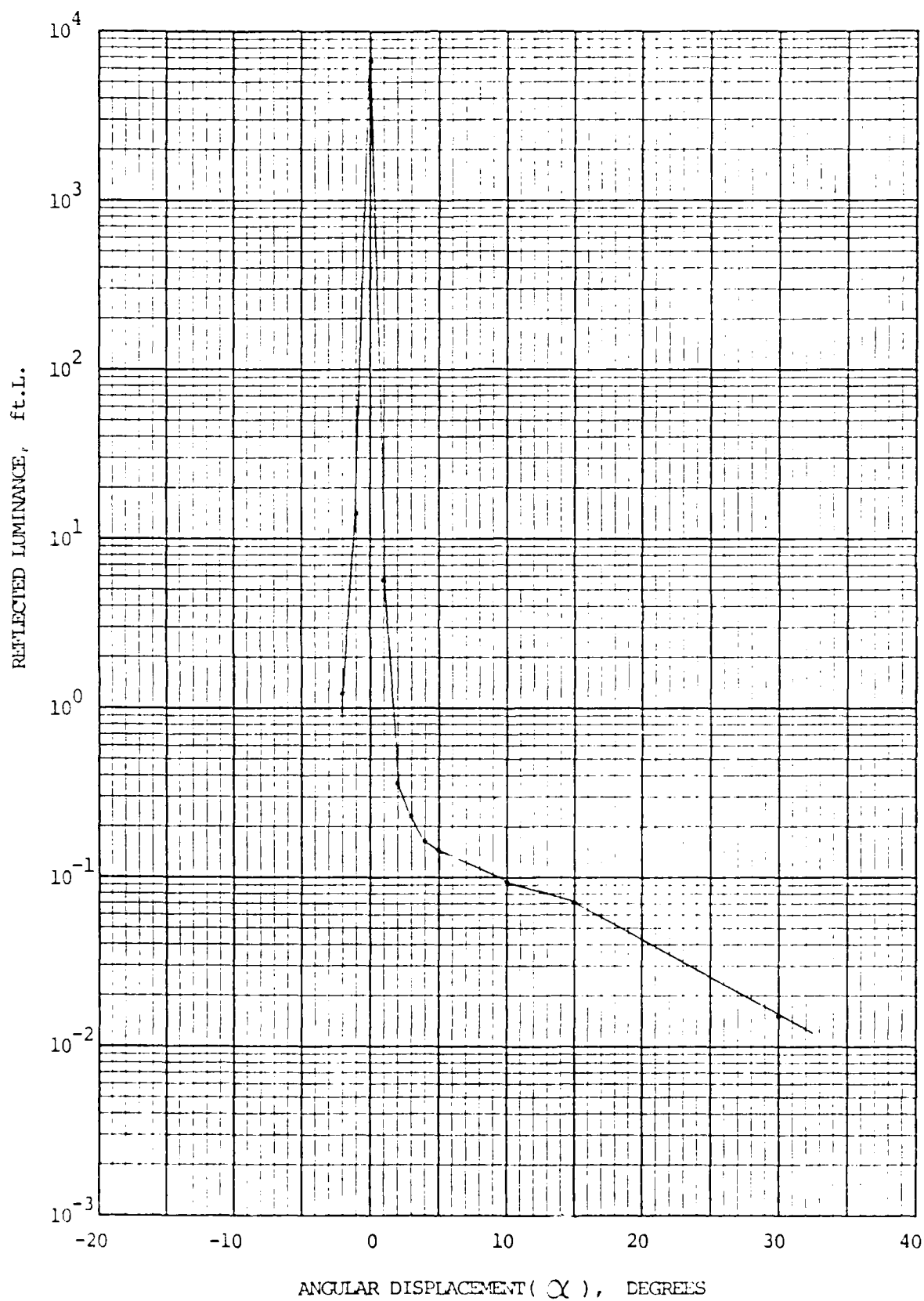


Fig. 36 Reflectance, Faceplate No. 48

Table 8

REFLECTANCE OF LOT 4 FACEPLATES (Sapphire in Percentage)

| Faceplate No.          | 0    | Angular Displacement from Specular, Degrees |                       |                       |                       |                       |                       |
|------------------------|------|---|-----------------------|-----------------------|-----------------------|-----------------------|-----------------------|
|                        |      | 1   | 3                     | 5                     | 10                    | 15                    | 30                    |
| 75                     | 8.47 | $3.05 \times 10^{-4}$                       | $5.74 \times 10^{-5}$ | $3.67 \times 10^{-5}$ | $2.32 \times 10^{-5}$ | $1.67 \times 10^{-5}$ | $4.93 \times 10^{-6}$ |
| 76                     | 9.25 | $3.35 \times 10^{-4}$                       | $7.36 \times 10^{-5}$ | $4.40 \times 10^{-5}$ | $2.47 \times 10^{-5}$ | $1.71 \times 10^{-5}$ | $4.10 \times 10^{-6}$ |
| 77                     | 8.92 | $2.40 \times 10^{-4}$                       | $2.43 \times 10^{-5}$ | $1.76 \times 10^{-5}$ | $1.25 \times 10^{-5}$ | $9.72 \times 10^{-6}$ | $3.38 \times 10^{-6}$ |
| 78                     | 8.64 | $2.51 \times 10^{-4}$                       | $5.58 \times 10^{-5}$ | $3.22 \times 10^{-5}$ | $1.63 \times 10^{-5}$ | $1.23 \times 10^{-5}$ | $5.33 \times 10^{-6}$ |
| 79                     | 9.65 | $1.65 \times 10^{-6}$                       | $3.41 \times 10^{-5}$ | $2.48 \times 10^{-5}$ | $1.87 \times 10^{-5}$ | $1.76 \times 10^{-5}$ | $6.88 \times 10^{-6}$ |
| 80                     | 8.37 | $2.04 \times 10^{-4}$                       | $5.30 \times 10^{-5}$ | $3.98 \times 10^{-5}$ | $2.77 \times 10^{-5}$ | $2.14 \times 10^{-5}$ | $7.28 \times 10^{-6}$ |
| 81                     | 9.84 | $2.27 \times 10^{-4}$                       | $6.13 \times 10^{-5}$ | $4.41 \times 10^{-5}$ | $2.96 \times 10^{-5}$ | $2.34 \times 10^{-5}$ | $9.03 \times 10^{-6}$ |
| 82                     | 9.65 | $1.56 \times 10^{-4}$                       | $3.97 \times 10^{-5}$ | $3.32 \times 10^{-5}$ | $2.59 \times 10^{-5}$ | $2.15 \times 10^{-5}$ | $9.53 \times 10^{-6}$ |
| 83                     | 8.90 | $3.57 \times 10^{-4}$                       | $2.30 \times 10^{-5}$ | $1.60 \times 10^{-5}$ | $1.18 \times 10^{-5}$ | $9.85 \times 10^{-6}$ | $3.64 \times 10^{-6}$ |
| 84                     | 8.53 | $3.15 \times 10^{-4}$                       | $1.39 \times 10^{-4}$ | $7.74 \times 10^{-5}$ | $3.76 \times 10^{-5}$ | $2.32 \times 10^{-5}$ | $6.51 \times 10^{-6}$ |
| 85                     | 9.91 | $2.58 \times 10^{-4}$                       | $8.76 \times 10^{-5}$ | $6.87 \times 10^{-5}$ | $4.68 \times 10^{-5}$ | $3.62 \times 10^{-5}$ | $8.33 \times 10^{-6}$ |
| 86                     | 9.74 | $2.58 \times 10^{-6}$                       | $8.71 \times 10^{-5}$ | $5.18 \times 10^{-5}$ | $3.91 \times 10^{-5}$ | $3.10 \times 10^{-5}$ | $8.46 \times 10^{-6}$ |
| 87                     | 8.63 | $2.73 \times 10^{-6}$                       | $6.29 \times 10^{-5}$ | $5.16 \times 10^{-5}$ | $3.61 \times 10^{-5}$ | $2.95 \times 10^{-5}$ | $1.06 \times 10^{-5}$ |
| Corning 1720, Uncoated | 7.97 | $1.82 \times 10^{-6}$                       | $1.25 \times 10^{-5}$ | $5.26 \times 10^{-6}$ | $7.00 \times 10^{-7}$ | -                     | -                     |
| Sapphire, Uncoated     | 14.9 | $2.99 \times 10^{-4}$                       | $9.36 \times 10^{-6}$ | $4.05 \times 10^{-6}$ | $1.45 \times 10^{-6}$ | $1.14 \times 10^{-6}$ | $1.21 \times 10^{-7}$ |
| Aluminum Mirror        | 88.0 | $2.69 \times 10^{-3}$                       | $4.03 \times 10^{-4}$ | $1.96 \times 10^{-4}$ | $6.77 \times 10^{-4}$ | $3.64 \times 10^{-6}$ | $5.22 \times 10^{-5}$ |

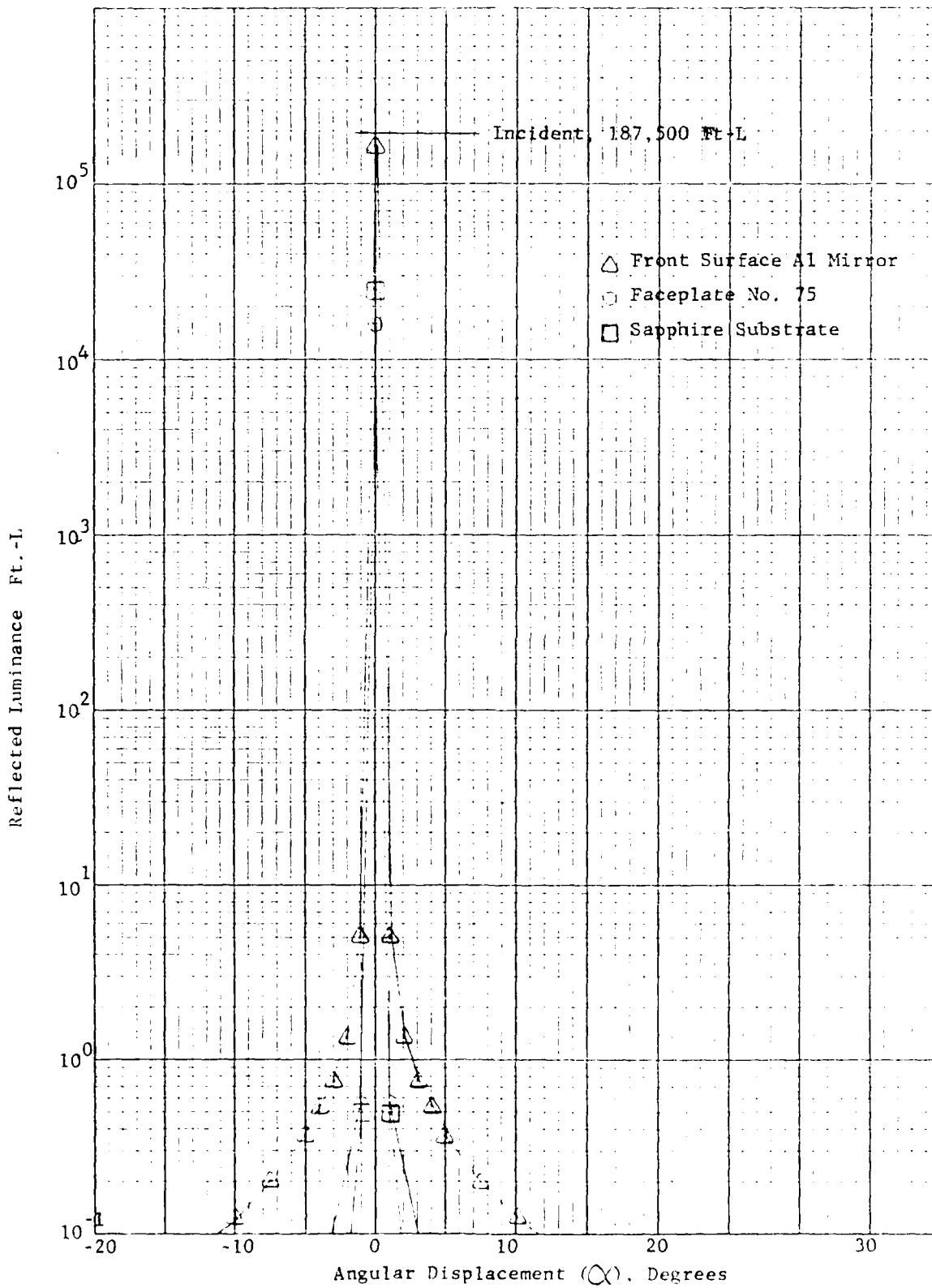


Fig. 37 Mirror vs. Faceplate 75 and Sapphire Substrate

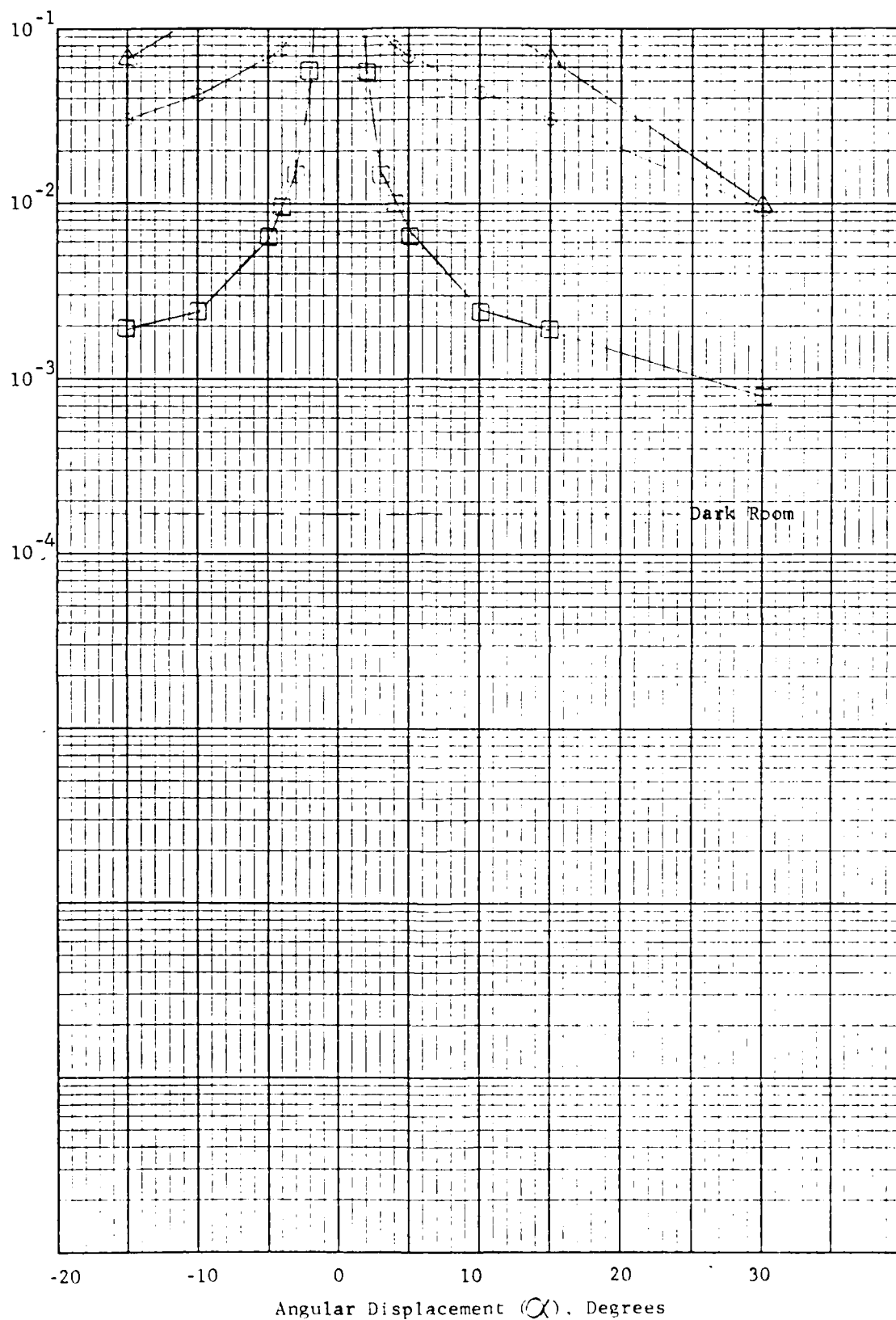


Fig. 37 Mirror vs. Faceplate 75 and Sapphire Substrate (Cont.).

K&E SEMI-LOGARITHMIC 46 6463  
7 CYCLES X 60 DIVISIONS  
MADE IN U.S.A.  
KLUFFEL & EBBEN CO.

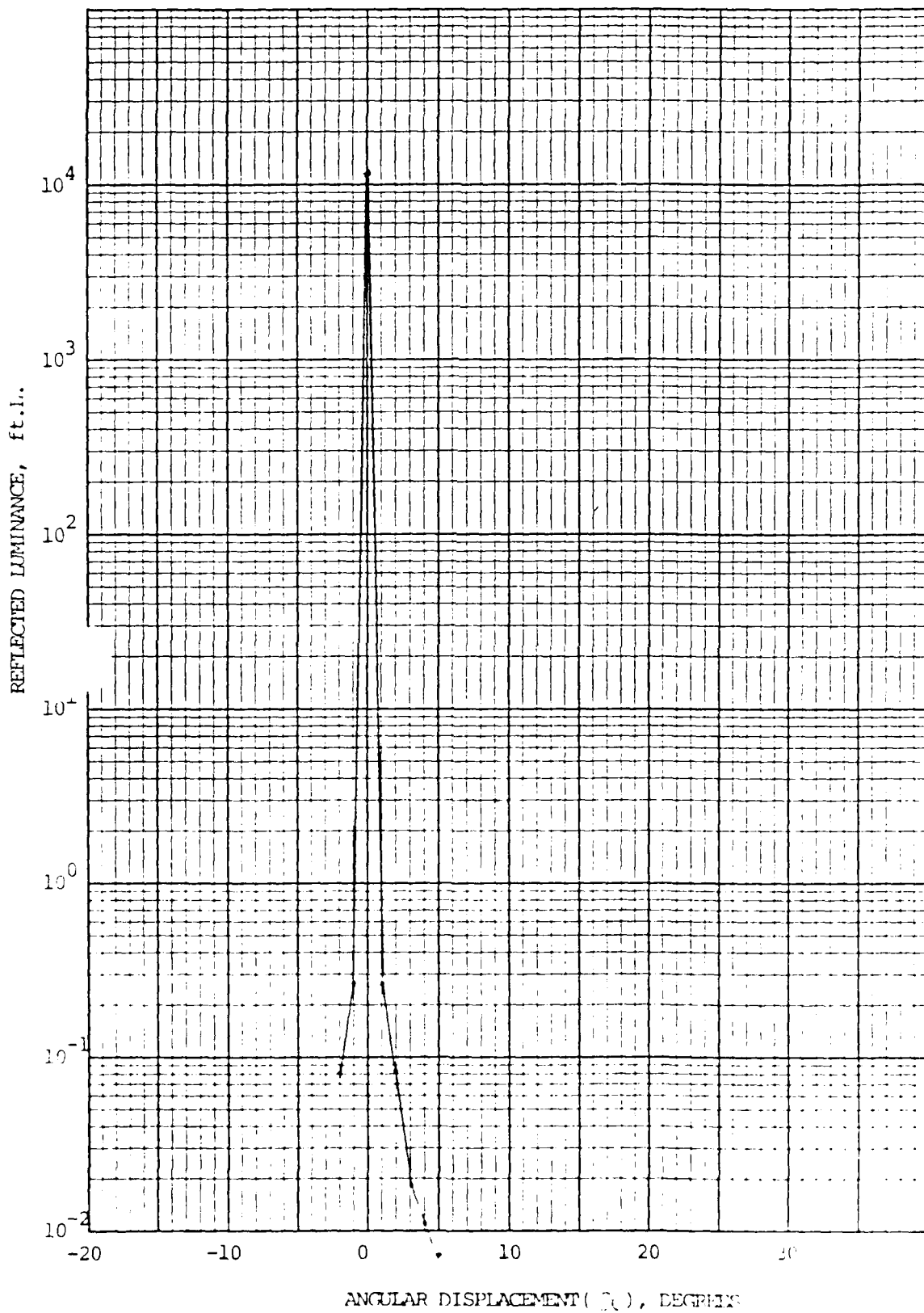


Fig. 38 Reflectance Uncoated 1720 Glass

K&E SEMI-LOGARITHMIC 46 6463  
7 CYCLES X 60 DIVISIONS  
KEUFFEL & ESSER CO.

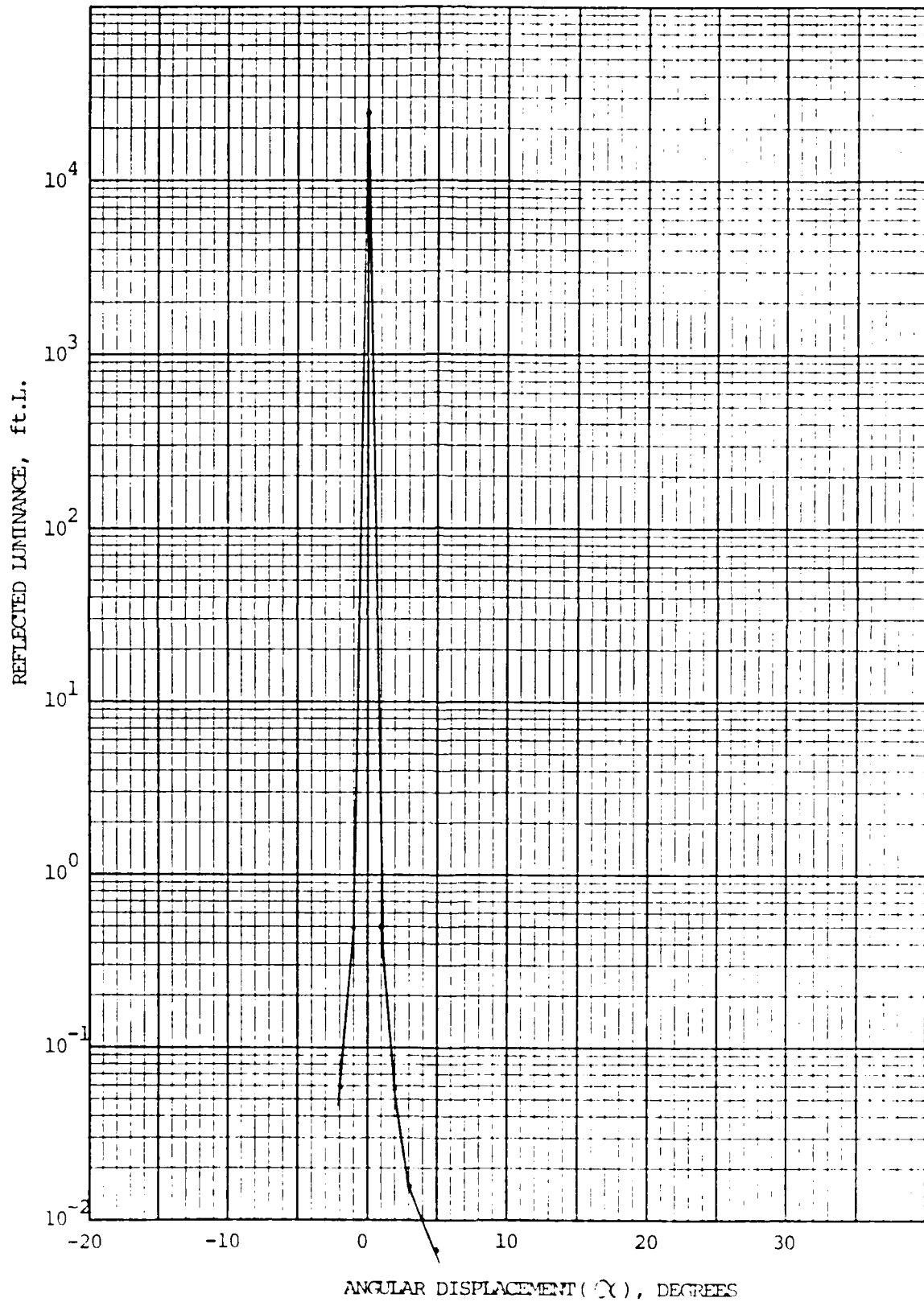


Fig. 39 Reflectance, Uncoated Sapphire

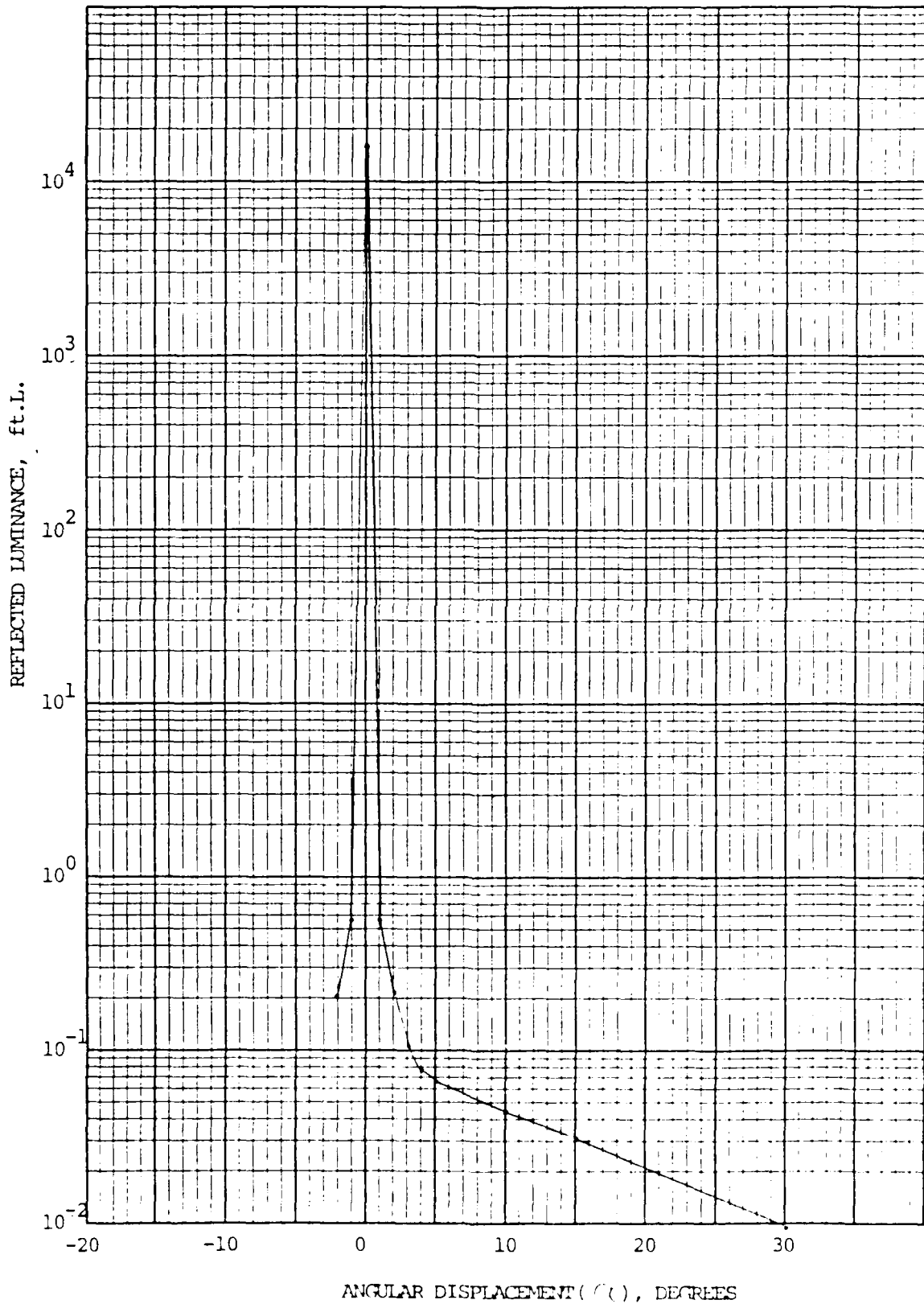


Fig. 40 Reflectance. Faceplate No. 75

K&E SEMI-LOGARITHMIC 46 6463  
7 CYCLES X 80 DIVISIONS  
KUPPEL & BEER CO.

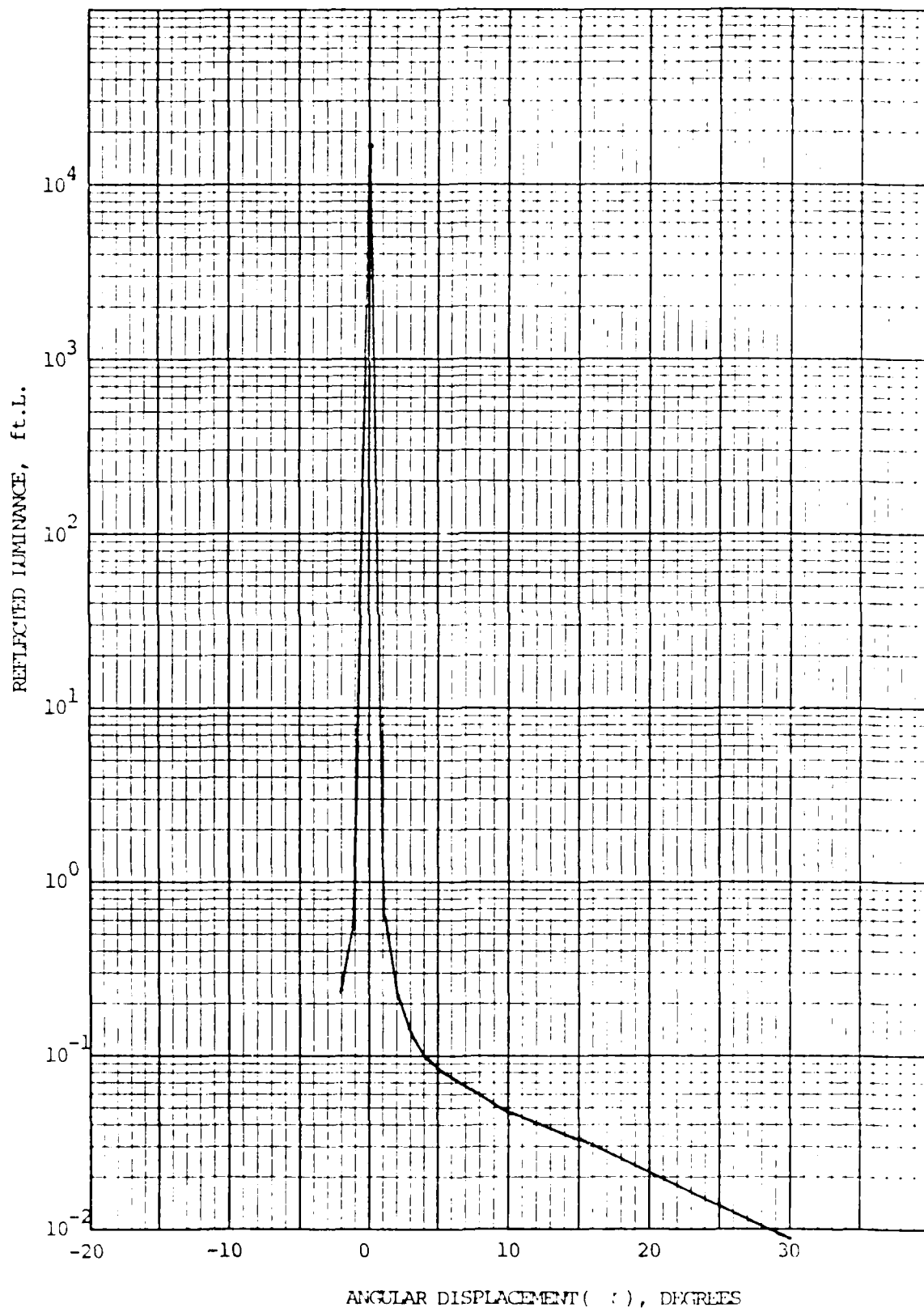


Fig.41 Reflectance Faceplate No. 76

KE SEMILOGARITHMIC 46 6463  
 1 CYCLES PER DIVISION  
 REUPPEL & EBBEL CO

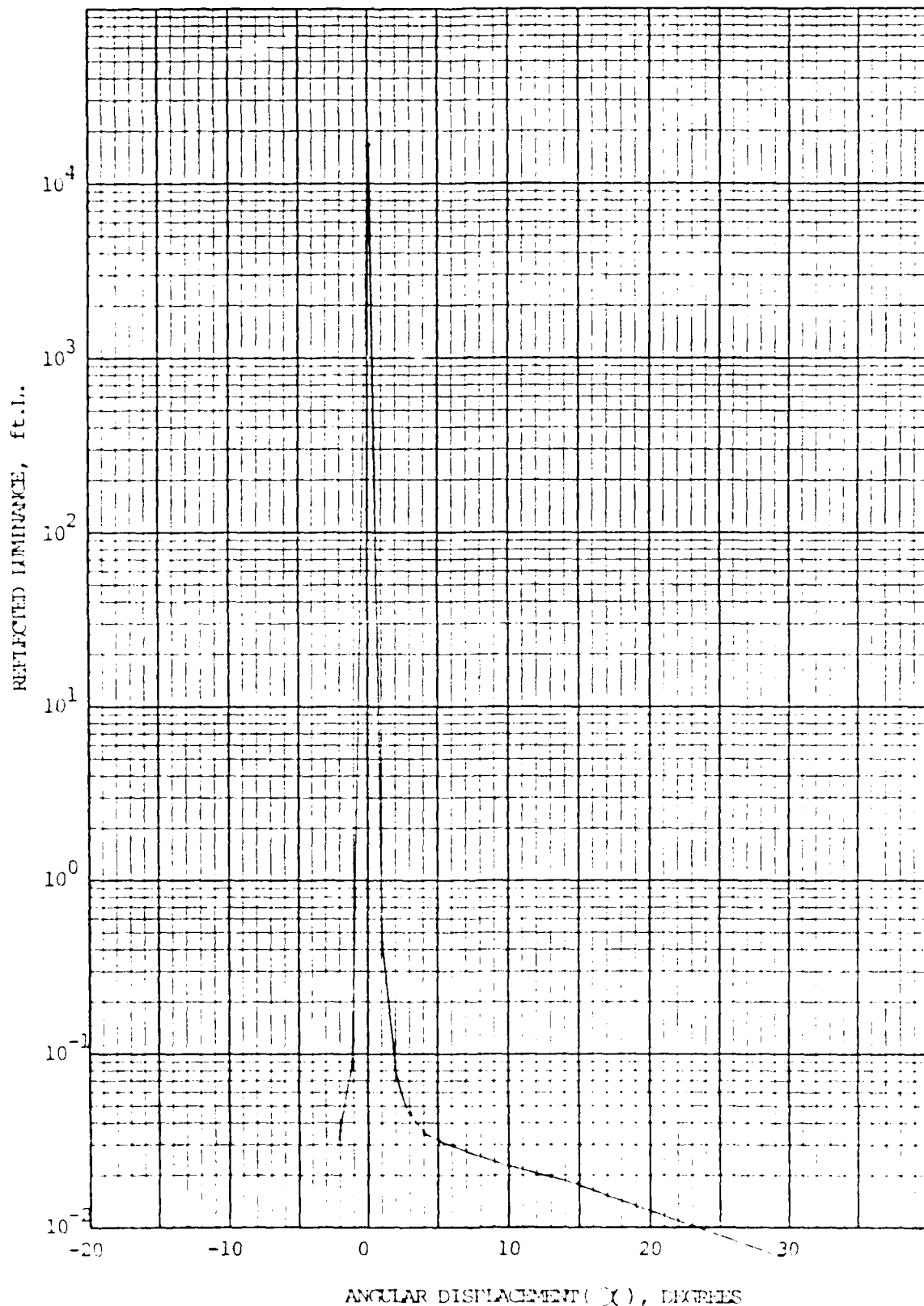


Fig. 42 Reflectance Faceplate No. 77

K $\odot$  $\Sigma$  SEMI-LOGARITHMIC 46 6463  
7 CYCLES X 60 DIVISIONS  
KEUFFEL & ESSER CO.

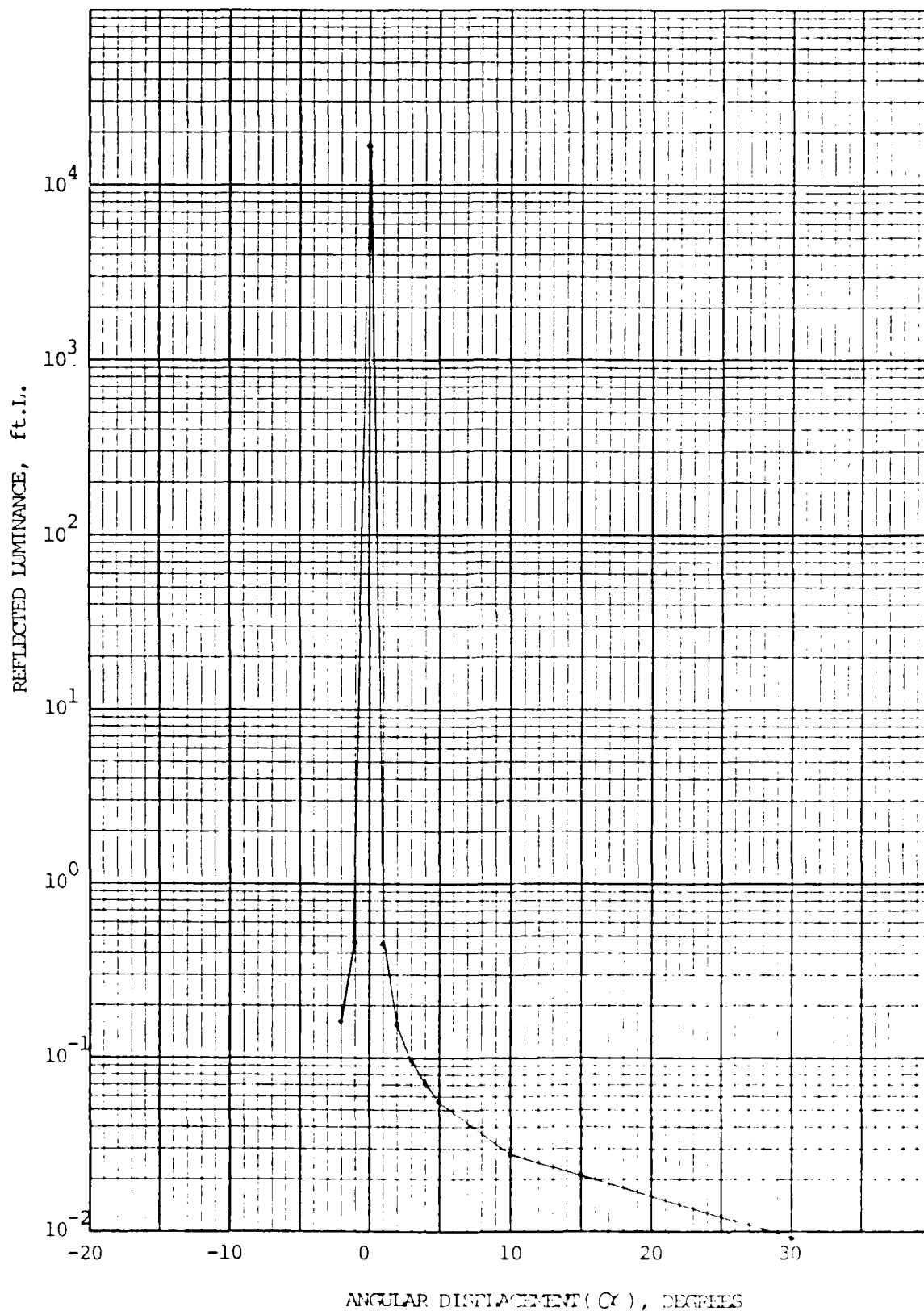


Fig. 43 Reflectance - Plate No. 78

K $\sigma$  SEMI-LOGARITHMIC 48 6463  
7 CYCLES X 40 DIVISIONS  
KRAUFF & ESSER CO.

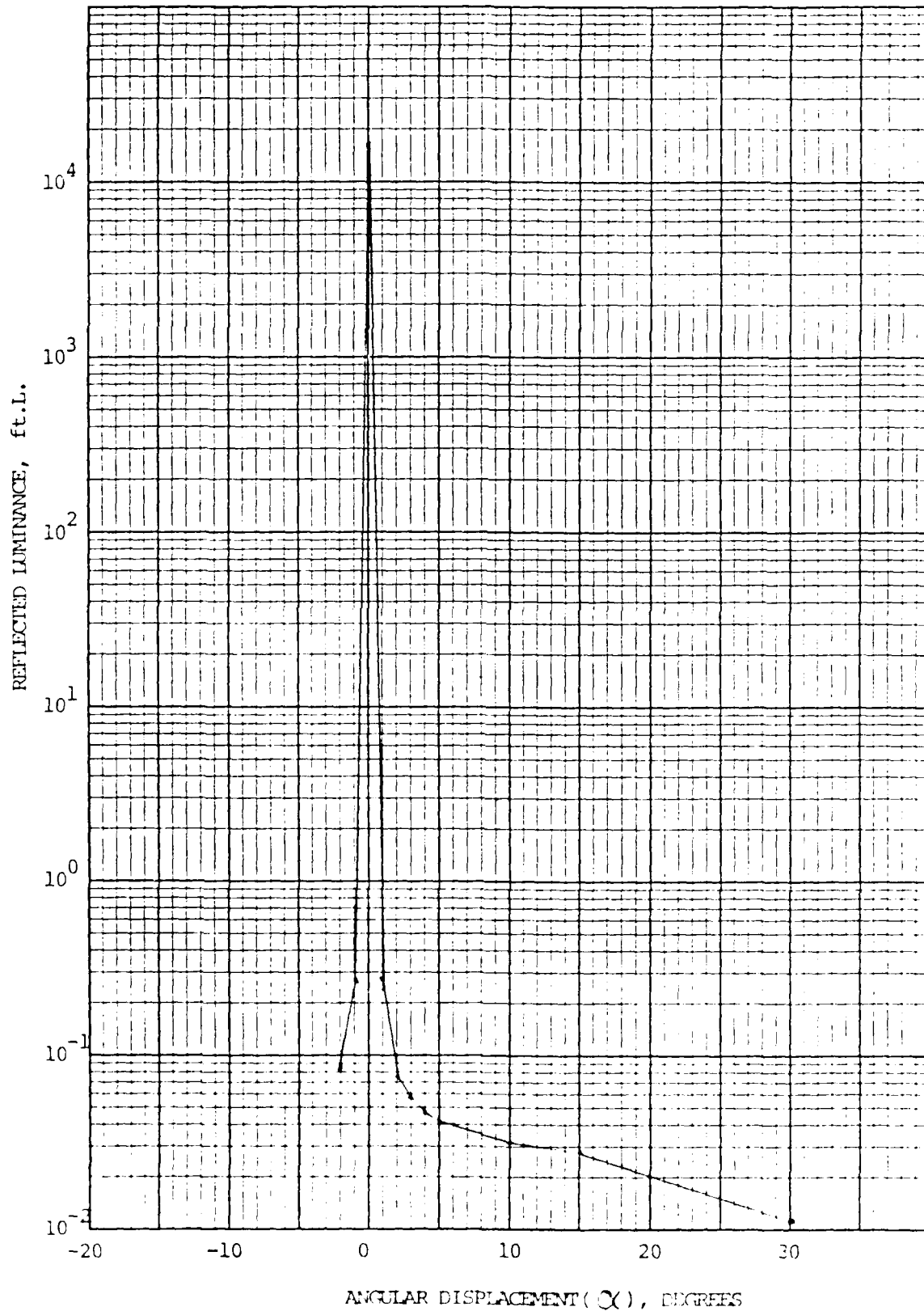


Fig 44 Reflectance Faceplate No. 79

K&E SEMI-LOGARITHMIC 46 6463  
7 CYCLES X 80 DIVISIONS MADE IN U.S.A.  
NEUPPEL & ESSER CO.

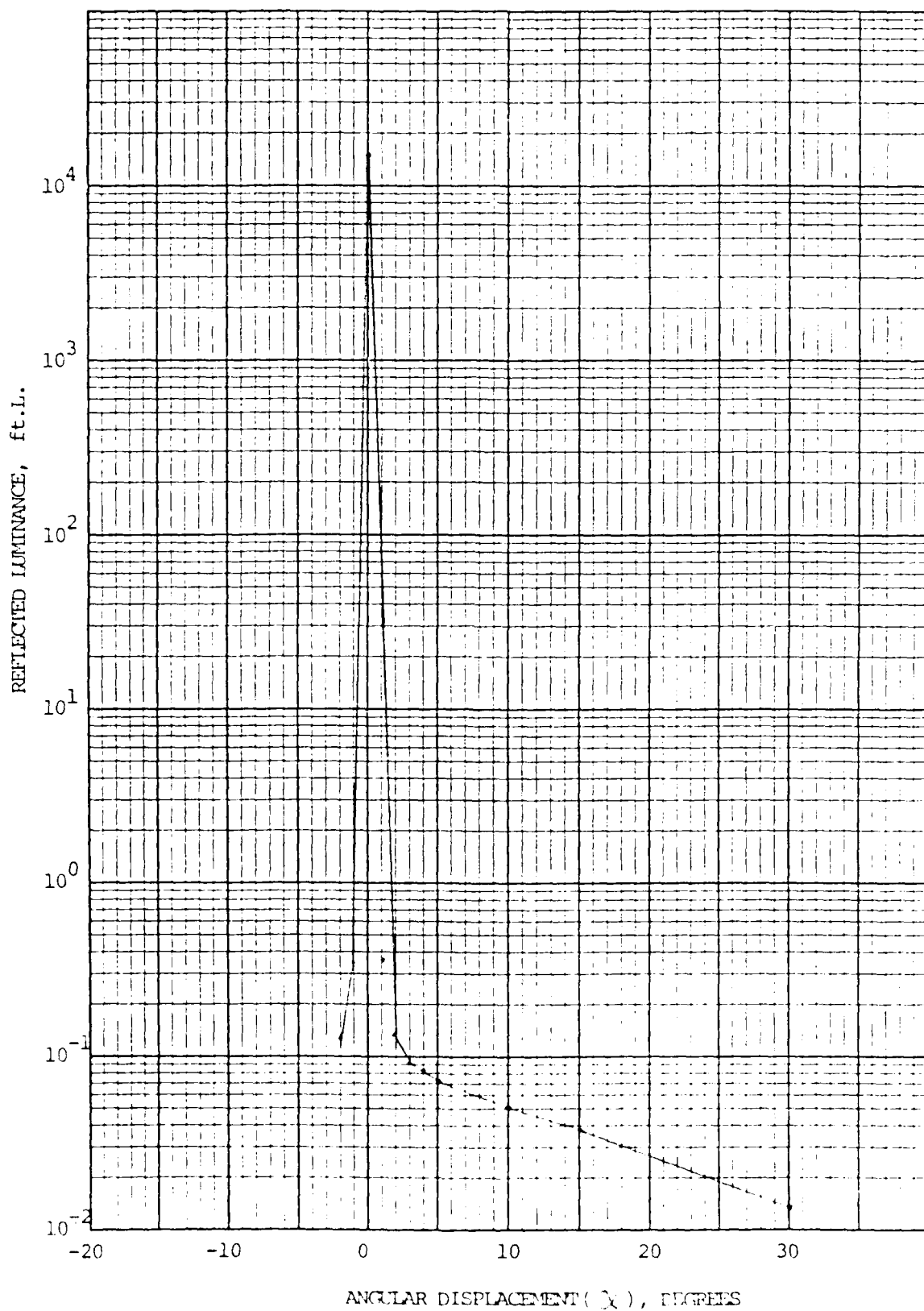


Fig. 45 Reflectance Faceplate No. 80

KE SEMILOGARITHMIC 46 8463  
7 CYCLES X 80 DIVISIONS  
NEUPPEL & EBBEL CO.

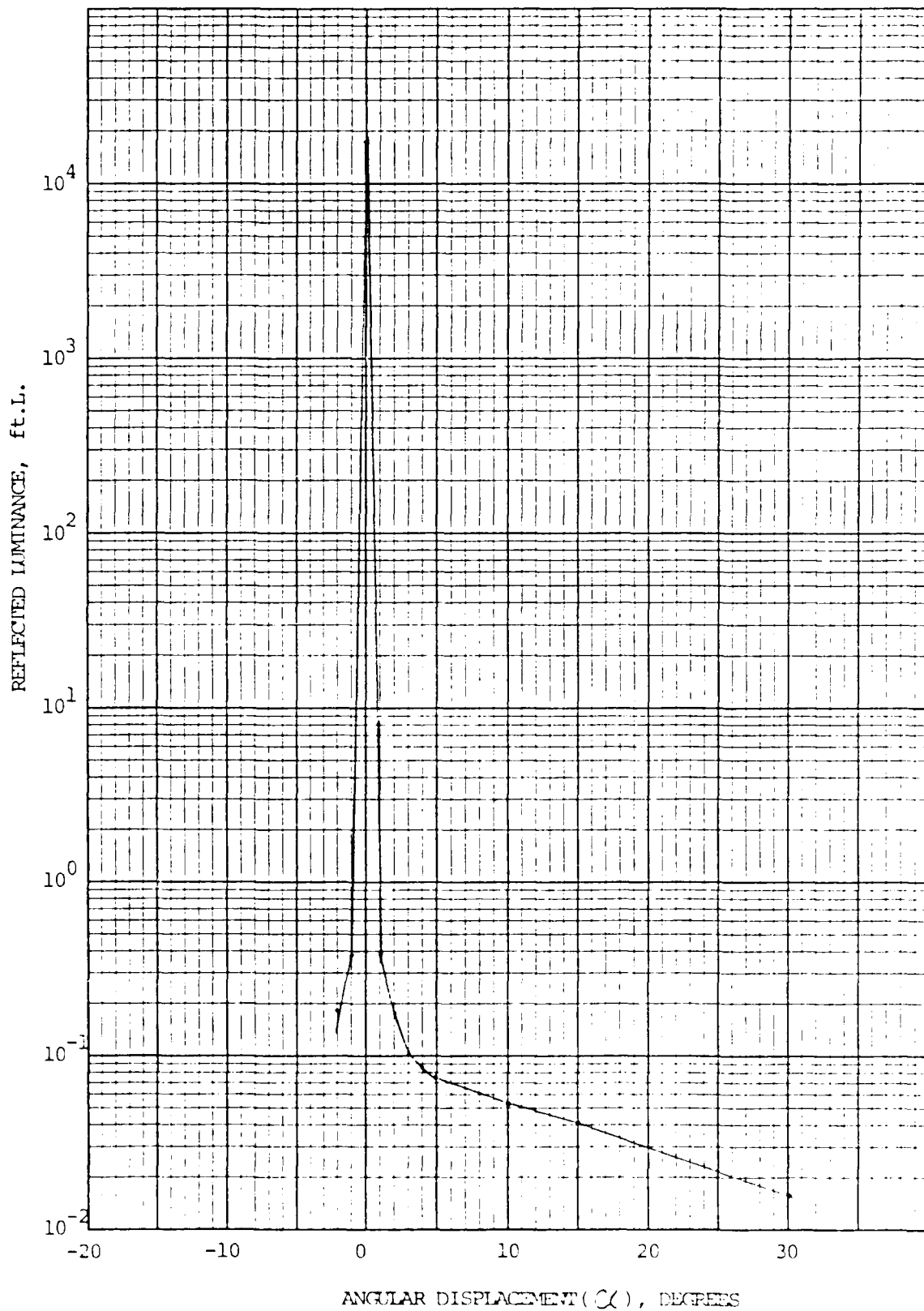


Fig.46 Reflectance Faceplate No. 81

K&E SEMI-LOGARITHMIC 48 6463  
7 CYCLES X 60 DIVISIONS  
KRUH & EBER CO.

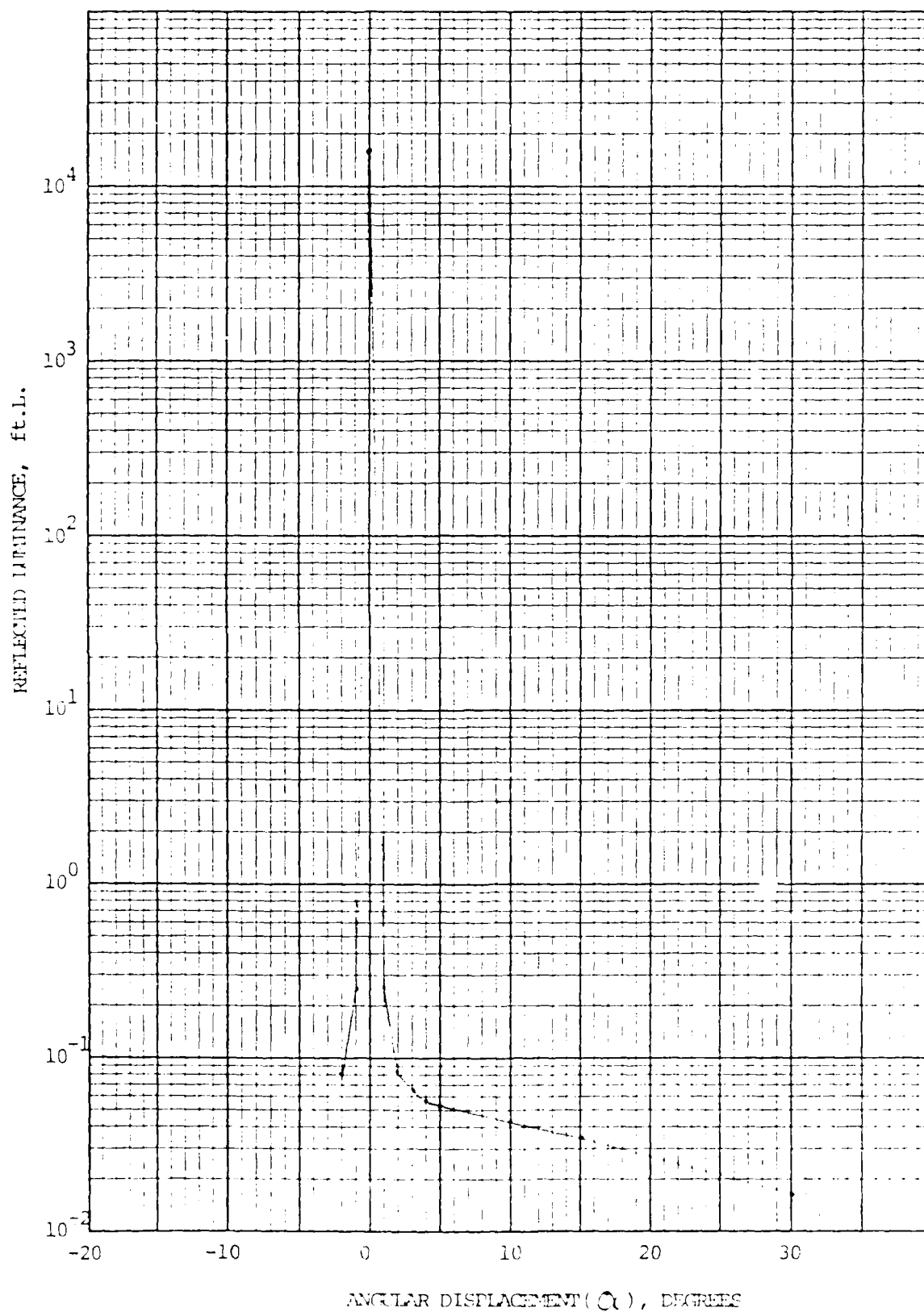


Fig. 47 Reflectance Faceplate No. 82

KE SEMI-LOGARITHMIC 46 6463  
7 CYCLES X 60 DIVISIONS  
KEUPPEL & ESSER CO.

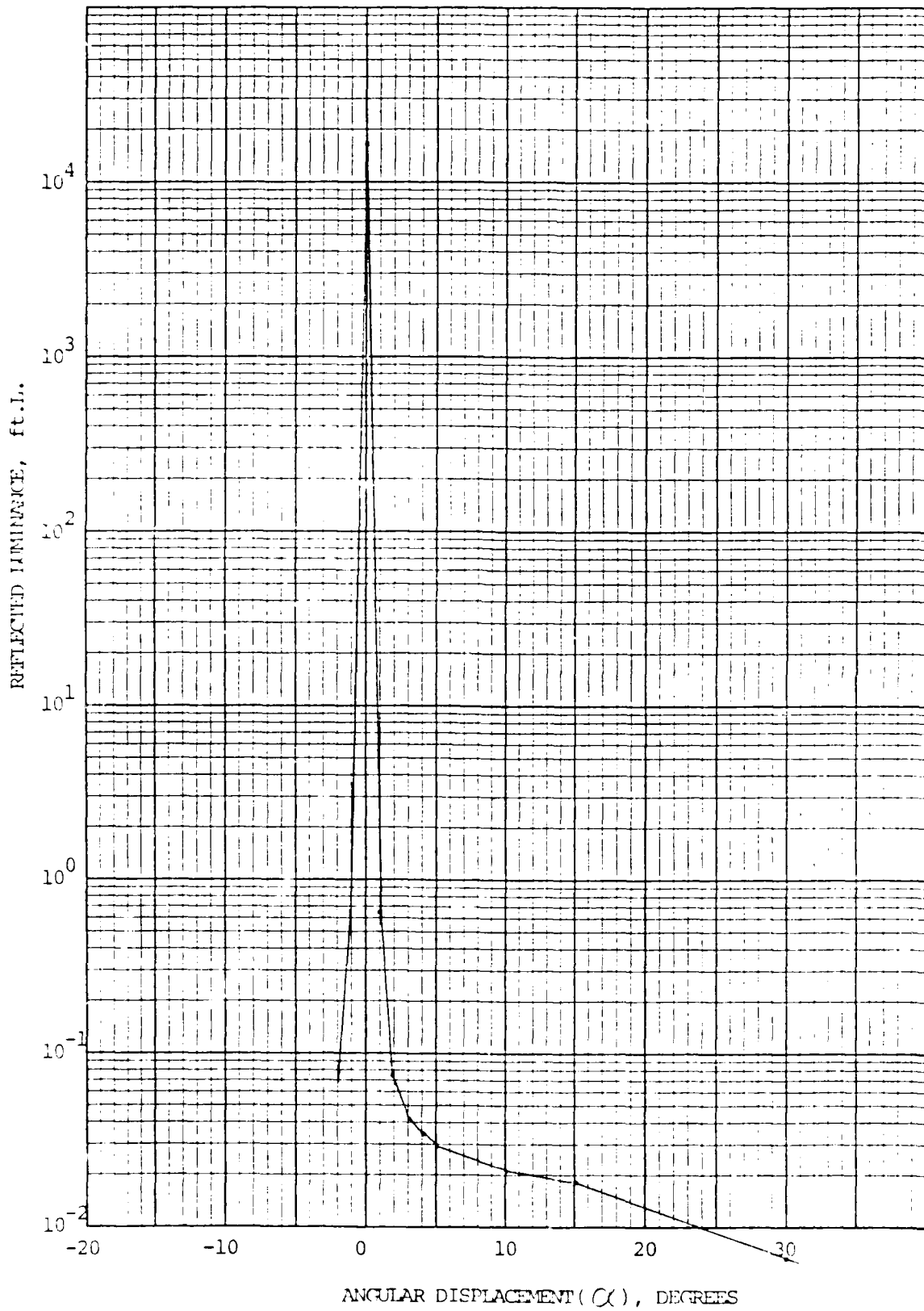


Fig.48 Reflectance Faceplate No. 83

K-E SEMI-LOGARITHMIC 46 6463  
7 CYCLES X 60 DIVISIONS  
MADE IN U.S.A.  
KEUFFEL & ESSER CO.

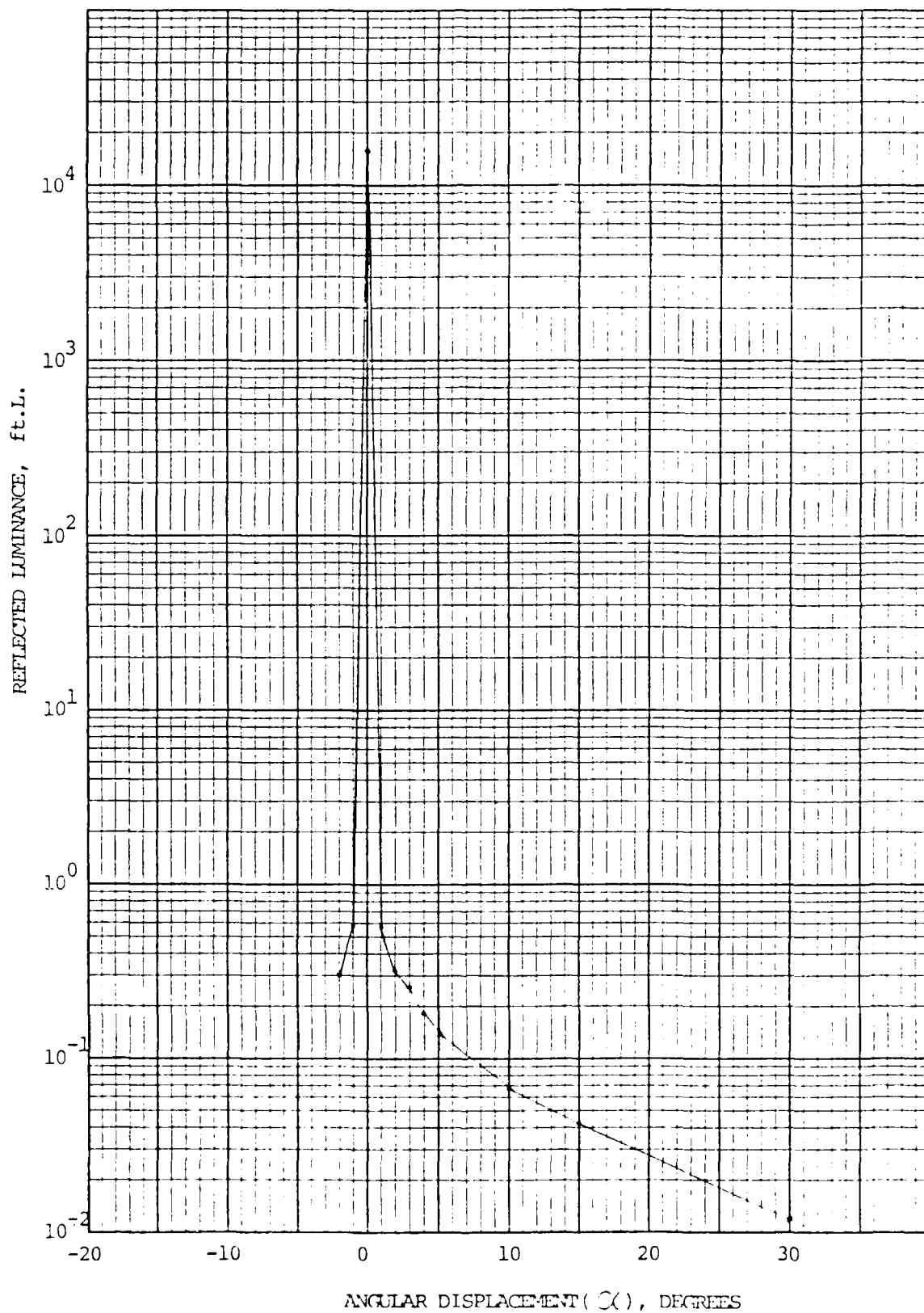
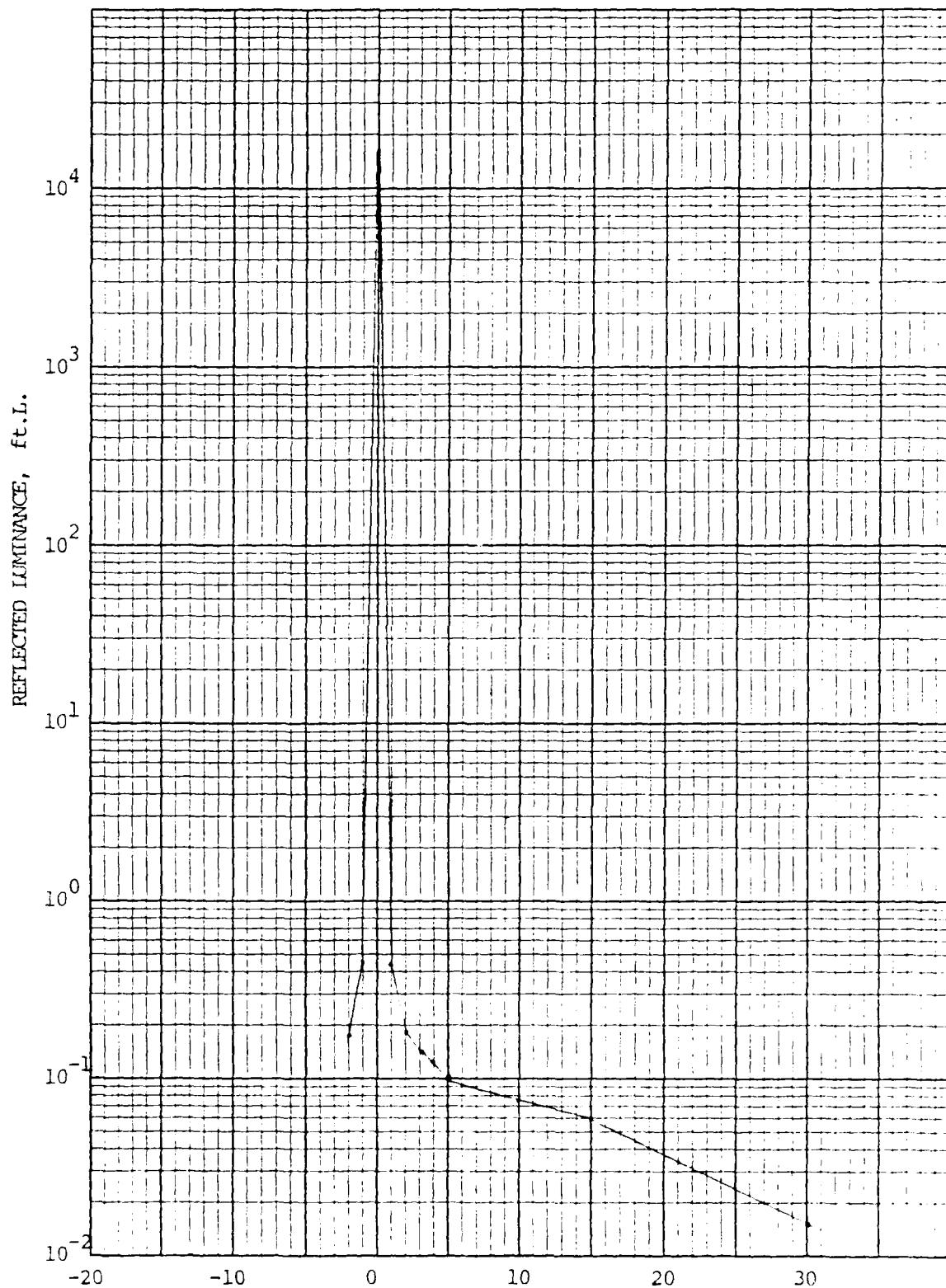


Fig.49 Reflectance, Faceplate No. 84

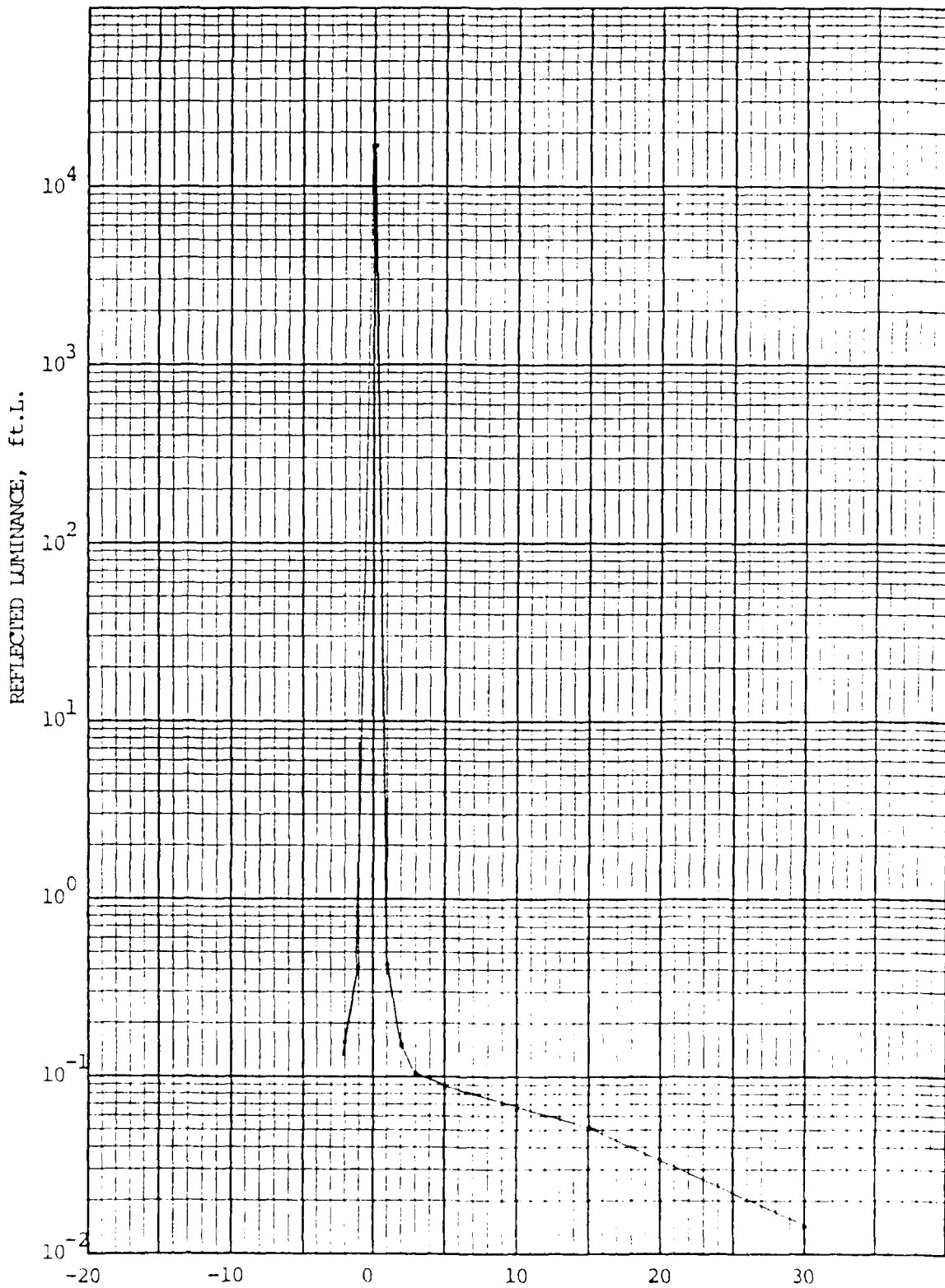
K $\Sigma$  SEMI-LOGARITHMIC 46 6463  
7 CYCLES X 80 DIVISIONS MADE IN U.S.A.  
KEUFFEL & ESSER CO.



ANGULAR DISPLACEMENT (α), DEGREES

Fig 50 Reflectance, Faceplate No. 85

175 SEMI-LOGARITHMIC 46 6463  
 1 CYCLES X 60 DIVISIONS  
 MADE IN U.S.A.  
 KNUFFEL & EBER CO.



ANGULAR DISPLACEMENT (α), DEGREES

Fig. 51 Reflectance, Faceplate No. 86

K&E SEMI-LOGARITHMIC 46 6463  
7 CYCLES X 80 DIVISIONS MADE IN U.S.A.  
KEUPPEL & EBER CO.

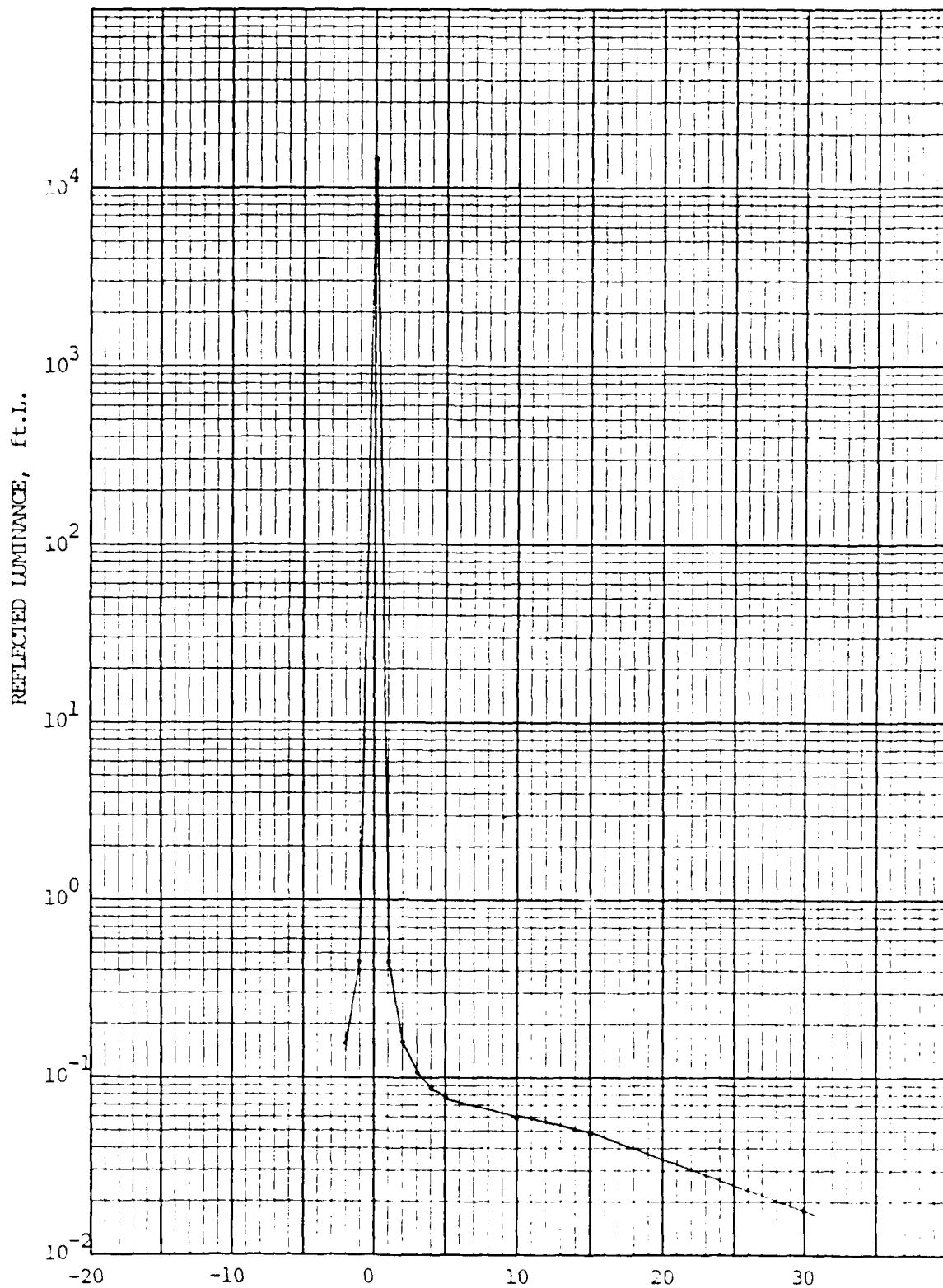


Fig. 52 Reflectance. Faceplate No. 87

It should be noted, however, that the sapphire substrates are single crystal material cut from boules grown from the melt; they are, therefore, free of bubbles, inhomogeneities, and other inclusions that may occur in glassmaking and are known to present a problem for aluminosilicate glasses. Melts of the latter have higher viscosity than common glasses and are difficult to free from bubbles. In fact, we have been advised by the Corning Glass Works that 1710 and 1720 glass is exclusively produced for drawing tubing and no attempt is made at "fining" because bubbles are not detrimental to the use for which the tubing is intended. In view of the general reputation of the firm which cut and polished the 1710 and 1720 glass substrates for this program, we believe the apparently greater diffuse reflection of these as compared to the sapphire substrate is due to inclusions in the glass rather than any lesser perfection of polish.

#### 4.3.3 Lot 5

Results of the optical reflectance measurements on Lot 5 are summarized in Table 9. Figures 53 through 63 are plots for the individual faceplates.

Table 9

## REFLECTANCE OF LOT 5 FACEPLATES

In Percentage

| FACEPLATE NO. | ANGULAR DISPLACEMENT FROM SPECULAR |                       |                       |                       |                       |                       |
|---------------|------------------------------------|-----------------------|-----------------------|-----------------------|-----------------------|-----------------------|
|               | 0                                  | 1                     | 3                     | 5                     | 10                    | 15                    |
| 88            | 8.32                               | 2.34 $\times 10^{-4}$ | 1.43 $\times 10^{-5}$ | 1.14 $\times 10^{-5}$ | 1.06 $\times 10^{-5}$ | 9.60 $\times 10^{-6}$ |
| 87            | 9.52                               | 3.73 $\times 10^{-4}$ | 3.74 $\times 10^{-5}$ | 3.03 $\times 10^{-5}$ | 2.43 $\times 10^{-5}$ | 1.74 $\times 10^{-5}$ |
| 90            | 8.42                               | 3.55 $\times 10^{-4}$ | 3.03 $\times 10^{-5}$ | 2.65 $\times 10^{-5}$ | 2.26 $\times 10^{-5}$ | 1.55 $\times 10^{-5}$ |
| 92            | 9.05                               | 3.61 $\times 10^{-4}$ | 5.17 $\times 10^{-5}$ | 3.25 $\times 10^{-5}$ | 2.44 $\times 10^{-5}$ | 1.95 $\times 10^{-5}$ |
| 93            | 10.2                               | 4.48 $\times 10^{-4}$ | 1.59 $\times 10^{-5}$ | 4.25 $\times 10^{-5}$ | 2.85 $\times 10^{-5}$ | 2.12 $\times 10^{-5}$ |
| 95            | 9.37                               | 1.61 $\times 10^{-4}$ | 3.49 $\times 10^{-5}$ | 2.97 $\times 10^{-5}$ | 2.59 $\times 10^{-5}$ | 2.06 $\times 10^{-5}$ |
| 96            | 9.53                               | 3.51 $\times 10^{-4}$ | 6.66 $\times 10^{-5}$ | 3.25 $\times 10^{-5}$ | 1.91 $\times 10^{-5}$ | 1.37 $\times 10^{-5}$ |
| 97            | 9.85                               | 4.74 $\times 10^{-4}$ | 5.29 $\times 10^{-5}$ | 3.73 $\times 10^{-5}$ | 2.81 $\times 10^{-5}$ | 2.06 $\times 10^{-5}$ |
| 98            | 10.3                               | 1.00 $\times 10^{-4}$ | 3.11 $\times 10^{-5}$ | 2.40 $\times 10^{-5}$ | 1.95 $\times 10^{-5}$ | 1.37 $\times 10^{-5}$ |

REFLECTANCE OF LOT 5 FACE PLATES

LMSC-D767020

$$I_0 = 8.33 \times 10^4$$

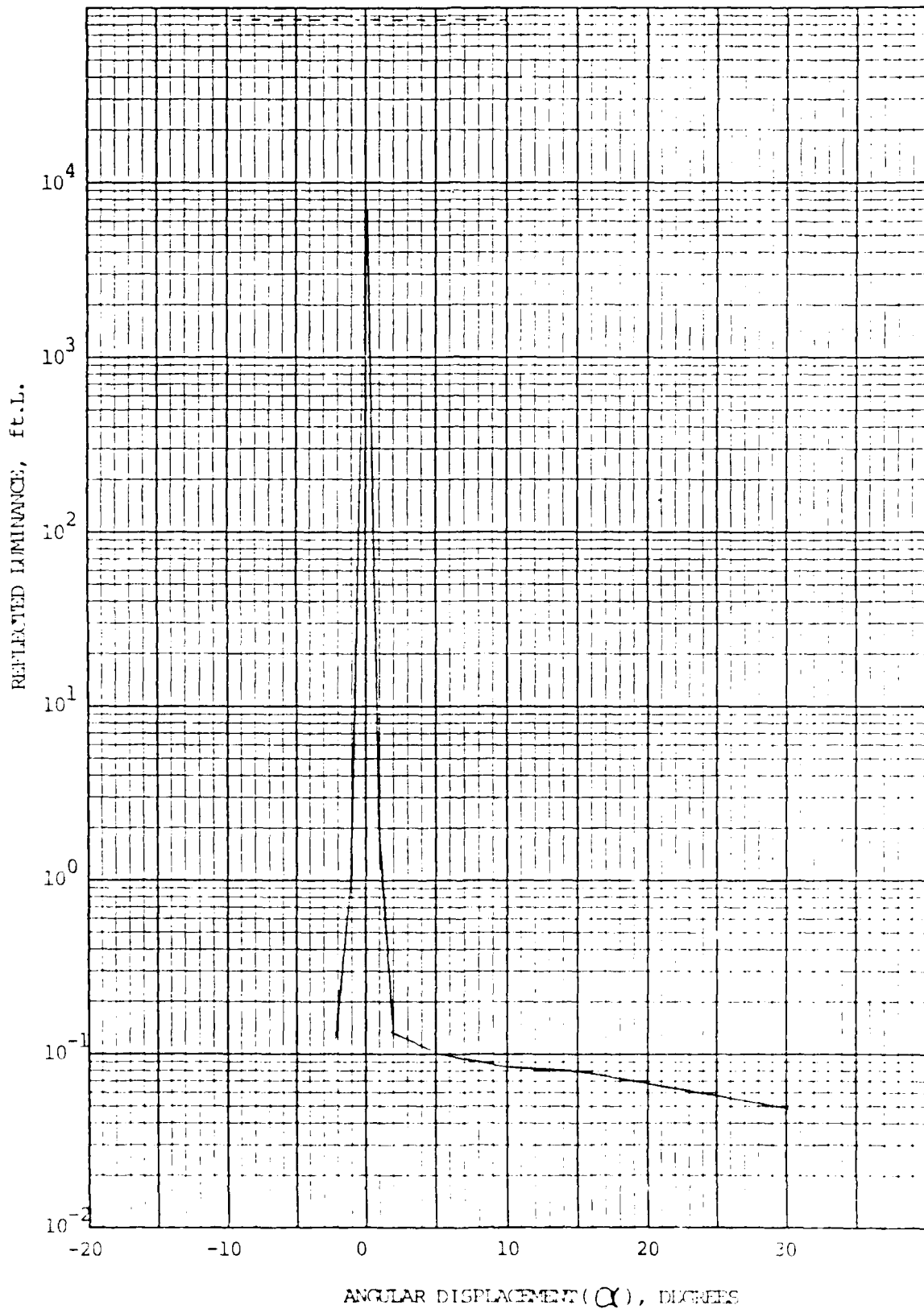
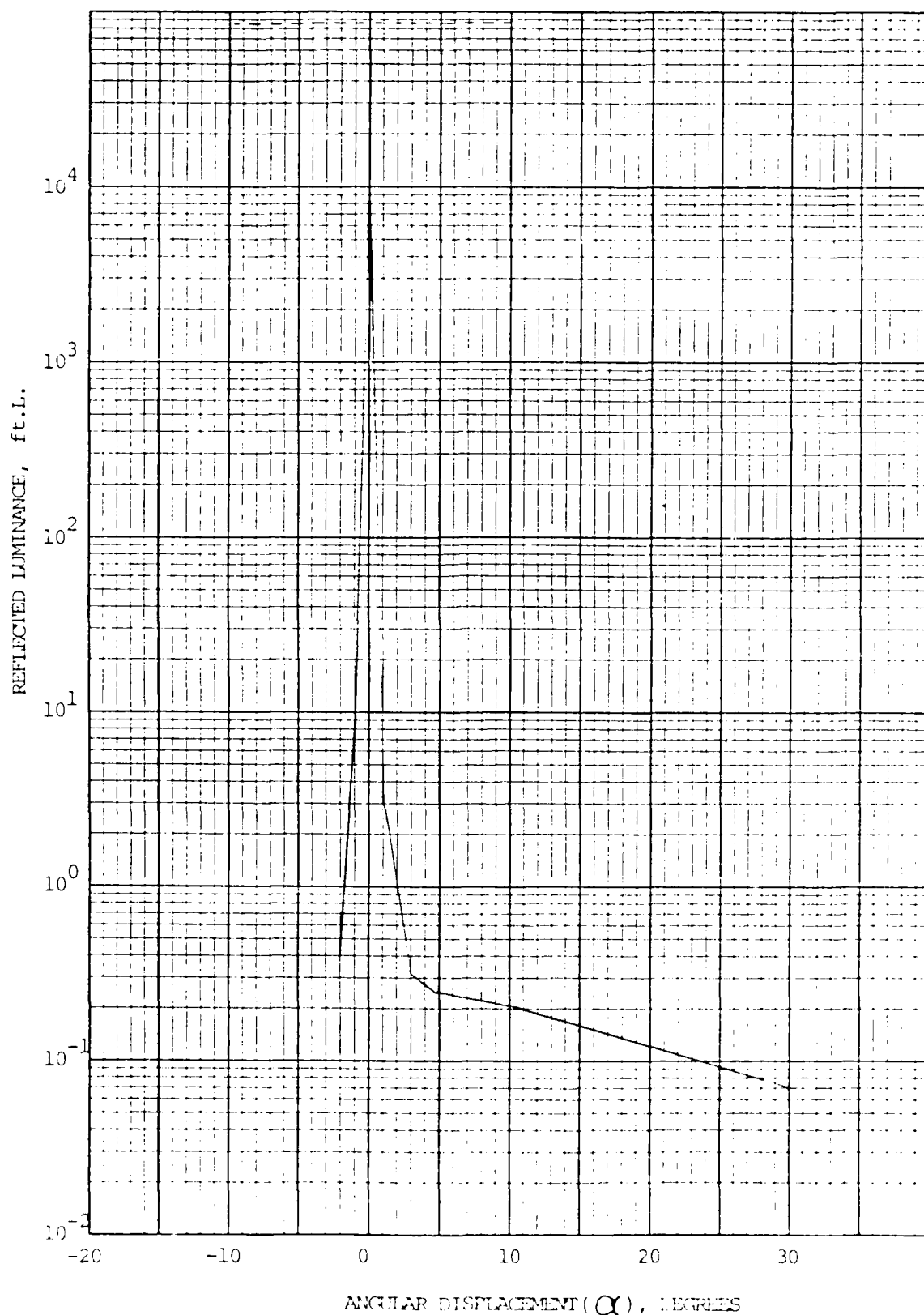


Fig. 53 Reflectance, Faceplate No. 88

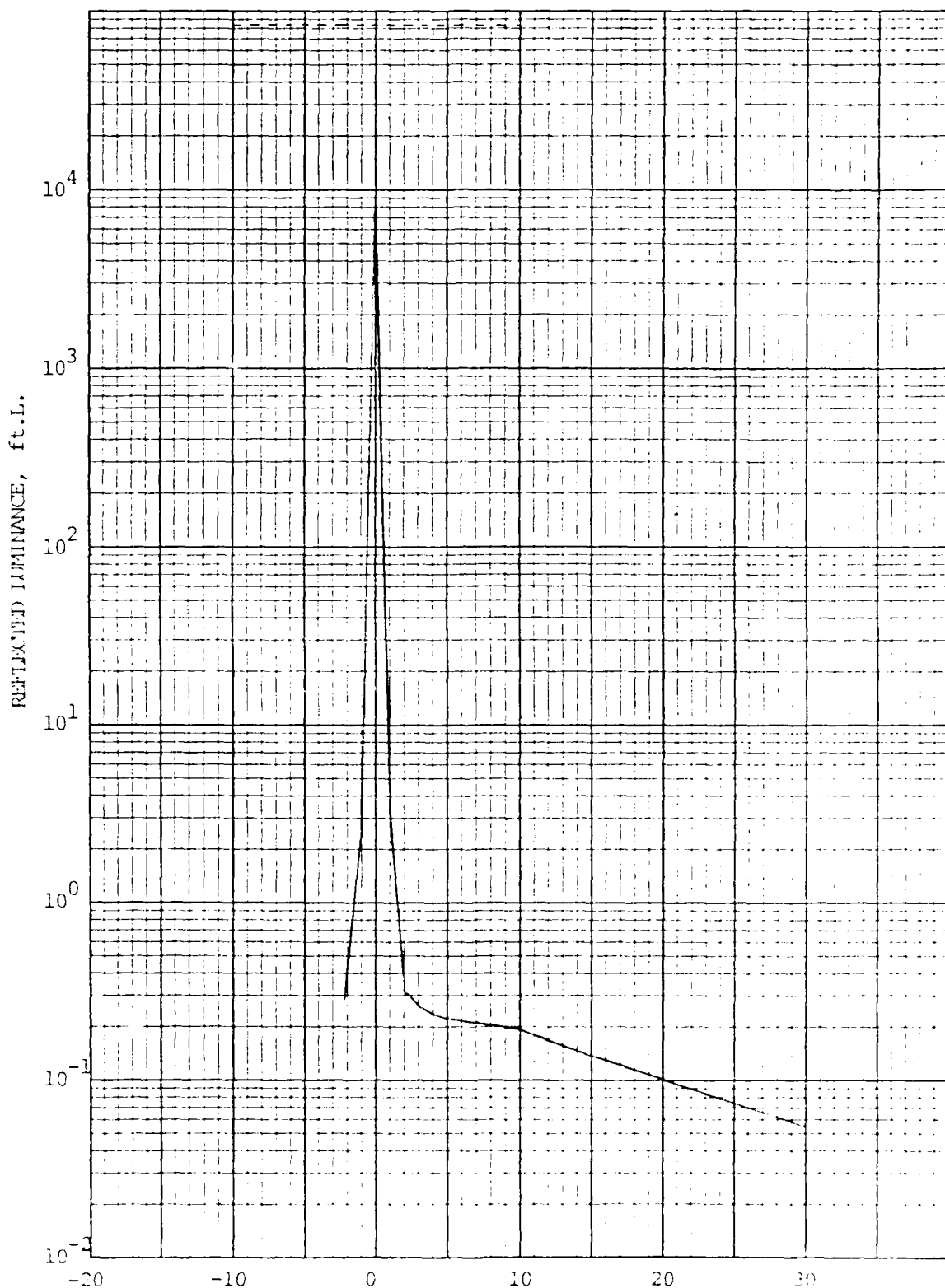
$$I_o = 8.50 \times 10^4$$



K&E SEMI-LOGARITHMIC 46 6483  
 75 CENTS x 60 DIVISIONS MADE IN U.S.A.  
 KUPFER & ESSER CO.

Fig.54 Reflectance, Faceplate No. 89

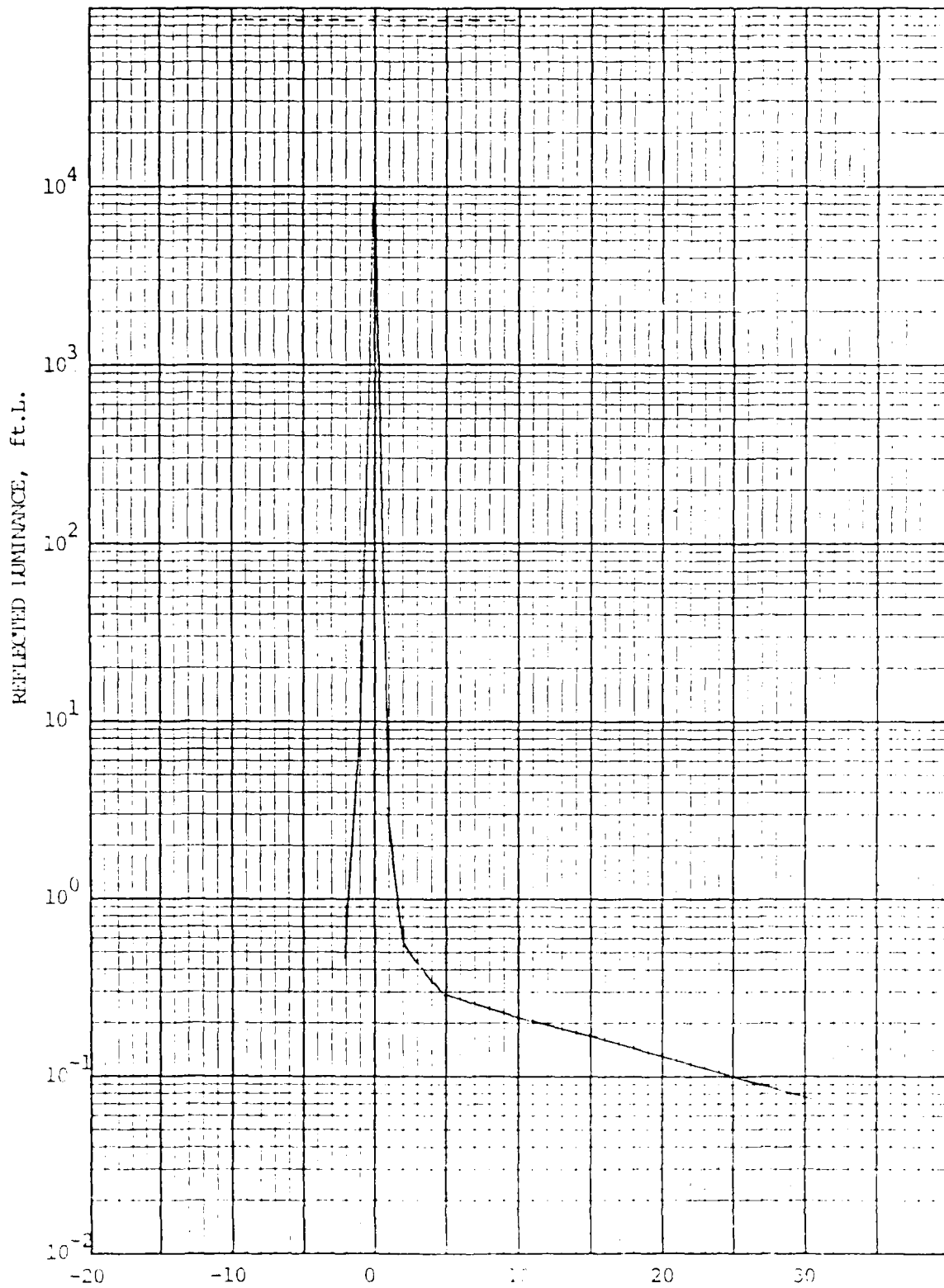
$$I_o = 8.68 \times 10^4$$



REFLECTANCE  
SEMI-LOGARITHMIC 46 6463  
FACILITIES DIVISIONS  
NEUPHEL & EBER CO

Fig. 55 Reflectance, Faceplate No. 90

$$I_0 = 8.72 \times 10^4$$



ANGULAR DISPLACEMENT (α), IN DEGREES

Fig. 56 Perfection Faceplate No. 92

$$I_0 = 8.70 \times 10^4$$

K&E SEMI LOGARITHMIC 46 6463  
7 CYCLES X 60 DIVISIONS  
KEUFFEL & ESSER CO.

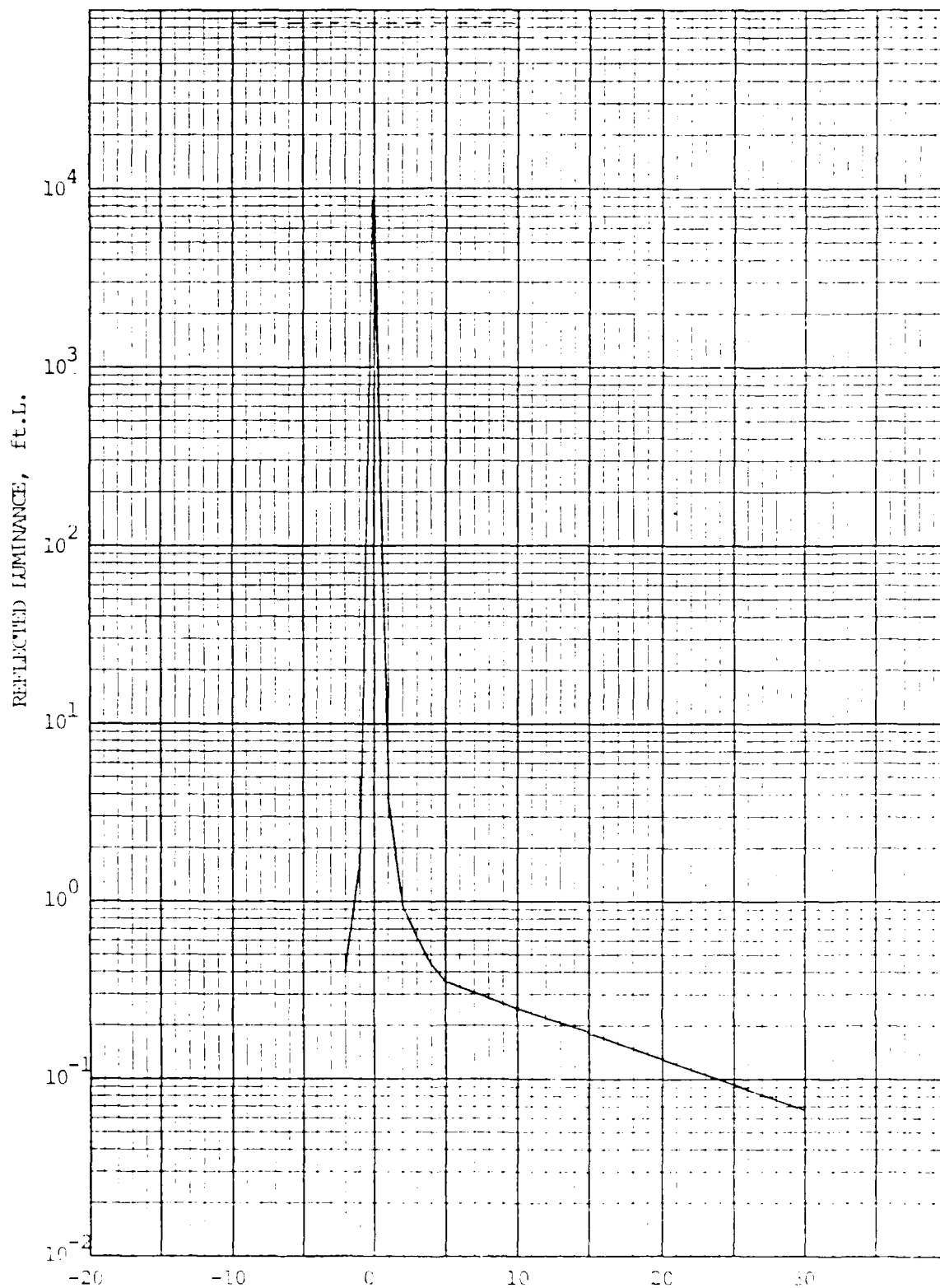
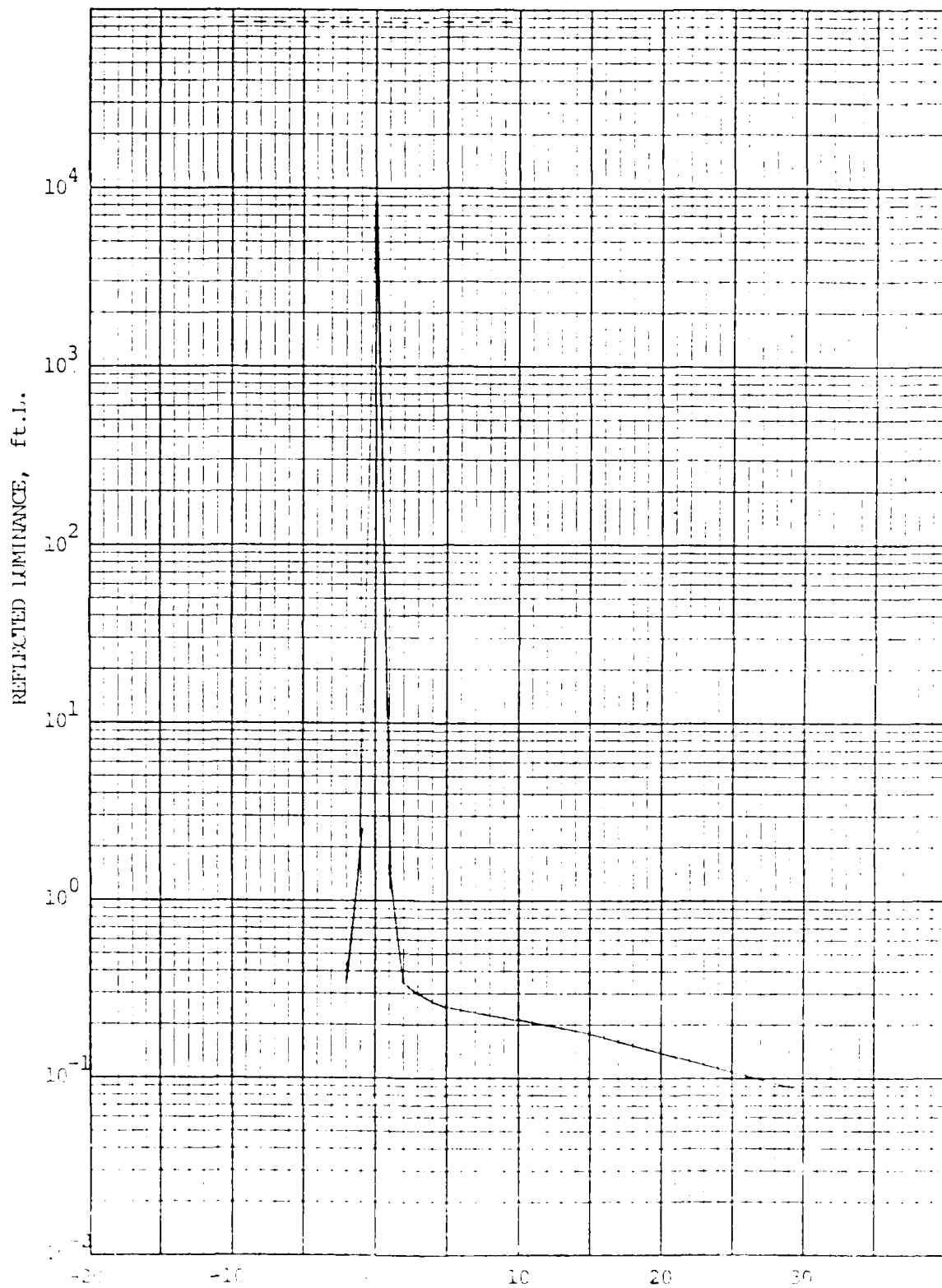


Fig. 57 Reflectance, Facerlate No. 93

$$I_0 = 8.75 \times 10^4$$

NE SEMILOGARITHMIC 46 6483  
7 CYCLES X 80 DIVISIONS  
KEUFFEL & ESSER CO.



ANGULAR DISPLACEMENT, α, DEGREES

Fig. 3- Reflectance, Faceplate No. 95

AD-A096 969

LOCKHEED MISSILES AND SPACE CO INC SUNNYVALE CA ADVA--ETC F/G 9/1  
HIGH CONTRAST CRT FACEPLATE, (U)

JAN 81 T G MAPLE, I D LIU, G COX

DAAK20-79-C-0282

UNCLASSIFIED

LMSC/D767020

DELET-TR-79-0282-F

NL

2 OF 2

NO A  
OFFERED



END

DATE  
FILMED

4-81

DTIC

$$I_o = 8.67 \times 10^4$$

LMSC-D767020

K&E SEMI-LOGARITHMIC 46 6463  
7 CYCLES X 60 DIVISIONS  
KEUFFEL & ESSER CO.

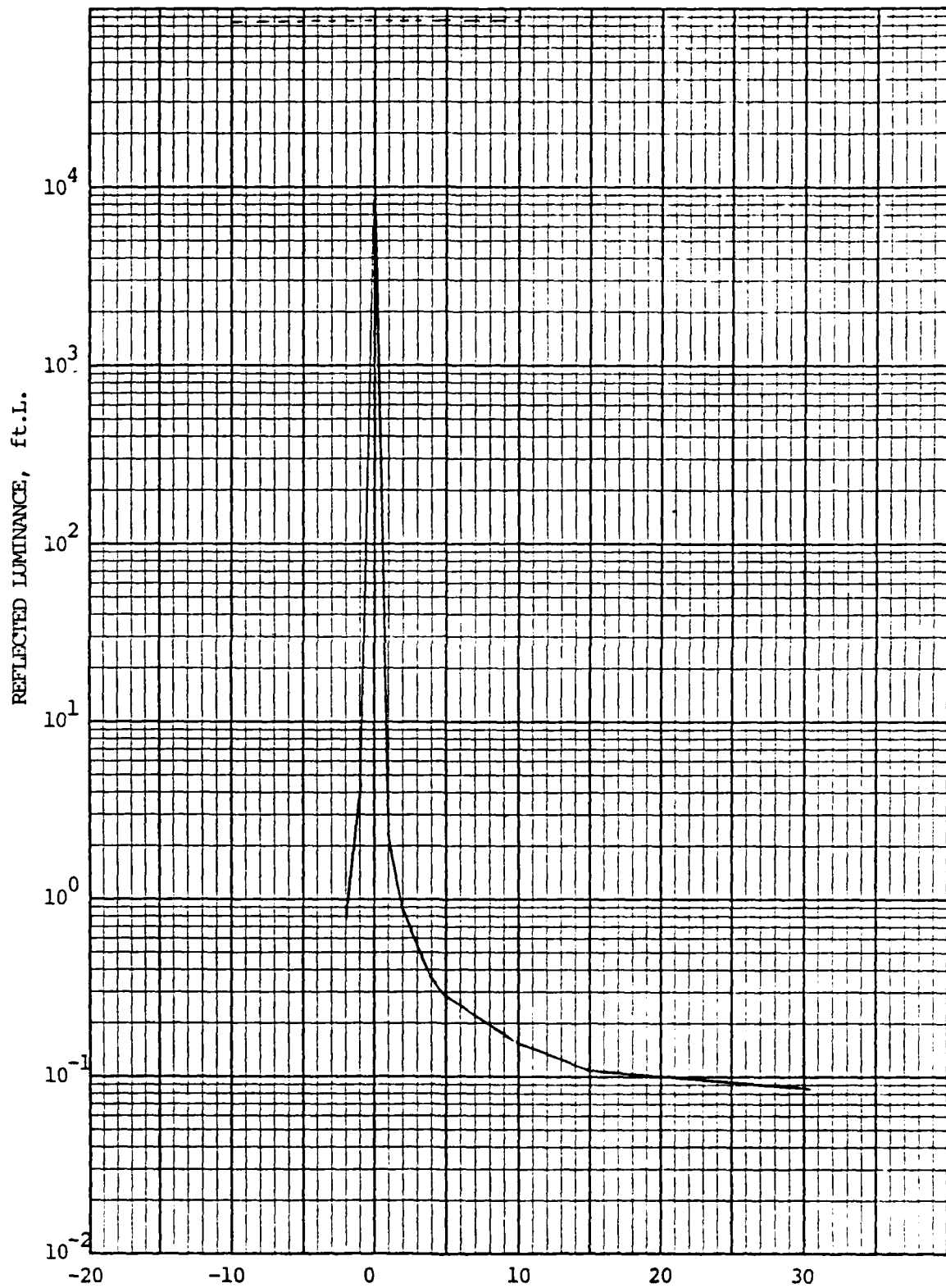
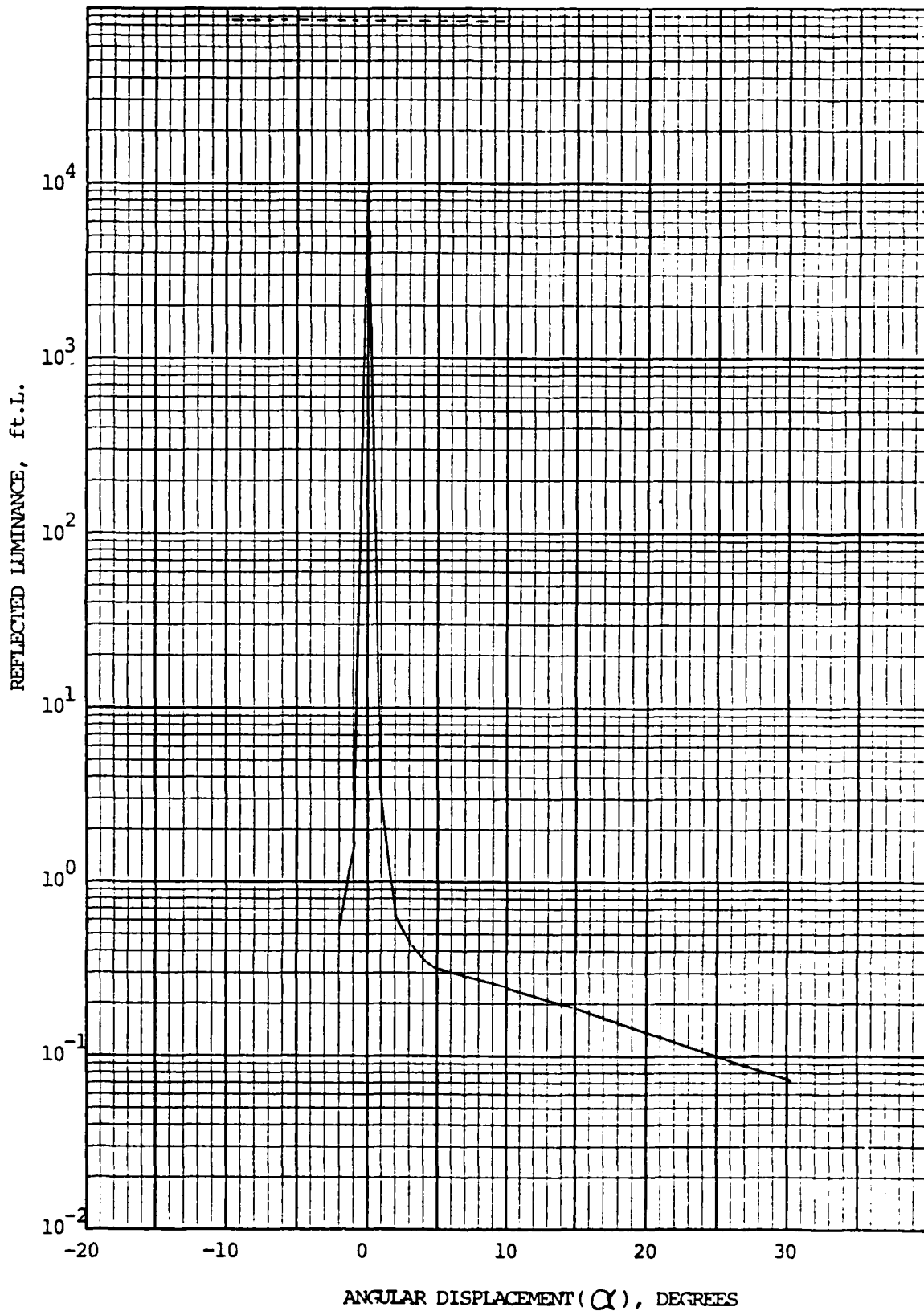


Fig.59 Reflectance, Faceplate No. 96

$$I_o = 8.75 \times 10^4$$



K $\odot$ E SEMI-LOGARITHMIC 46 6463  
7 CYCLES X 80 DIVISIONS  
KEUFFEL & ESSER CO.

Fig. 60 Reflectance, Faceplate No. 97

$$I_o = 8.66 \times 10^4$$

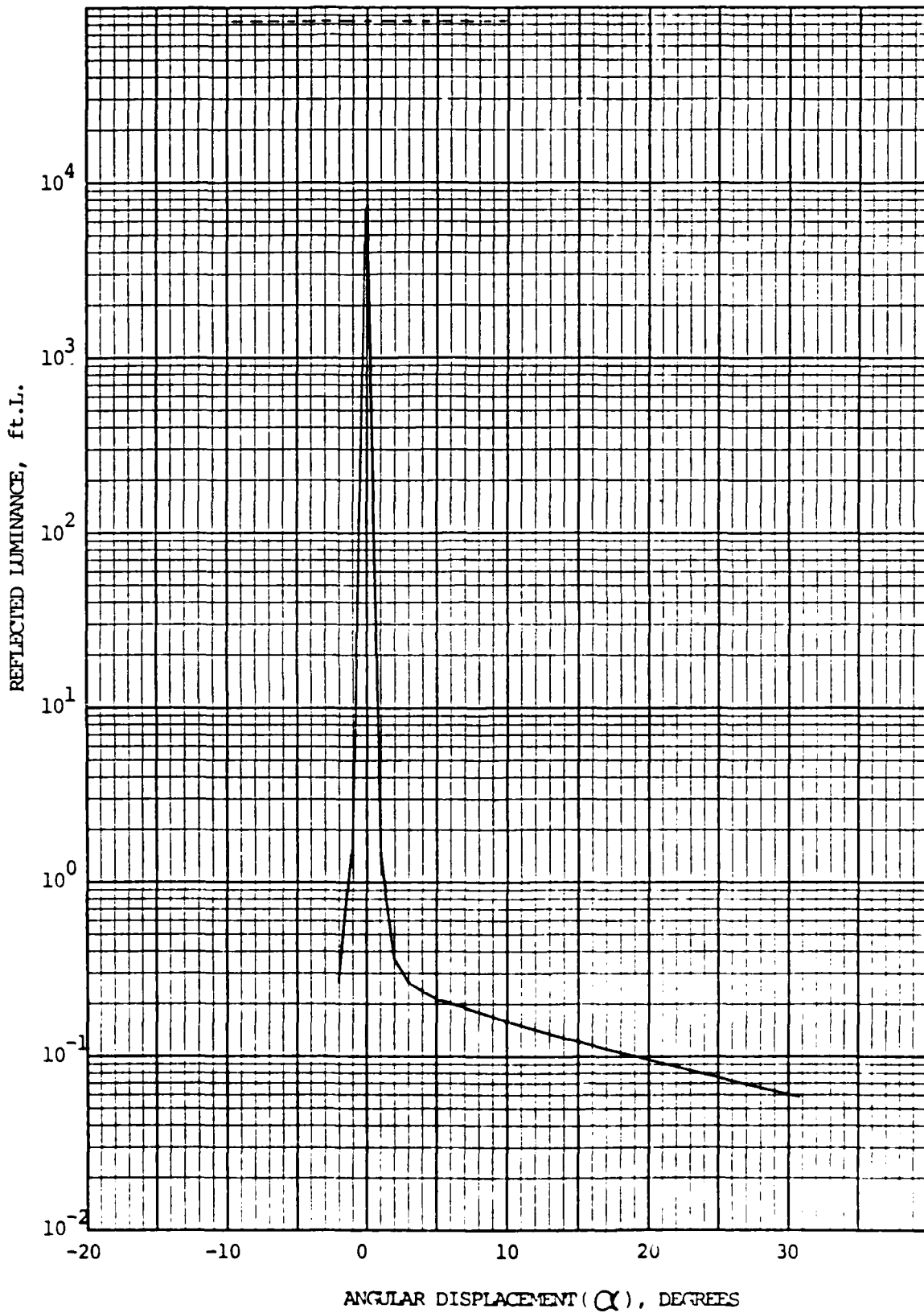
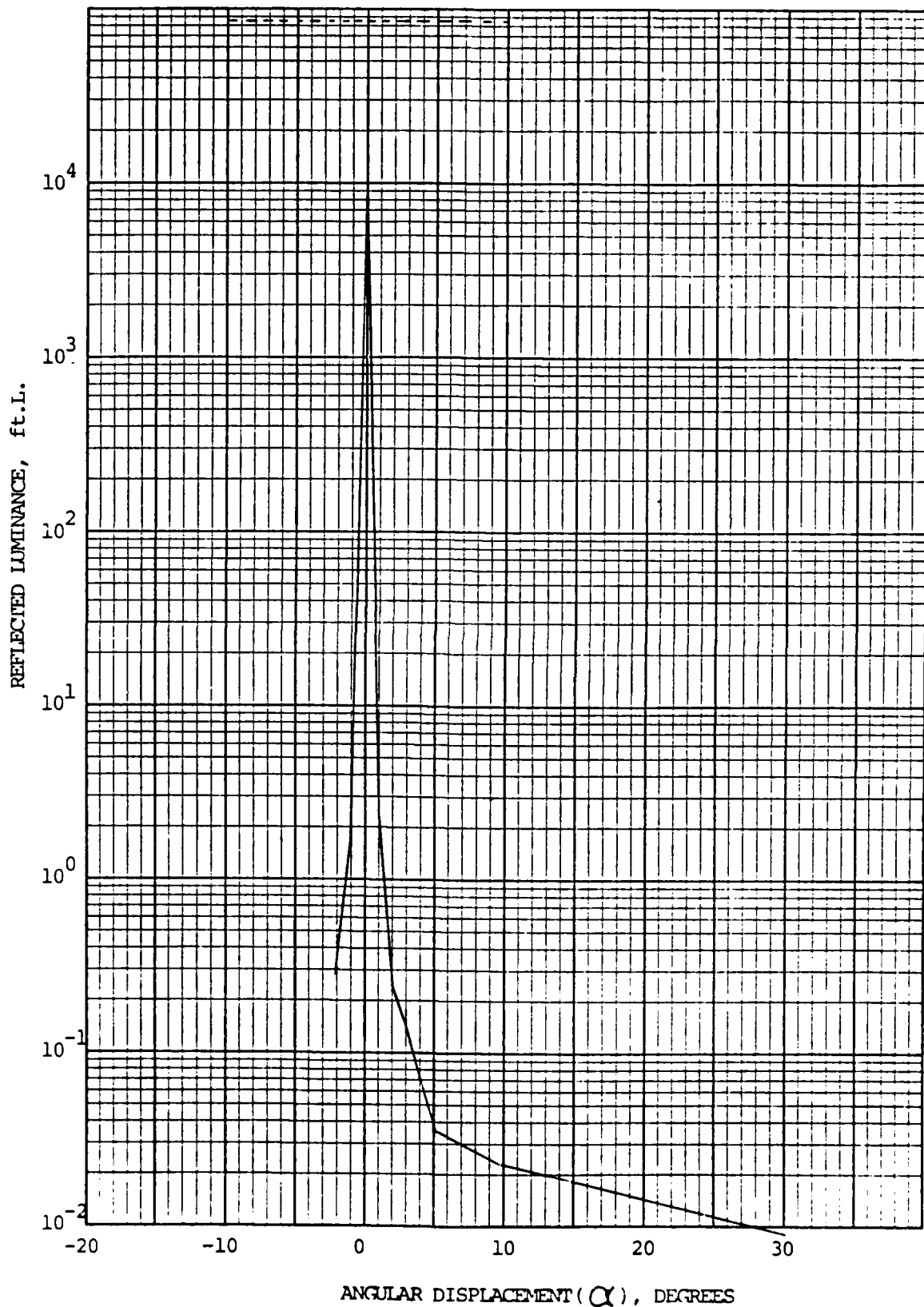


Fig. 61 Reflectance, Faceplate No. 98

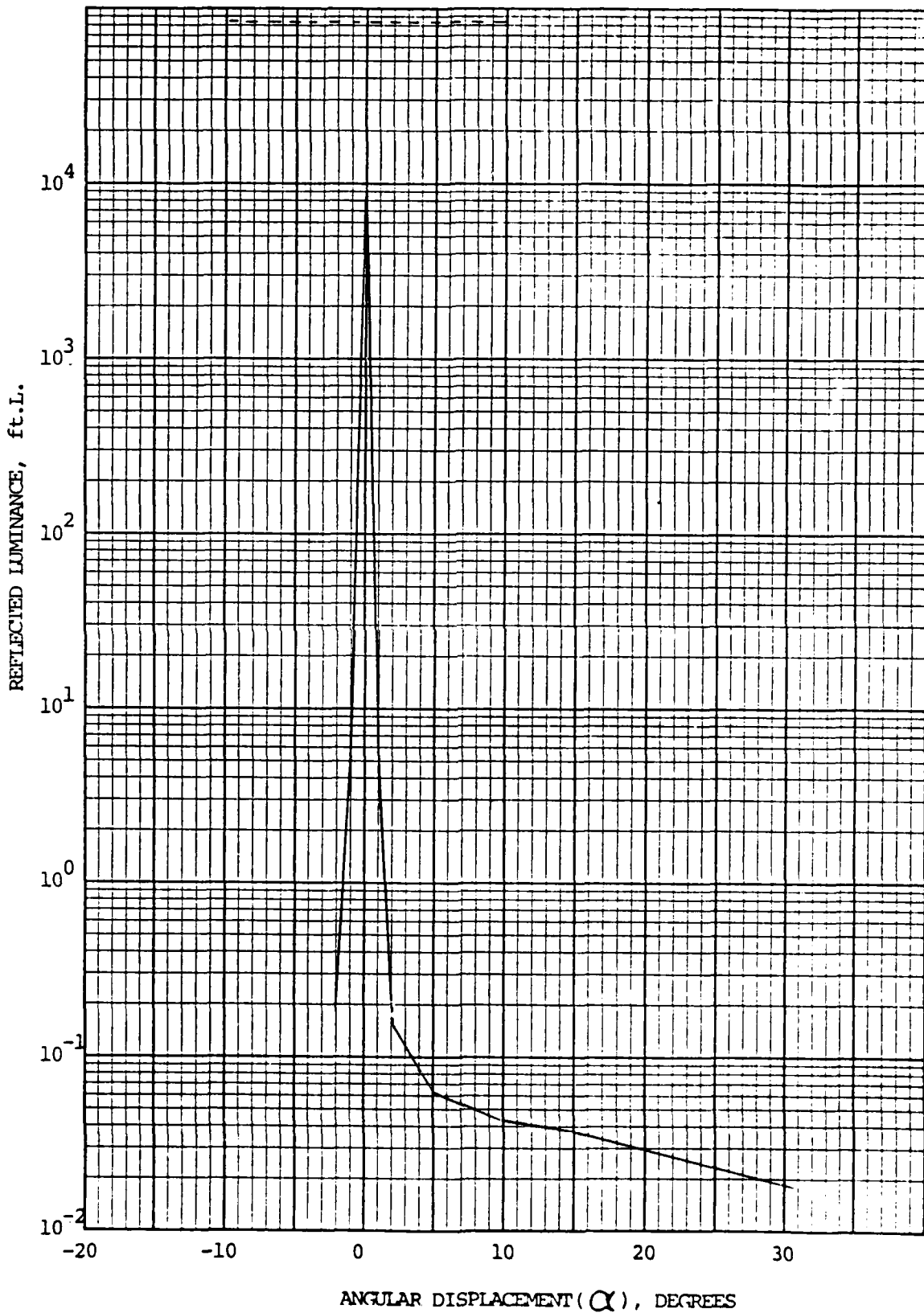
$$I_o = 8.88 \times 10^4$$



ANGULAR DISPLACEMENT ( $\alpha$ ), DEGREES

Fig. 62 Reflectance, Faceplate No. 107

$$I_o = 8.58 \times 10^4$$



K<sub>0</sub>E SEMI-LOGARITHMIC 46 6463  
7 CYCLES X 60 DIVISIONS MADE IN U.S.A.  
KEUFFEL & ESSER CO.

Fig.63 Reflectance, Faceplate No. 108

## 4.4

## REFLECTIVITY CALCULATIONS FOR SAPPHIRE FACEPLATES

In the Second Interim Report, DELET-TR-79-0282-2, May 1980, expressions were presented for the optical reflectance of a glass plate, a glass plate with a nonabsorbing film on its back surface, and a glass plate with a phosphor film and an ideal NR film. The results of calculations for an aluminosilicate glass plate having a refractive index of 1.53 were also presented in both tabular and graphic form.

We present here the results of calculations where the substrate is a sapphire plate with refractive index 1.708. The calculations are based on the expressions for reflectance at oblique incidence presented in Section 4.9 of the Second Interim Report. For a nonabsorbing plate, the reflectance is:

$$R_p = \frac{R_1 + R_2 - 2R_1R_2}{1 - R_1R_2},$$

where  $R_1$  and  $R_2$  are the reflectances at the first and second interface, respectively.

For a plate with a nonabsorbing film on its back,  $R_2$  is replaced with

$$R_2 = R_f = \frac{r_{1f}^2 + r_{2f}^2 + 2r_{1f}r_{2f}\cos \theta_f}{1 + r_{1f}^2 r_{2f}^2 + 2r_{1f}r_{2f}\cos \theta_f},$$

where  $r_{1f}$  and  $r_{2f}$  are the Fresnel reflection coefficients for the glass-film and film-air interfaces, respectively, and

$$\theta_f = \frac{4\pi n_f d_f \cos \theta_f}{\lambda},$$

where  $\theta_f$  is the angle at which light is refracted in the film.  $n_f$  is the refractive index of the film, and  $d_f$  the film thickness.  $\theta_f$  is determined by Snell's law

$$n_o \sin \theta_o = n_f \sin \theta_f.$$

where  $\theta_0$  is the angle at which light is incident upon the film.

Tables 10, 11, and 12 present the results calculated for a sapphire plate, a sapphire plate with an  $\text{La}_2\text{O}_3$  film of 12,272 Å thickness, and a sapphire plate with an  $\text{La}_2\text{O}_3$  film and an ideal NR film. The reflectivity of the sapphire plate plus  $\text{La}_2\text{O}_3$  film is a minimum at  $\theta_0 = 0^\circ$  for a 12,272 Å film thickness and a maximum for a 12,886 Å film thickness (compare Tables 11 and 13). The calculated overall reflectivities are shown graphically in Fig. 64. The curve labeled "Plate +  $\text{La}_2\text{O}_3$  Film" is for the 12,272 Å thickness. The hump in the curve peaking at  $45^\circ$  is the result of interference in the film.

The curves are similar to those previously obtained for the aluminosilicate 1720 glass plate (see Fig. 65), but the reflectances are greater for the sapphire faceplate due to the larger refractive index and consequent larger front surface reflectance of sapphire.

The contribution of the substrate-phosphor interface to the overall reflectance is, however, less for sapphire. At normal incidence, the reflectance for this interface is

$$R_2 = \left( \frac{n_1 - n_2}{n_1 + n_2} \right)^2$$

where  $n_1$  is the refractive index of the substrate and  $n_2$  that of the phosphor. For  $\text{La}_2\text{O}_3$   $n_2 = 2.2$ . Thus for 1720 glass ( $n_1 = 1.53$ )

$$R_2 = \left( \frac{1.53 - 2.2}{1.53 + 2.2} \right)^2 = 0.03227$$

For sapphire ( $n_1 = 1.768$ )

$$R_2 = \left( \frac{1.768 - 2.2}{1.768 + 2.2} \right)^2 = 0.01185.$$

If the faceplate were provided with an ideal front surface anti-reflection coating ( $R_1 = 0$ ) in addition to the ideal NR film on the phosphor, the overall reflectiveness would be reduced to only that of the substrate-phosphor interface, so that the reflectivity of the sapphire faceplate would be less than that of the 1720 faceplate.

Real anti-reflection coatings approach, but do not achieve, zero reflectance. In addition, polishing defects can constitute a diffuse reflectance component. Nevertheless, these calculations show that with suitable front surface anti-reflection coating, somewhat lower reflectance would be expected for a sapphire faceplate than for the 1720 faceplate.

Table 10  
SAPPHIRE PLATE  
Oblique Incidence

| Media          | Index | $\theta_o$ , Deg. | $I_p^r$ | $I_s^r$ | R       |
|----------------|-------|-------------------|---------|---------|---------|
| Air $n_o$      | 1     | 0                 | .14296  | .14296  | .14296  |
| Sapphire $n_1$ | 1.768 | 5                 | .14181  | .14411  | .14296  |
| Air $n_2$      | 1     | 10                | .13836  | .14760  | .14298  |
|                |       | 15                | .13255  | .15360  | .14307  |
|                |       | 20                | .12431  | .16236  | .14333  |
|                |       | 25                | .11355  | .17428  | .14392  |
|                |       | 30                | .10021  | .18991  | .14506  |
|                |       | 35                | .08434  | .20993  | .14713  |
|                |       | 40                | .06615  | .23522  | .14069  |
|                |       | 45                | .04632  | .26687  | .15659  |
|                |       | 50                | .02629  | .30612  | .16620  |
|                |       | 55                | .00902  | .35436  | .18169  |
|                |       | 60                | .00010  | .41300  | .20655  |
|                |       | 65                | .00958  | .48325  | .24642  |
|                |       | 70                | .05423  | .56588  | .31006  |
|                |       | 75                | .15850  | .66080  | .40965  |
|                |       | 80                | .34955  | .76674  | .55814  |
|                |       | 85                | .63950  | .88108  | .76029  |
|                |       | 90                | 1.00000 | 1.00000 | 1.00000 |

Table 11

SAPPHIRE PLATE +  $\text{La}_2\text{O}_3$  FILM  
Oblique Incidence

| Media                         | Index | $\theta_o$ , Deg. | $I_p^r$ | $I_p^r$ | R       |
|-------------------------------|-------|-------------------|---------|---------|---------|
| Air $n_o$                     | 1     | 0                 | .14296  | .14296  | .14296  |
| Sapphire $n_1$                | 1.768 | 5                 | .14190  | .14419  | .14305  |
| $\text{La}_2\text{O}_3$ $n_2$ | 2.2   | 10                | .13969  | .14897  | .14433  |
| Air $n_3$                     | 1     | 15                | .13888  | .16039  | .14964  |
|                               |       | 20                | .14229  | .18269  | .16249  |
|                               |       | 25                | .15058  | .21892  | .18475  |
|                               |       | 30                | .16025  | .26764  | .21394  |
|                               |       | 35                | .16394  | .32170  | .24282  |
|                               |       | 40                | .15389  | .37130  | .26260  |
|                               |       | 45                | .12617  | .40894  | .26756  |
|                               |       | 50                | .08418  | .43276  | .25847  |
|                               |       | 55                | .03972  | .44779  | .24375  |
|                               |       | 60                | .00972  | .46956  | .23784  |
|                               |       | 65                | .00996  | .50274  | .25635  |
|                               |       | 70                | .05379  | .56850  | .31115  |
|                               |       | 75                | .15838  | .66109  | .40974  |
|                               |       | 80                | .34762  | .76967  | .55864  |
|                               |       | 85                | .63668  | .88423  | .76046  |
|                               |       | 90                | 1.00000 | 1.00000 | 1.00000 |

 $\lambda = 5400 \text{ \AA}$ 
 $d_1 = 12272.7 \text{ \AA}$  (min for  $\theta_o = 0^\circ$ )

Table 12

SAPPHIRE PLATE +  $\text{La}_2\text{O}_3$  FILM + IDEAL NR  
Oblique Incidence

| Media                         | Index | $\theta_o$ , Deg. | $I_p^r$ | $I_s^r$ | R       |
|-------------------------------|-------|-------------------|---------|---------|---------|
| Air $n_o$                     | 1     | 0                 | .08709  | .08709  | .08709  |
| Sapphire $n_1$                | 1.768 | 5                 | .08640  | .08778  | .08709  |
| $\text{La}_2\text{O}_3$ $n_2$ | 2.2   | 10                | .08433  | .08989  | .08711  |
| $\lambda = 5400 \text{ \AA}$  |       | 15                | .08086  | .09351  | .08719  |
|                               |       | 20                | .07598  | .09884  | .08741  |
|                               |       | 25                | .06968  | .10613  | .08790  |
|                               |       | 30                | .06198  | .11578  | .08888  |
|                               |       | 35                | .05295  | .12831  | .09063  |
|                               |       | 40                | .04279  | .14446  | .09362  |
|                               |       | 45                | .03191  | .16518  | .09854  |
|                               |       | 50                | .02110  | .19179  | .10645  |
|                               |       | 55                | .01186  | .22604  | .11895  |
|                               |       | 60                | .00687  | .27025  | .13856  |
|                               |       | 65                | .01111  | .32753  | .16929  |
|                               |       | 70                | .03341  | .40193  | .21767  |
|                               |       | 75                | .09066  | .49876  | .29271  |
|                               |       | 80                | .21503  | .62477  | .41990  |
|                               |       | 85                | .47147  | .78843  | .62995  |
|                               |       | 90                | 1.00000 | 1.00000 | 1.00000 |

## Plate 13

SAPPHIRE PLATE +  $\text{La}_2\text{O}_3$  FILM

## Oblique Incidence

| Media  |       | Index | $\theta_o$ , Deg. | $I_p^r$ | $I_s^r$ | R       |
|--|-------|-------|-------------------|---------|---------|---------|
| Air  | $n_o$ | 1     | 0                 | .26423  | .26423  | .26423  |
| Sapphire   | $n_1$ | 1.768 | 5                 | .26262  | .26569  | .26416  |
| $\text{La}_2\text{O}_3$                          | $n_2$ | 2.2   | 10                | .25698  | .26729  | .26313  |
| Air  | $n_3$ | 1     | 15                | .24497  | .27274  | .25886  |
|  |       |       | 20                | .22359  | .27273  | .24816  |
|  |       |       | 25                | .19079  | .26609  | .22844  |
| $\lambda = 5400\text{\AA}$                       |       |       | 30                | .14815  | .25237  | .20026  |
| $d_1 = 12886.36$ (Max for $\theta_o = 0^\circ$ ) |       |       | 35                | .10328  | .23779  | .17053  |
|  |       |       | 40                | .06788  | .23817  | .15302  |
|  |       |       | 45                | .04912  | .27249  | .16080  |
|  |       |       | 50                | .04224  | .34467  | .19346  |
|  |       |       | 55                | .03566  | .43673  | .23620  |
|  |       |       | 60                | .02321  | .52720  | .27520  |
|  |       |       | 65                | .01260  | .60709  | .30984  |
|  |       |       | 70                | .02810  | .67899  | .35354  |
|  |       |       | 75                | .10796  | .75002  | .42899  |
|  |       |       | 80                | .29310  | .82641  | .55976  |
|  |       |       | 85                | .60211  | .91051  | .75631  |
|  |       |       | 90                | 1.00000 | 1.00000 | 1.00000 |

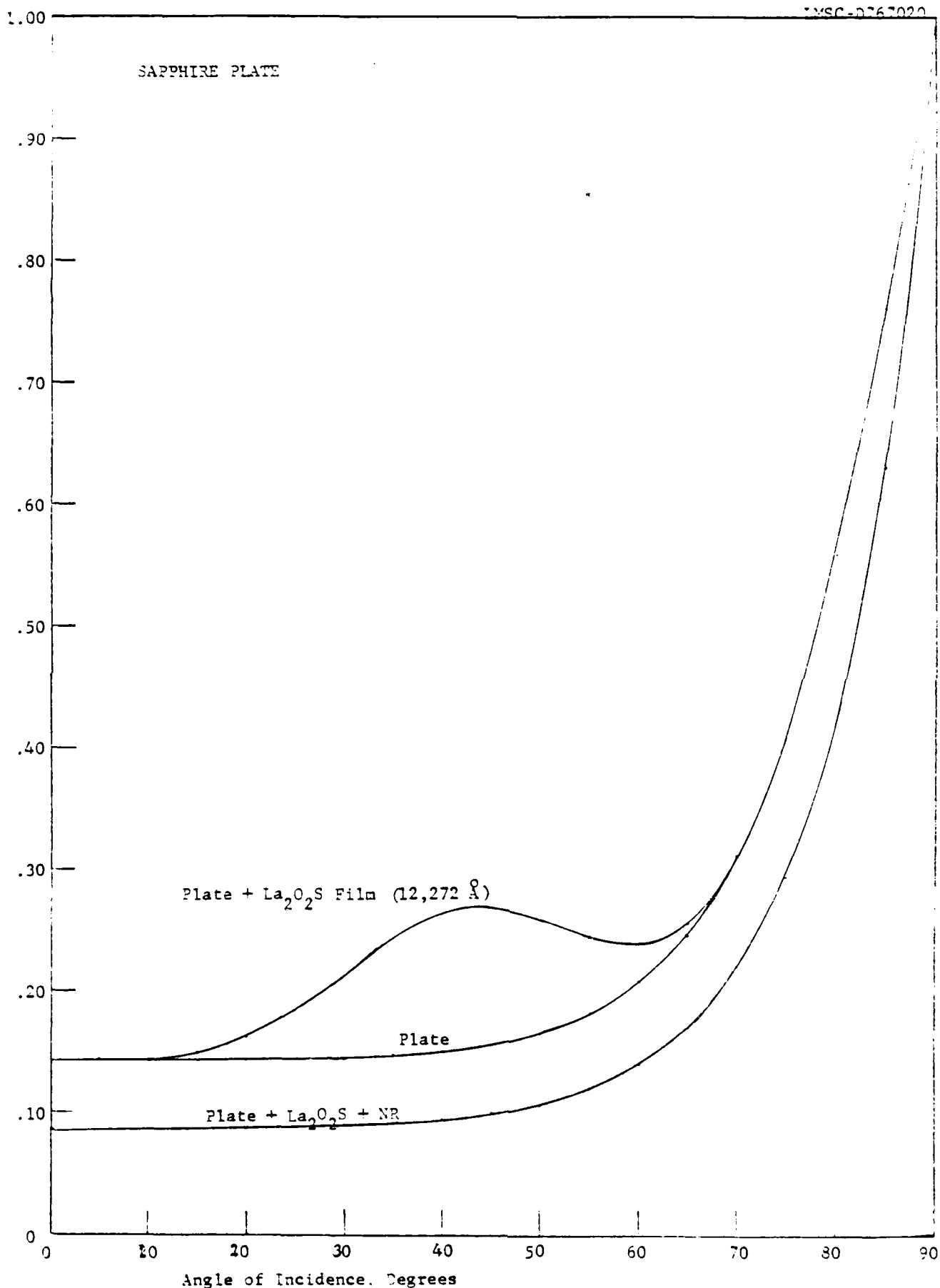
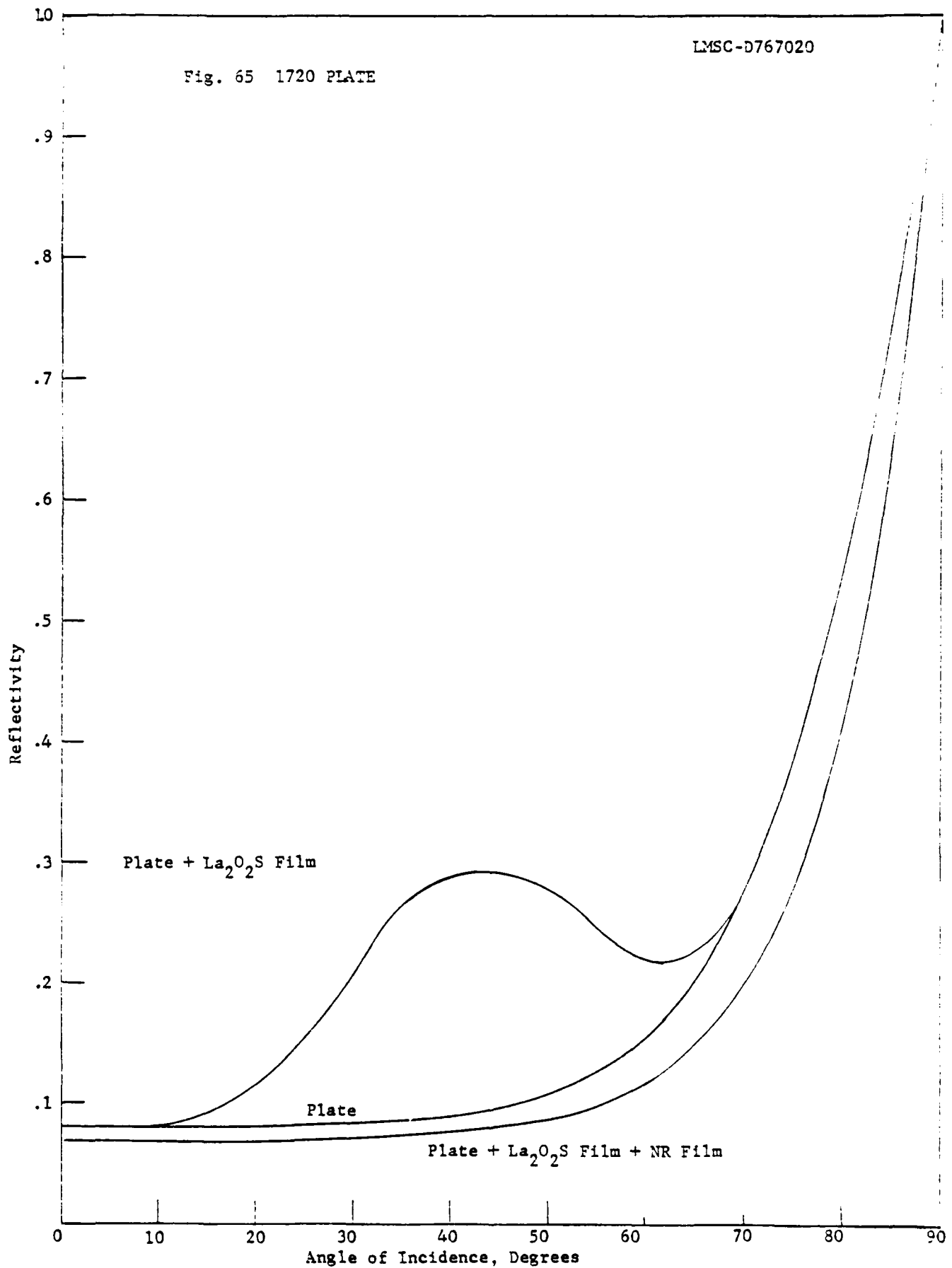


Fig. 64 Sapphire Plate

Fig. 65 1720 PLATE



#### 4.5 DELIVERY OF FACEPLATES

The ten sapphire faceplates of Lot 4 were shipped to ERADCOM via Federal Express on July 23, 1980.

The nine sapphire faceplates of Lot 5 were shipped to ERADCOM via Federal Express on September 16, 1980.

## 5.0 SUMMARY OF RESULTS

During the period of this program, a total of 45 high contrast CRT faceplates were fabricated and delivered to ERADCOM. Twenty-six utilized Type 1720 (or the equivalent Type 1710) aluminosilicate glass as substrates and 19 utilized single crystal sapphire as substrates.

Although gross distortion and some warpage of substrates was initially a problem during the high temperature sulfurization treatment, as the result of expansion coefficient mismatch between glass and phosphor film, it was found possible to solve this problem by a carefully programmed preheating and cooling schedule. A similar schedule was also found desirable for avoiding incipient cracking of the sapphire substrates.

Sapphire substrates were found to have distinct advantages in comparison to aluminosilicate glass. The high melting point of sapphire permitted the sulfurization treatment to be made at the optimum temperature of 1050°C for maximum brightness, whereas the softening point of the aluminosilicate glass necessitated reducing the sulfurization treatment temperature to 850°C, with a consequent reduction in cathodoluminescent brightness.

In addition, it was observed that the brightness of a raster display on a 1720 glass faceplate decreased by 40 percent during a 30 second period following turning on a high current density electron beam. Under the same conditions, sapphire faceplates did not exhibit a significant decrease. The difference in behavior is attributed to the high thermal conductivity of sapphire, some two orders of magnitude greater than that of 1720 glass; the thermal conductivity of 1720 glass was insufficient to prevent thermal quenching of the phosphor film luminescence.

## 6.0

## CONCLUSIONS

Sapphire has been found to possess several advantages over aluminosilicate glass as a substrate for high contrast CRT faceplates:

- Phosphor films on sapphire substrates can be processed at the optimum temperature for maximum cathodoluminescence.

Sapphire is totally inert toward the sulfurization atmosphere and the oxysulfide film at the optimum treatment temperature of 1050°C.

- No distortion or warpage of sapphire faceplates occurs in processing. With a melting point of 2040°C, sapphire readily withstands the stress of a moderate temperature coefficient mismatch with the oxysulfide film without effect. The sapphire is completely rigid at 1050°C; surfaces remain completely flat and retain the perfection of the initial polish.

1710 and 1720 aluminosilicate glasses, on the other hand, have a softening point of 915°C. The maximum processing temperature has been found limited to 850°C because the stress of the temperature coefficient mismatch with the oxysulfide film is sufficiently large to cause gross distortion of the glass and warpage of the film unless great care is taken during preheating and cooling down after the sulfurization treatment. Although the glasses are chemically inert toward the sulfurizing atmosphere, and the oxysulfide film at 850°C, the surface of the glass reproduces imperfections in the support plate. Carbon plates must be used to support the glass during treatment because the glass will fuse to quartz or alumina. Carbon plates cannot be provided with a finish of optical quality.

- Luminescence of phosphor films on a sapphire substrate is not reduced by thermal quenching.

The greater part of the energy of an electron beam is dissipated as heat. The thermal conductivity of sapphire is some two orders of magnitude greater than that of 1710 or 1720 glass; as a result, the heat generated in the phosphor film is conducted away by the sapphire fast enough that

temperature of the film does not rise into the range at which thermal quenching of the film luminescence becomes appreciable, even at average power densities of 8 watts/cm<sup>2</sup>.

On the other hand, the luminescence of the film on 1720 glass has been observed to decrease by 40% within 30 seconds exposure to a power density of only 1.1 watt/cm<sup>2</sup>.

7.0 REFERENCES

1. Research and Development Technical Report ECOM-77-2689-2 May 1978, Contract DAAB-07-77-C-2639, Watkins Johnson Company
2. Research and Development Technical Report DELET-TR-77-2639-3, August, 1979, Contract DAAB-07-77-C-2639, Watkins Johnson Company
3. K. A. Wickersheim, R. A. Buchanan, and E. C. Yates, "Multiphonon Relaxation of Trivalent Europium in Lanthanum Oxysulfide", Proc. 7th Rare Earth Research Conference, Coronado, Calif., 28-30 Oct. 1968, Vol. II, p. 835

DISTRIBUTION:

|  |  |
|--|--|
| 101 Defense Technical Information Center<br>Attn: DTIC-TCA<br>Cameron Station (Bldg. 5)<br>012 Alexandria, Va. 22314 | 602 Cdr. Night Vision & Electro-Optics<br>ERADCOM<br>Attn: DELMV-D<br>001 Fort Belvoir, Va. 22060                |
| 203 GIDEP Engineering & Support Dept.<br>TE Section<br>P.O. Box 398<br>001 NORCO, Ca. 91760                          | 603 Cdr. Atmospheric Sciences Lab<br>ERADCOM<br>Attn: DELAS-SY-S<br>001 White Sands Missile Range,<br>N.M. 88002 |
| 205 Director<br>Naval Research Laboratory<br>Attn: Code 2627<br>001 Washington, D.C. 20375                           | 607 Cdr. Harry Diamond Labs<br>Attn: DELHD-CO, TD (In Turn)<br>2800 Powder Mill Road<br>001 Adelphi, Md. 20783   |
| 301 Rome Air Development Center<br>Attn: Documents Library (TILD)<br>001 Griffiss AFB, N.Y. 13441                    | 609 Cdr. ERADCOM<br>Attn: DRDEL-CG, CD, CS (In Turn)<br>2800 Powder Mill Road<br>001 Adelphi, Md. 20783          |
| 437 Deputy for Science & Technology<br>Office, Ass't Sec. Army (R&D)<br>001 Washington, D.C. 20310                   | 612 Cdr. ERADCOM<br>Attn: DRDEL-CT<br>2800 Powder Mill Road<br>001 Adelphi, Md. 20783                            |
| 438 HQDA (DAMA-ARZ-D/Dr. F.D. Verderame)<br>001 Washington, D.C. 20310   | 680 Commander<br>U.S. Army Electr R&D Command<br>000 Fort Monmouth, N.J. 07703                                   |
| 482 Director<br>U.S. Army Mat'l Systems Analy. Actv<br>Attn: DRXSY-T<br>001 Aberdeen Proving Ground, Md. 21005       | 1 DELEW-D<br>1 DELET-DD<br>1 DELSD-L (Tech Library)<br>2 DELSD-L-S (STINFO)<br>4 Originating Office              |
| 563 Commander, DARCOM<br>Attn: DRCDE<br>5001 Eisenhower Ave.<br>001 Alexandria, Va. 22333                            | 681 Commander<br>U.S. Army Communicatns R&D Command<br>Attn: USMC-LNO<br>001 Fort Monmouth, N.J. 07703           |
| 564 Cdr. U.S. Army Signals Wfres Lab<br>Attn: DELSW-OS<br>Vint Hill Farms Station<br>001 Warrenton, Va. 22185        | 705 Advisory Group on Electron Devices<br>201 Varick Street, 9th Floor<br>002 New York, New York 10014           |
| 579 Cdr. PM Concept Analysis Ctrs.<br>Attn: DRCPM-CAC<br>Arlington Hall Station<br>001 Arlington, Va. 22212          |  |

|     |   |  |
|-----|---|--|
| 103 | Code R123, Tech Library<br>DCA Defense Comm Engrg Ctr<br>1800 Hienle Ave.<br>001 Resten, Va. 22090                          | Dr. Robert Trimmier<br>Sperry Flight Systems<br>Mail Station 109B<br>21111 N. 19th Ave.<br>001 Phoenix, Ariz. 55027                                      |
| 104 | Defense Communications Agency<br>Technical Library Center<br>Code 205 (P. A. Tolovi)<br>001 Washington, D.C. 20305          | Mr. Robert Perutz<br>LORAL Electronics System<br>999 Central Park Ave.<br>001 Yonkers, N.Y. 10704  |
| 206 | Commander<br>Naval Electronics Lab Center<br>Attn: Library<br>001 San Diego, Ca. 92152                                      | Applied Physics Laboratory<br>John Hopkins University<br>John Hopkins Road<br>Attn: Mr. Charles Feldman<br>001 Laurel, Md. 20810                         |
| 406 | Commandant<br>U.S. Army Aviation Center<br>Attn: ATZQ-D-MA<br>001 Fort Rucker, Al. 36362                                    | General Electric Company<br>50 Fordham Road<br>Attn: Mr. Richard L. Skovhalt<br>001 Wilmington, Ma. 01887  |
| 475 | Cdr. Harry Diamond Laboratories<br>Attn: Library<br>2800 Powder Mill Road<br>001 Adelphi, Md. 20783                         | Naval Research Laboratory<br>4555 Overlook Ave. S.W.<br>Code 5333<br>Attn: Mr. Paul Thibaud<br>001 Washington, D.C. 20375                                |
| 507 | Cdr. AVRADCOM<br>Attn: DRSAB-E<br>P.O. Box 209<br>001 St. Louis, Mo. 63166  | General Electric Company<br>P.O. Box 5000<br>Mail Drop 120<br>Attn: Mr. Sam S. Jobs<br>001 Birmingham, N.Y. 13902  |
| 604 | Chief<br>Office of Missile Electron Warfare<br>Electronic Warfare Lab, ERADCOM<br>001 White Sands Missile Range, N.M. 88002 | Westinghouse Electric Corp.<br>Industrial and Government<br>Tube Division<br>Westinghouse Circle<br>Attn: Mr. N. J. Taylor<br>001 Horseheads, N.Y. 14545 |
| 701 | MIT Lincoln Laboratory<br>Attn: Library (RM A-082)<br>P.O. Box 73<br>002 Lexington, Ma. 02173                               | XEROX Corporation<br>Attn: Dr. Benjamin Kazan<br>Palo Alto Research Center<br>3333 Coyote Hill Road<br>001 Palo Alto, Ca. 94304                          |
| 703 | NASA Scientific & Tech Info Facility<br>Baltimore/Washington Intl Airport<br>P.O. Box 8757<br>001 Md. 21240                 |  |

Thomas Electronics, Inc.  
Attn: Mr. Peter Seats  
100 Riverview Drive  
001 Wayne, N.J. 07470

Dumont Electron Tubes and Devices Corp.  
Attn: Mr. E. W. Swenarton  
750 Bloomfield Ave.  
001 Clifton, N.J. 07015

Northrop Corporation  
Attn: Mr. Walter Goede  
Electronics Division  
1 Research Park  
001 Palos Verdes, Ca. 90274

Watkins-Johnson Co.  
Attn: Mr. Norman Lehrer  
442 Mount Herman Road  
001 Scotts Valley, Ca. 95066

DATE  
FILMED  
-8